Award Number: W81XWH-12-1-0275

TITLE: Dual-Targeting of AR and Akt Pathways by Berberine in Castration-Resistant Prostate Cancer

PRINCIPAL INVESTIGATOR: Haitao Zhang

CONTRACTING ORGANIZATION: Tulane University
New Orleans, LA 70112-2699

REPORT DATE: October 2016

TYPE OF REPORT: Final Report

PREPARED FOR: U.S. Army Medical Research and Materiel Command
Fort Detrick, Maryland 21702-5012

REPORT DOCUMENTATION PAGE

Form Approved
OMB No. 0704-0188

1. REPORT DATE	2. REPORT TYPE	3. DATES COVERED
October 2016	FINAL	19Jul2012 - 18Jul2016

4. TITLE AND SUBTITLE

Dual-Targeting of AR and Akt Pathways by Berberine in Castration-Resistant Prostate Cancer

5a. CONTRACT NUMBER

5b. GRANT NUMBER
W81XWH-12-1-0275

5c. PROGRAM ELEMENT NUMBER

6. AUTHOR(S)

Haitao Zhang

E-Mail: hzhang@tulane.edu

5d. PROJECT NUMBER

5e. TASK NUMBER

5f. WORK UNIT NUMBER

7. PERFORMING ORGANIZATION NAME(S) AND ADDRESS(ES)

Tulane University
1430 Tulane Ave, EP-15
New Orleans, LA 70112

8. PERFORMING ORGANIZATION REPORT NUMBER

9. SPONSORING / MONITORING AGENCY NAME(S) AND ADDRESS(ES)

U.S. Army Medical Research and Materiel Command
Fort Detrick, Maryland 21702-5012

10. SPONSOR/MONITOR'S ACRONYM(S)

11. SPONSOR/MONITOR'S REPORT NUMBER(S)

12. DISTRIBUTION / AVAILABILITY STATEMENT

Approved for Public Release; Distribution Unlimited

13. SUPPLEMENTARY NOTES

14. ABSTRACT

We have demonstrated that berberine (BBR) inhibits AR expression by downregulating its mRNA and inducing degradation of the AR protein. In contrast, BBR inhibition of AKT expression is mediated mainly by inducing protein degradation. By using a PTEN conditional knockout mouse model, we have demonstrated that BBR is effective in blocking the development and castration-resistant progression of prostate cancer. These effects seem to be confined to the cancerous tissues, as normal prostates and other tissues are not affected by BBR. These results provide strong support for BBR as a chemoprevention agent targeting the development and progression of prostate cancer. Additionally, we have demonstrated that BBR inhibits the growth of castration-resistant xenografts driven by a constitutively active AR splice variant, and that BBR sensitizes AR-V-expressing tumors to enzalutamide treatment. These results suggest a role for BBR in the treatment of advanced prostate cancer, particularly in overcoming therapeutic resistance mediated by constitutively active AR splice variants. Finally, we have shown BBR blocks steroidogenesis by inhibiting the activity of AKR1C3, pointing to a new direction of drug development using BBR as the lead compound.

15. SUBJECT TERMS

Prostate cancer; Androgen receptor; Berberine; natural compound; castration resistant prostate cancer; AR splice variants; steroidogenesis.

16. SECURITY CLASSIFICATION OF:			17. LIMITATION OF ABSTRACT	18. NUMBER OF PAGES	19a. NAME OF RESPONSIBLE PERSON
a. REPORT	b. ABSTRACT	c. THIS PAGE			USAMRMC
Unclassified	Unclassified	Unclassified	Unclassified	71	19b. TELEPHONE NUMBER *(include area code)*

Table of Contents

1. Introduction

Advanced prostate cancer is notorious for developing resistance to therapies. One of the underpinnings for the resistance mechanism is that cancer cells rely on multiple intracellular signaling pathways for growth and survival. When one of these pathways is shut down therapeutically, cancer cells adapt by shifting to alternative pathways, rendering the treatment ineffective. Therefore, it is of utmost importance to target multiple pathways to combat the development of resistance in our pursuit of more effective treatments. Preliminary studies conducted in our lab have shown that a berberine (BBR), a plant-derived isoquinoline alkaloid, suppresses both androgen receptor (AR) and AKT signaling pathways in prostate cancer cells. Supported by this grant, we set out to understand the mechanisms of BBR-induced downregulation of different AR isoforms (Task 1) and to evaluate the efficiency of BBR in various disease settings in animal models of prostate cancer (Tasks 2&3).

2. Body

2.1 Task 1. To investigate the mechanisms of berberine-induced downregulation of full-length and splice variants of AR.

2.1.1 Berberine inhibits the transcription of the AR gene. We have previous concluded that BBR does not affect the mRNA level of full-length AR (1). The conclusion was drawn when β-actin was used as the housekeeping gene. However, we have since found that β-actin is ill-suited for this purpose since its transcript level was affected by BBR (data not shown). We decided to re-examine and compare the effects of BBR on the transcript levels of full-length AR (AR-FL) and AR-V7. We chose ribosome protein L30 (RPL30), which has been identified as one of the most stably expressed gene (2), to normalize the gene expression data in this analysis. 22Rv1 cells were treated with 100 μM BBR and for up to 24 h and transcript levels of AR-FL and AR-V7 were analyzed by qRT-PCR. As shown in Fig. 1, both AR and AR-V7 mRNAs were reduced by BBR, starting at the 4 h time point. The suppression became more significant as a function of time. Interestingly, the change of AR-V7 mRNA paralleled that of AR in this experiment. This observation is supported by a recent publication by Liu et al, showing that AR-V7 transcript levels were highly correlated with those of AR-FL (3). The authors concluded that the splicing of AR-V7 RNA is coupled to the transcription rate of the AR gene. Based on these results, we conclude that BBR inhibits AR transcription and thereby decreases AR-FL and AR-V7 to similar magnitudes.

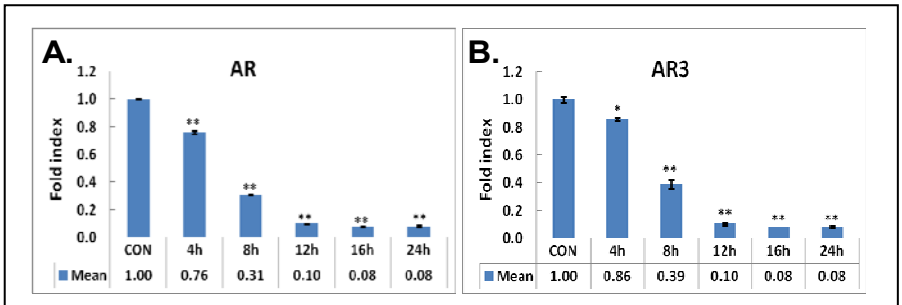

Fig. 1. BBR decreases mRNA levels of AR-FL (A) and AR-V7/AR3 (B). 22Rv1 cells were cultured in RPMI 1640 supplemented with 10% FBS and treated with 100 μM BBR for various durations. The transcripts were measured by qRT-PCR, with RPL30 as the housekeeping gene. The results were averaged from three independent experiments, and presented as mean ± standard deviation (SD). *, $P<0.05$; **, $P<0.01$.

2.1.2 BBR does not induce the degradation of AR splice variants. We have previously shown that BBR decreases the half-life of AR-FL (1). To determine if BBR exerts a similar effect on the splice variants, 22Rv1 cells were pretreated with cycloheximide to stop protein synthesis and then treated with BBR. Cells were lysed at different intervals for Western blotting analysis, using antibodies recognize all isoforms (AR and ΔAR) or AR-V7 only. Normalized AR protein levels were analyzed by linear regression to determine the half-life. The results are shown in Fig. 2. The half-life of AR-FL was estimated to be ~18 hr, and it was decreased by BBR treatment (Fig. 2 B&E). This is consistent with our previous data from LNCaP cells. However, the splice variants (ΔAR) were much less stable than AR, with a much shorter half-life than that of AR-FL (Fig. 2 C&E). Surprisingly, BBR treatment had little effect on the degradation of the splice variants. These results were confirmed by using an antibody specific for AR-V7 (Fig. 2 D &E). Similar results were obtained from LNCaP95 cells (data not shown).

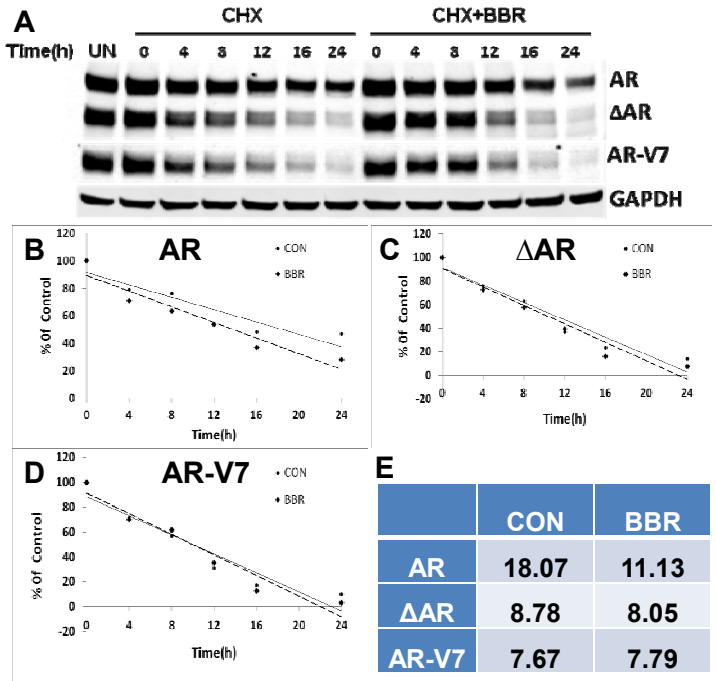

E

	CON	BBR
AR	18.07	11.13
ΔAR	8.78	8.05
AR-V7	7.67	7.79

Fig. 2. Berberine does not induce the degradation of AR splice variants. 22Rv1 cells were treated with 50 μg/mL cycloheximide (CHX) for 30 minutes and then with 100 μM BBR. **A**, Western analysis of cell lysates obtained at different intervals. **B-D**, normalized AR protein levels were analyzed by linear regression. **E**, half-life (hr) of AR proteins calculated from B-D.

2.1.3 BBR induces AR ploy-ubiquitinatin. To determine the effect of BBR on AR poly-ubiquitination, we performed an *in vivo* ubiquitination assay. As shown in Fig. 3, BBR markedly increased the intensity of ubiquitinated-AR in the presence of the proteasome inhibitor MG-132.

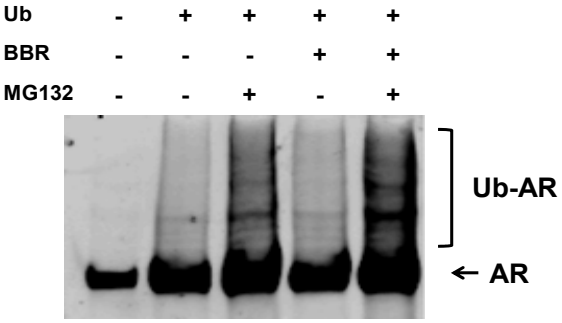

Fig 3. BBR induces AR poly-ubiquitination. LNCaP cells were transfected with plasmids encoding AR and his-tagged ubiquitin. Forty-eight hours after transfection, cells were treated with 100 μM BBR for 8h, then with 10 μM MG132 for 4 h. Following His-tag pulldown using Ni-NTA magnetic agarose beads, ubiquitinated proteins were detected by Western blot using an anti-AR antibody.

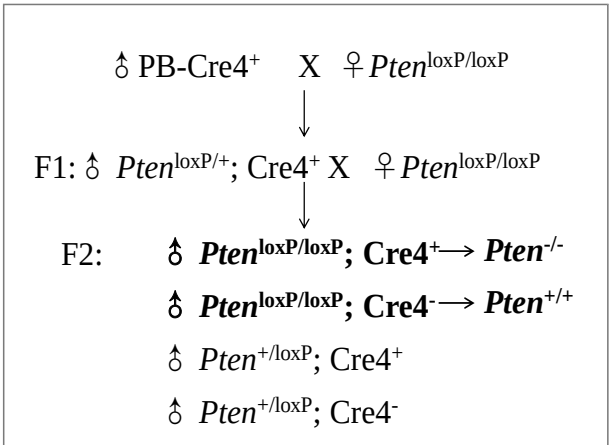

Fig. 4. Breeding scheme to generate *Pten* knockout and wild-type mice. Genotyping was done by PCR using Cre- and Pten-specific primers.

This result suggested that BBR-induced AR degradation is mediated through the ubiquitin-proteasome pathway.

2.2 Task 2. To evaluate the in vivo efficacy of berberine against prostate cancer growth in Pten knockout mice.

2.2.1 BBR inhibits prostate cancer growth in Pten knockout mice. Conditional Pten-KO mice were generated in-house by crossing $PTEN^{loxP/loxP}$ mice with PB-Cre4 mice, wherein the Cre recombinase is under the control of a modified prostate-specific probasin promoter (see Breeding scheme, Fig. 4). Genotyping was performed by PCR using primers specific for Pten and Cre. Male F2 mice (Pten-/- and Pten+/+) were randomly assigned to control or BBR treatment group (n=6) at the age of 12 weeks and received vehicle (DMSO) or 5 mg/kg/day of BBR, respectively, through i.p. injection. The treatment continued for 9 weeks and body weight of the mice was measured weekly. At the end of experiment, animals were sacrificed by CO_2 inhalation. The genitourinary bloc (GU bloc), consisting of the prostate lobes, seminal vesicles, ampullary glands, bladder, proximal ductus deferens, and proximal urethra was excised *en bloc*. The weight of the GU bloc is proportional to the prostate weight, thus it is widely used to represent prostate tumor burden (4–6). As shown in Fig. 5, Pten knockout mice have a markedly higher GU bloc weight than the wild-type mice, suggesting the presence of prostate tumors. In Pten knockout mice, treatment with BBR significantly reduced the weight of GU blocs (P<0.001). In contrast, there is no difference between treatment and control groups in wild-type mice. These results show that BBR inhibits prostate cancer growth without affecting the normal prostate. This result is consistent with our observation from the xenograft study, suggesting that the inhibitory action of BBR may be specific to the malignant tissue (1).

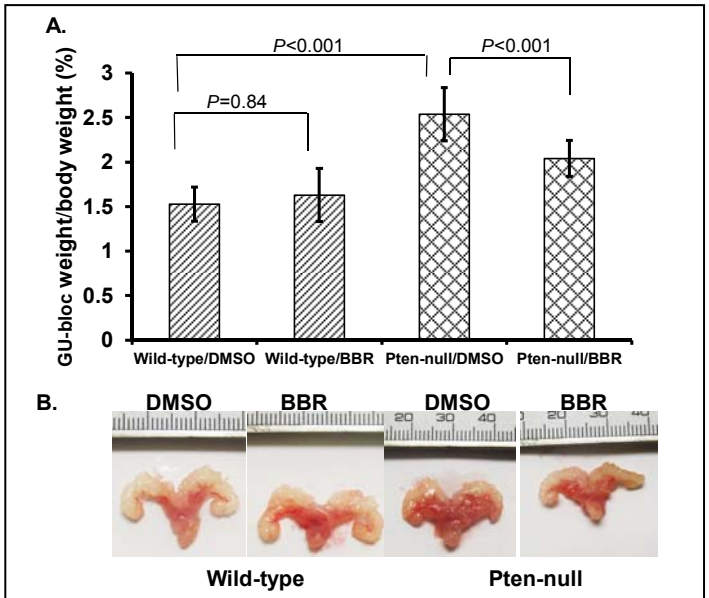

Fig. 5. Berberine treatment decreased prostate cancer growth in Pten knockout mice. A. The weight of the GU-bloc is normalized by body weight and presented as mean±standard deviation, n=6. **B.** Representative photos of the GU bloc in each group.

2.2.2 BBR inhibits the expression of AR and AKT *in vivo*. Prostatic tissues obtained from aforementioned animal experiment were analyzed by immunohistochemistry (IHC) staining for the expression of AR, total and phosphorylated AKT (serine 308 and 473), as previously described (1). The staining intensity was scored as high, medium, and low, and cells in each category were counted. While having no effect on the distribution of cells in wild-type mice (Fig. 6A), BBR treatment significantly lowered the cell population with high AR staining, and

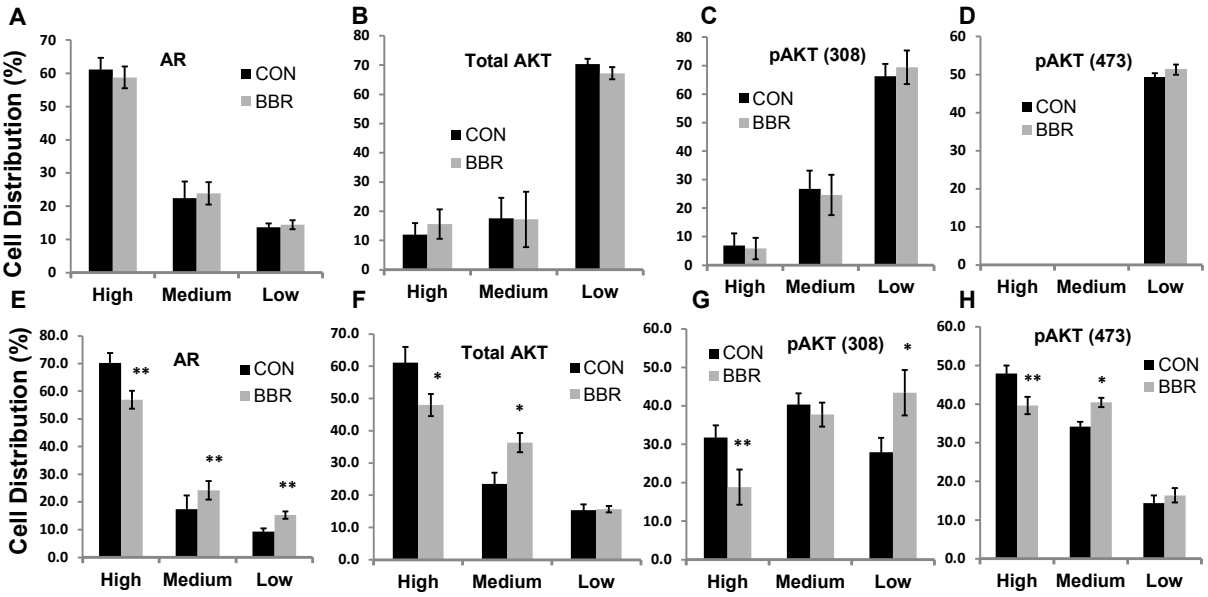

Fig. 6. IHC staining for AR and AKT expression in prostatic tissues. A-D, tissues from Pten wild-type mice. **E-H**, tissues from Pten knockout mice. Image analysis was performed by the NIH Image J software. The staining intensity in each cell was scored as high, medium, and low. The results were presented as percentage of cells in each category. *, $P<0.05$; **, $P<0.01$.

increased those with medium or low staining for AR in PTEN-null mice (Fig. 6E). Similar observations were made for total AKT (Fig. 6, B vs F), pAKT308 (Fig. 6, C vs G), and pAKT (Fig. 6, D vs H). In summary, the IHC data showed BBR suppresses both the AR and the AKT pathways simultaneously. The selectivity of BBR in AR and AKT inhibition in cancerous tissues is consistent with the tumor growth data.

2.2.3. Mono-targeting of AKT is ineffective to block prostate cancer development in Pten-null mice. To evaluate the benefit of dual-targeting of AR and AKT by BBR, we tested the efficacy of BEZ235, a PI3K and mTORC1/2 dual inhibitor which inhibits AKT phosphorylation by PDK1 and mTORC2 (7), in the Pten-null model. The experimental design is similar to that described above. Vehicle (10% 1-methyl-2-pyrrolidone/ 90% PEG 400) or BEZ235 (45 mg/kg) was given daily to mice through oral gavage and continued for 9 weeks. As shown in Fig. 7, little or no difference in GU bloc weight was found between the control and BEZ235 groups. The ineffectiveness of BEZ235 is not due to a loss of potency of the compound, as IHC staining clearly demonstrated that BEZ235 reduced AKT phosphorylation in prostatic tissues (Fig. 8, B&E). Instead, we postulated that inhibition of AKT by BEZ235 treatment led to induction of AR expression, based on the reciprocal inhibition between AR and

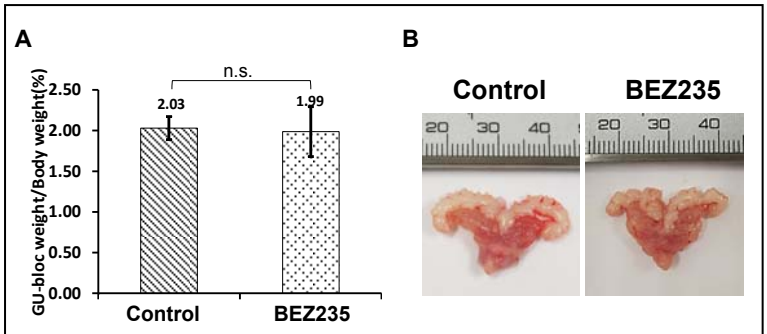

Fig. 7. BEZ235 is ineffective in blocking prostate cancer development in Pten KO mice. A, The weight of the GU-bloc is normalized by body weight and presented as mean ± standard deviation, n=6. **B,** Representative photos of the GU bloc in each group.

AKT. Indeed, IHC analysis showed an increase of AR staining in these tissues (Fig. 8 C&F). These results suggest that suppression of the AKT pathway by BEZ235 is negated by a compensatory AR induction in prostatic cells. By comparing the efficacies of BBR and BEZ235, we conclude that it is necessary to inhibit both AR and AKT pathways, at least in this Pten-null model of prostate cancer.

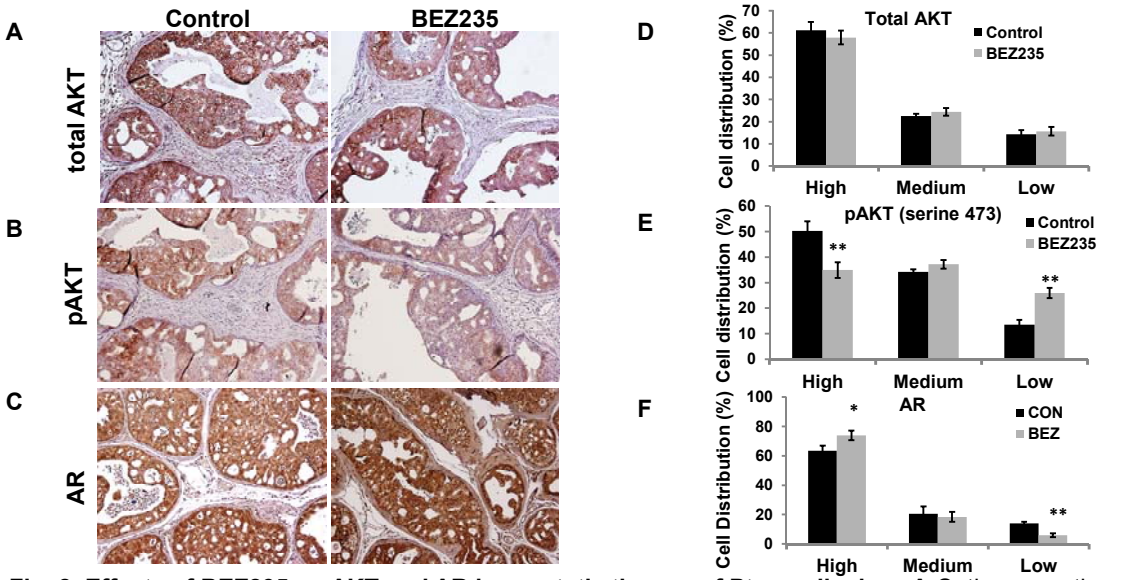

Fig. 8. Effects of BEZ235 on AKT and AR in prostatic tissues of Pten null mice. **A-C**, tissue sections were stained with antibodies for of total, phosphorylated AKT (serine 473), and AR, respectively. **D-F**, quantitation of the IHC staining results. The intensity was scored as high, medium or low, and the results are presented as percentage of cell population in each category.

2.2.4 BBR inhibits castration-resistant progression of Pten-null prostate cancer. Pten-null mice were castrated at 12 weeks of age and randomly assigned to control and treatment groups (n=9) and received vehicle (DMSO) or 5 mg/kg/day of BBR, respectively, through i.p. injection. The treatment continued for 20 weeks and animals were sacrificed at the end of 32 weeks. As shown in Fig. 9, BBR treatment significantly lowered the weight of the GU bloc. IHC analysis showed BBR reduced the expression of AR and AKT in these tissues as well.

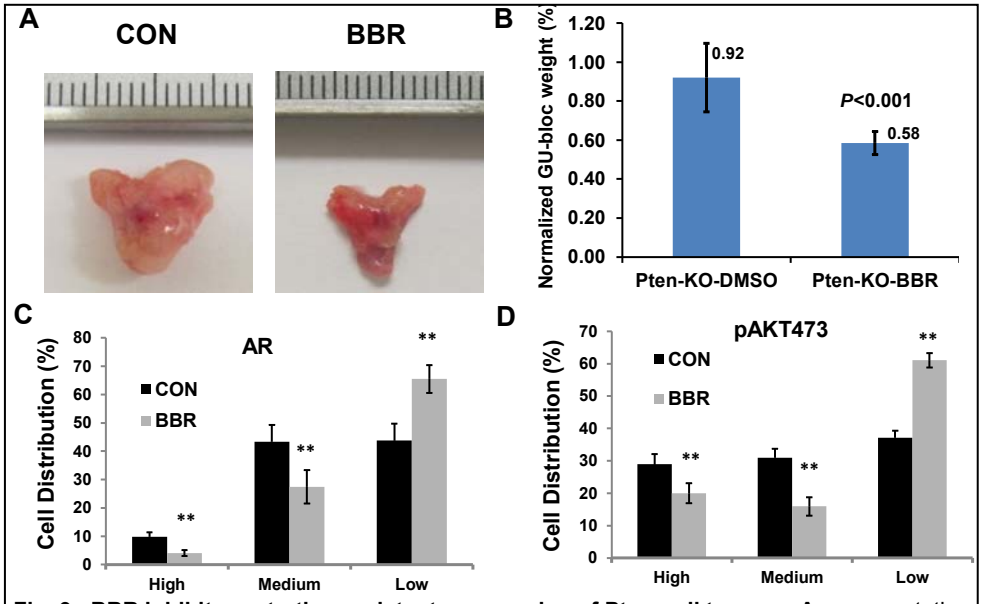

Fig. 9. BBR inhibits castration-resistant progression of Pten-null tumors. A, representative images of GU-bloc. **B**, normalized GU bloc weight. The results are presented as mean ± S.D. **C& D**, quantitation of IHC staining for AR and pAKT, respectively. *, *P*<0.05; **, *P*<0.01.

These results suggest BBR is effective in blocking castration-resistance progression following androgen deprivation.

2.2.5 BBR has low toxicity in mice. The dose of BBR used in this study appears to be well tolerated: no signs of stress were observed in mice in both experiments (2.2.1 & 2.2.4). Body weight was measured in intact mice (2.1) and no difference was detected between treatment and control groups (Fig. 10 A&B). In addition, no difference was found in the weights of various organs, including liver, heart, lung, spleen, kidney, and testis among different groups (Fig. 10C). These results suggest BBR has a low toxicity profile.

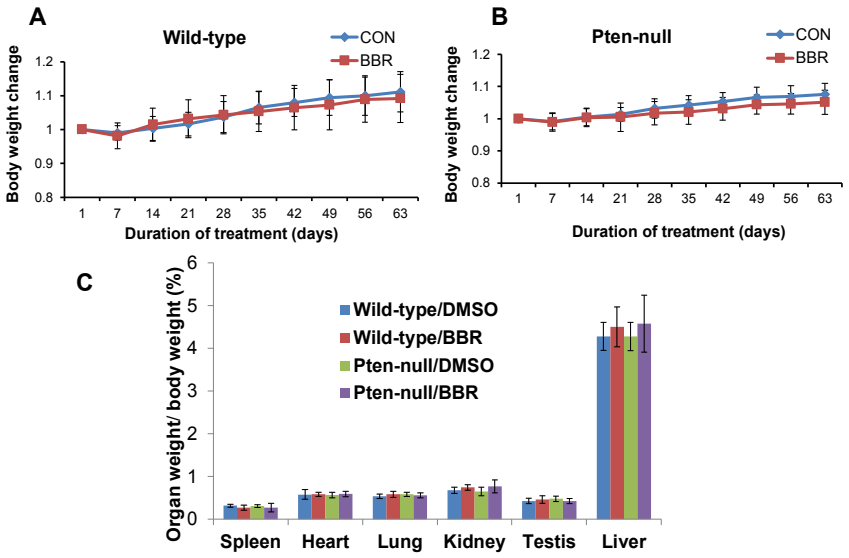

Fig. 10. Toxicity evaluation of berberine. **A** and **B**, change of body weight during the course of the experiment in wild-type and Pten-null mice, respectively. Body weight is expressed as fold of initial body weight. **C.** weight of various organs normalized by body weight and presented as mean± SD.

2.3 Task 3. To evaluate the *in vivo* efficacy of berberine against AR-FL- or AR-V-promoted CRPC growth.

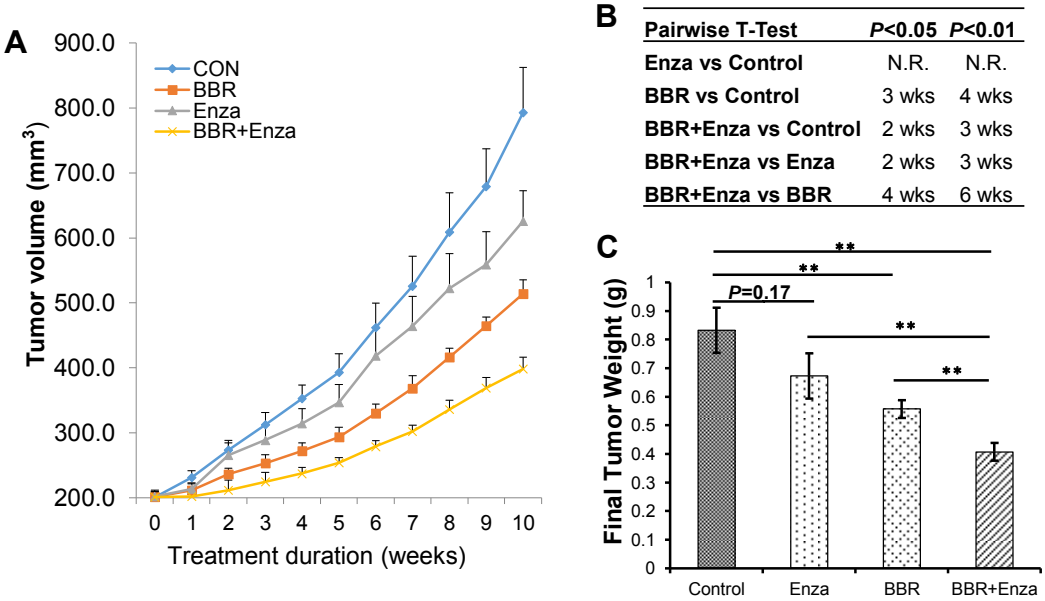

Fig. 11. BBR inhibits the growth of AR^{v567es}–expressing tumors and sensitizes them to enzalutamide. LuCaP86.2 xenografts were established in castrated SCID mice and treated with vehicle, enzalutamide (Enza), BBR, or BBR+Enza, for 10 weeks. **A**, tumor growth curves during the treatment duration. Tumor volumes are presented as mean ± SEM (n=7). **B**, the tumor growth data were analyzed by pairwise T-test and the results indicate the time points at which the significance levels were reached. N.R., not reached. **C**, final tumor weight. **, *P*<0.01.

2.3.1 BBR inhibits the growth LuCaP86.2 tumor xenografts and sensitizes them to enzalutamide treatment. LuCaP86.2 was chosen for this study because it expresses predominantly a constitutively active AR-V (AR^{v567es}), along with the AR-FL (8). The xenografts were maintained by serial passaging in castrated SCID mice. The tumors were cut into 25 mm^3 pieces and implanted subcutaneously into castrated SCID mice at 8 weeks of age. When tumor size reaches 200 mm^3, mice were randomized to one of four groups and receive vehicle, enzalutamide (MDV3100) at 10 mg/kg/day, BBR at 5 mg/kg/day, or the combination of enzalutamide and BBR, respectively, through i.p. injection. The treatments continued for 10 weeks before the animals were sacrificed. As can be seen in Fig. 11, the antiandrogen enzalutamide did not significantly change the growth of AR^{v567es}–driven LuCaP86.2 tumors throughout this treatment period. This is expected since AR^{v567es} lacks the ligand-binding domain and therefore escapes the action of the enzalutamide. In contrast, BBR treatment significantly reduced the growth of LuCaP86.2 xenografts. Interestingly, the combination of enzalutamide and BBR was more effective than BBR alone. The tumor growth data were confirmed by the final tumor weights (Fig. 11C).

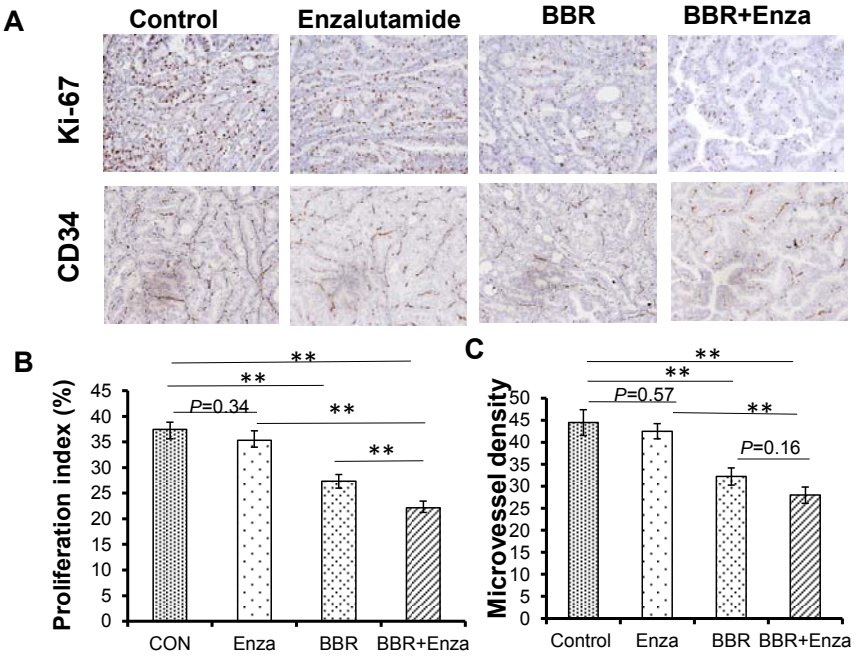

Fig. 12. BBR and BBR+Enza combination inhibit cell proliferation and angiogenesis in LuCaP86.2 tumor xenografts. A, Sections from LuCaP86.2 xenografts were stained for Ki-67 (cell proliferation) and CD34 (blood vessel). **B**, the proliferation index is the percentage of Ki-67+ cells. **C**, Microvessel density was obtained by counting the number of stained blood vessels. **, $P<0.01$.

To further understand the inhibitory effects on tumor growth, sections of the LuCaP86.2 tumors were stained for the cell proliferation marker Ki-67 and the endothelial marker CD34. As can be seen in Fig. 2, BBR treatment reduced Ki-67 staining and microvessel density, suggesting the growth inhibitory effect is mediated by inhibition of cell proliferation and angiogenesis. Once again, the combination of BBR and enzalutamide was more effective than either agent alone.

Taken together, the above data suggest BBR not only is effective against tumor growth driven predominantly by a constitutively active AR-V, but also could boost the therapeutic efficacy of enzalutamide in these tumors.

2.4 Additional tasks (not included in original SOW)

2.4.1 BBR induces proteasome-dependent AKT degradation. To understand the mechanism of AKT downregulation, LNCaP cells were treated with cycloheximide and then with 100 μM BBR, the modulation of AKT mRNA was assessed by qRT-PCR. The results show that BBR decreased the AKT transcript, but the decrease was small and not evident until the 50 μM dose was used (Fig. 13A). On the other hand, the half-life of AKT was reduced from 37.3 h to 24.6 h (Fig. 13B). These results suggest BBR downregulates AKT mainly through inducing protein degradation. To test the involvement of the proteasome pathway, LNCaP cells were treated with 100 μM BBR for 8 h. The proteasome inhibitor MG132 was added for the last 4 hours of treatment. The protocol was designed as such because co-treatment of MG132 and BBR for more than 4 h caused significant cytotoxicity. As shown in Fig. 13C, the presence of MG132 attenuated AKT degradation (lane 5 vs lane 4), suggesting that BBR induces AKT degradation through a proteasome-dependent pathway.

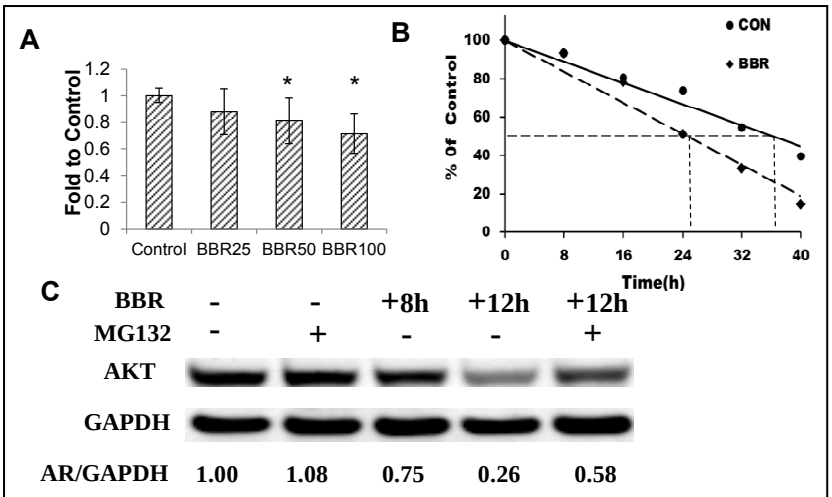

Fig. 13. BBR induces proteasome-dependent AKT degradation. **A,** LNCaP cells were treated with BBR at the indicated concentrations for 24 h. qRT-PCR was performed to determine the AKT mRNA level using a relative quantitation protocol and RPL30 was used as the housekeeping gene. *, $P<0.05$. **B**, LNCaP cells were pretreated with protein synthesis inhibitor cyclohexamide and then with 100 uM BBR for various durations. The levels of AKT protein were expressed as % of baseline and plotted to determine the half-life. **C**, effect of the proteasome inhibitor MG132 on berberine-induced AKT degradation. LNCaP was treated with 100 μM BBR for 8 h before MG-132 was added for another 4 h.

To corroborate the above result, we conducted *in vivo* ubiquitination assay. As shown in Fig. 14, BBR markedly increased the intensity of polyubiquitinated AKT in the presence of the proteasome inhibitor MG-132. This result suggested that BBR-induced AKT degradation is mediated through the ubiquitin-proteasome pathway.

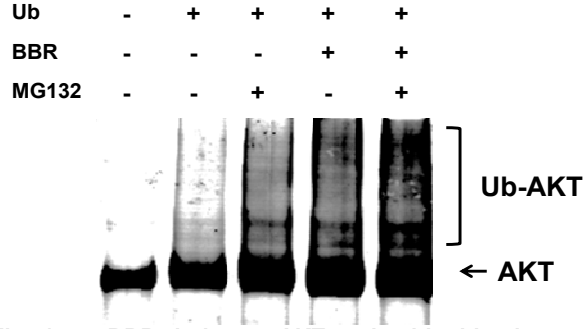

Fig 14. BBR induces AKT poly-ubiquitination. LNCaP cells were transfected with a plasmid encoding his-tagged ubiquitin. Forty-eight hours after transfection, cells were treated with 100 μM BBR for 8h, then with 10 μM MG-132 for 4 h. Following His-tag pulldown using Ni-NTA magnetic agarose beads, ubiquitinated proteins were detected by Western blot using an antibody recognizes AKT.

2.4.2 BBR blocks steroidogenesis by inhibiting AKR1C3 activity. Recent studies have demonstrated that prostate cancer cells acquired the ability of producing androgens from cholesterol or adrenal androgens in the absence of circulating androgens. Intratumoral steroidogenesis enables prostate cancer to evolve from an endocrine disease to an autocrine/paracrine one. AKR1C3 (Aldo-Keto Reductase Family 1, Member C3) is a key enzyme in steroidogenesis, catalyzing the conversion of weak androgens androstenedione and 5α-androstanedione to the highly active testosterone (T) and dihydrotestosterone (Fig. 15A, ref. 9), We have previously observed that BBR inhibits the growth of 22RV1 cells, and the inhibitory effect was attenuated with the addition of androstenedione to the culture medium (Fig. 15B). Western blot analysis showed that AKR1C3 is expressed in several prostate cancer cell line, and the expression level was highest in 22RV1 (Fig. 15C).

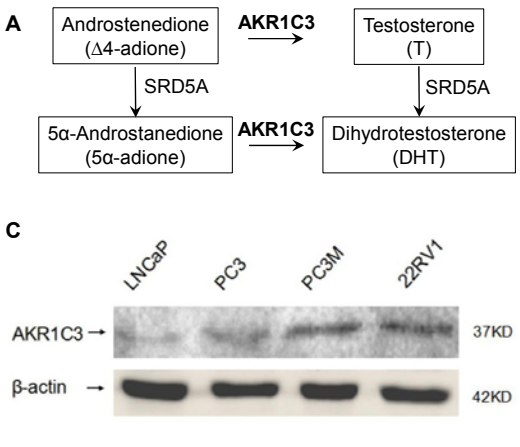

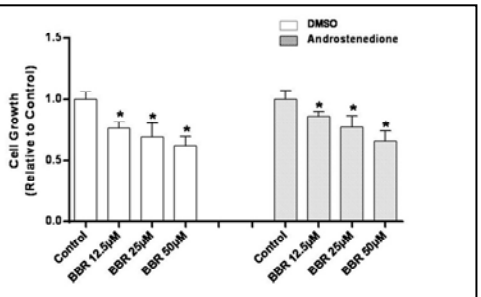

Fig. 15. **A**, conversion of androstenedione and 5α-androstenedione to T and DHT, respectively, by AKR1C3. T can be further reduced to DHT by 5α-reductase (SRD5A). **B**, effect of BBR on 22RV1 cell proliferation by MTT assay. Cells were treated with BBR in the presence or absence of 0.1 μM androstenedione for 48 h. * P< 0.05 vs control. **C**, Western blot analysis showed AKR1C3 is expressed in prostate cancer cells including 22RV1.

To explore whether BBR influenced androgen synthesis, T production was measured in 22RV1 conditioned medium following treatment with BBR, finasteride, and indomethacin (INN) for 48 h. Finasteride is an inhibitor for 5α-reductase; it is expected to increase T concentration due to the blockade of T to DHT and Δ4-adione to 5α-adione conversions (Fig. 15A).

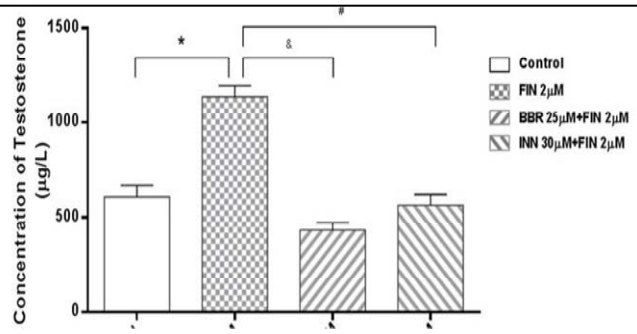

Fig. 16. **Berberine inhibits testosterone production by 22RV1**. Cells were cultured in medium containing 0.1 μM androstendione and treated for 48 h. Testosterone concentration in conditioned medium was determined by chemiluminesence immunoassay. Finasteride (FIN) is used to block the conversion of T to DHT. Indomethacin (INN), an inhibitor for AKR1C3, was included as a positive control. *, #, and &: P< 0.05, compared with the control.

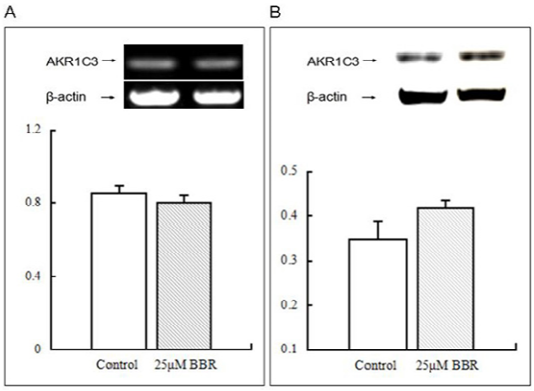

Fig. 17. **BBR does not inhibit AKR1C3 expression**. Following treatment with 25 μM BBR for 48 h, the expression of AKR1C3 in 22RV1 cells was measured by RT-PCR (**A**) and Western blot (**B**).

Indomethacin (INN) is an inhibitor for AKR1C3 and was included as a positive control. As shown in Fig 16, treatment with BBR significantly decreased testosterone concentration in the conditioned medium. This result suggests BBR inhibits the expression and/or the activity of AKR1C3.

To investigate the effect of BBR on AKR1C3 expression, RT-PCR and Western blot analysis were carried out in 22RV1 cells treated with 25 μM of BBR for 48 h. The results showed that neither the mRNA nor the protein level was decreased by BBR treatment (Fig 17). Furthermore, we performed AKR1C3 activity assay using Δ4-adione as the substrate and INN as a positive control. As shown in Fig. 18, both BBR and INN displayed potent inhibitory effects on the activity of recombinant human AKR1C3. The estimated IC50 for BBR and INN were 4.08 μM (95% CI: 3.47-4.69) and 7.26 μM (95% CI: 6.82-7.70), respectively. The lower IC50 for BBR suggests it is a more potent inhibitor than INN.

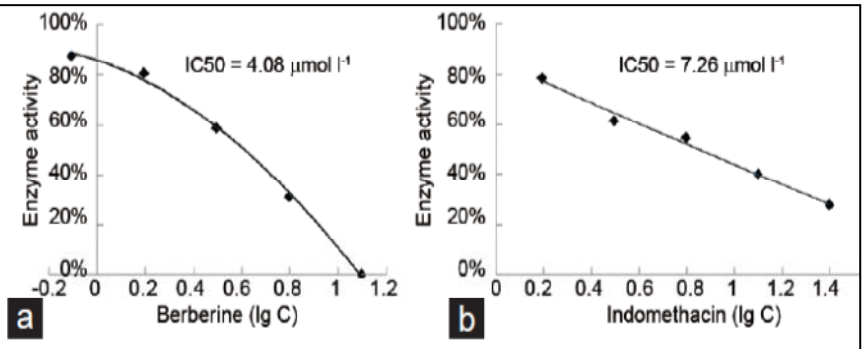

Fig. 18. **Berberine inhibits the activity of AKR1C3.** Recombinant human AKR1C3 was used in an *in vitro* activity assay. The results were plotted for BBR (a) and INN (b).

We next performed molecular docking analysis with AutoDock to better understanding the molecular mechanism of BBR on AKR1C3. The analysis revealed that BBR could enter the steroid binding pocket of AKR1C3 and form π-π interactions with residues Phe306 and Phe311 (Figure 19 Ic). Similarly, INN is capable of interacting with the pocket. By using the Discovery Studio (DS) 3.5 Visualizer software, the free energy of binding was estimated from the most stable conformation. The binding energies of BBR and INN were −9.63 and −9.79 kcal mol−1, respectively. These results provided an explanation of the inhibitory effects of BBR on AKR1C3 activity.

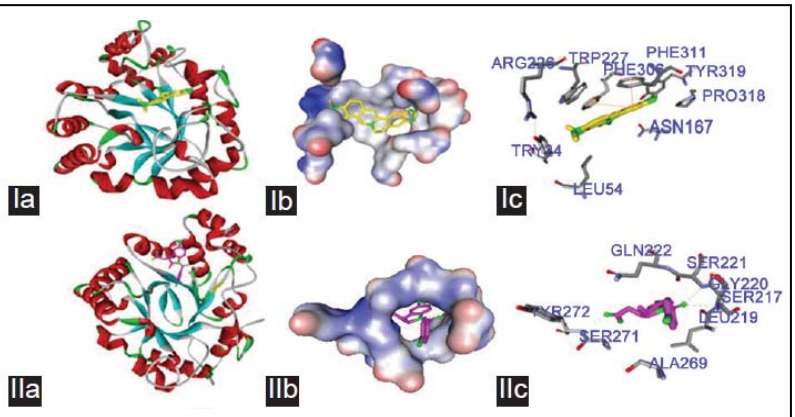

Fig. 19. **Molecular docking analysis of BBR (I) and INN (II) with AKR1C3.** BBR is shown in yellow and INN in purple. (a) The optimized 3D structure of AKR1C3 with a ligand. (b) Surface view of a ligand in the active center of AKR1C3. (c) Ligand binding residues of AKR1C3. Hydrogen bonds (green dash lines) and π-π interactions (yellow solid lines) formed between the ligand and the active center of AKR1C3 were shown.

In summary, these experiments have broadened our knowledge with regard to the molecular mechanisms of the inhibitory effects of BBR in prostate cancer. The potent inhibition

of AKR1C3 activity by BBR suggests a new dimension of drug development using BBR as the lead compound.

3. Key Research Accomplishments

- We have established that BBR downregulates full-length AR by inhibiting AR transcription and inducing AR degradation via the ubiquitin-proteasome pathway. In contrast, BBR downregulates AR splice variants mainly through inhibiting AR transcription, which in turn affects alternative splicing.
- BBR inhibits AKT expression through inducing AKT degradation.
- We have demonstrated BBR inhibits prostate cancer development and progression in Pten knockout mice, with simultaneous downregulation of AR and AKT. In contrast, mono-targeting AKT by BEZ235 failed to thwart cancer development, suggest it is necessary to target both AR and AKT.
- By using the LuCaP86.2 xenograft model, we have demonstrated that BBR is effective against tumor growth driven by a constitutively active AR-V, AR^{v567es}. In addition, BBR sensitizes these tumors to enzalutamide.
- In addition to its inhibition on AR, BBR also blocks testosterone synthesis from weak androgens by inhibiting the enzymatic activity of AKR1C3.

4. Reportable Outcomes

4.1 Manuscripts

1) Alison Egan, Yan Dong, Haitao Zhang, Yanfeng Qi, Steven P. Balk, Oliver Sartor. (2013). Castration-Resistant Prostate Cancer: Adaptive Responses in the Androgen Axis. Cancer Treatment Reviews 40:426-433.
2) Haitao Zhang*, Yang Zhan, Xichun Liu, Yanfeng Qi, Guanyi Zhang, Oliver Sartor, Yan Dong. (2013). Splicing variants of androgen receptor in prostate cancer. Am J Clin Exp Urol 2013;1(1):18-24.
3) Bo Cao, Yanfeng Qi, Guanyi Zhang, Duo Xu, Yang Zhan, Xavier Alvarez, Zhiyong Guo, Xueqi Fu, Stephen R. Plymate, Oliver Sartor, Haitao Zhang*, and Yan Dong. (2014). Androgen receptor splice variants activating the full-length receptor in mediating resistance to androgen-directed therapy. Oncotarget 2014. Mar 30;5(6):1646-56.
4) Guanyi Zhang, Xichun Liu, Jianzhuo Li, Elisa Ledet, Xavier Alvarez, Yanfeng Qi, Xueqi Fu, Oliver Sartor, Yan Dong, and Haitao Zhang*. Androgen Receptor Splice Variants Circumvent AR Blockade by Microtubule-Targeting Agents. Oncotarget 2015 Sep 15;6(27):23358-71.
5) Duo Xu, Yang Zhan, Yanfeng Qi, Bo Cao, Shanshan Bai, Wei Xu, Sanjiv Gambhir, Peng Lee, Oliver Sartor, Erik Flemington, Haitao Zhang, Chang-Deng Hu, and Yan Dong. Androgen receptor splice variants dimerize to transactivate target genes. Cancer Research 2015 Sep 1;75(17):3663-71.

6) Tian Y, Zhao L, Wang Y, Zhang H, Xu D, Zhao X, Li Y, Li J. Berberine inhibits androgen synthesis by interaction with aldo-keto reductase 1C3 in 22Rv1 prostate cancer cells. Asian J Androl. (2016) 18, 607–612.
7) Xichun Liu, Jing Li, Qiuyang Zhang, Bo Cao, Yanfeng Qi, Zhenggang Xiong, Sudesh Srivastav, Zongbing You, and Haitao Zhang. Co-targeting AR and AKT by berberine in castration-resistant prostate cancer. Manuscript in preparation.

4.2 Funding

07/01/14-06/30/18 American Cancer Society Research Scholar Grant (125766-RSG-14-016-01-CCE)
Title: Cotargeting AR and AKT by Berberine in Castration-resistant Prostate Cancer
Objective: This project will establish the functional significance of the simultaneous downregulation of AR and Akt by berberine and to further understand the underlying mechanisms.
Role: Principal Investigator

07/01/14-06/30/17 DOD Prostate Cancer Research Program Idea Development Award (W81XWH-14-1-0480, log#PC130570)
Title: *Androgen receptor splice variants and resistance to taxane chemotherapy*
Objective: This project is to establish the role of AR splice variants in the resistance to taxane-based chemotherapy and to delineate the underlying mechanism.
Role: Principle Investigator

5. Conclusion

By using a Pten conditional knockout mouse model of prostate cancer, we have demonstrated that berberine is effective in blocking the development and castration-resistant progression of prostate cancer. These effects of berberine seem to be confined to the cancerous tissues, as normal prostates and other tissues are not affected. These results support the use of berberine as a chemoprevention agent targeting the development and progression of prostate cancer. Additionally, we have demonstrated that berberine inhibits the growth of castration-resistant xenografts driven by a constitutively active AR splice variant, and that berberine sensitizes AR-V-expressing tumors to enzalutamide treatment. These results suggest berberine is effective in the treatment of advanced prostate cancer, particularly in overcoming therapeutic resistance mediated by AR-Vs. Finally, we have shown berberine interferes with testosterone synthesis by inhibiting AKR1C3 activity, pointing to a new direction of pharmacological development using berberine as the lead compound.

6. References

1. Li J, Cao B, Liu X, Fu X, Xiong Z, Chen L, et al. Berberine suppresses androgen receptor signaling in prostate cancer. Mol Cancer Ther. 2011;10:1346–56.

2. de Jonge HJM, Fehrmann RSN, de Bont ESJM, Hofstra RMW, Gerbens F, Kamps WA, et al. Evidence Based Selection of Housekeeping Genes. PLoS ONE. 2007;2:e898.

3. Liu LL, Xie N, Sun S, Plymate S, Mostaghel E, Dong X. Mechanisms of the androgen receptor splicing in prostate cancer cells. Oncogene. 2013;

4. Gupta S, Ahmad N, Marengo SR, MacLennan GT, Greenberg NM, Mukhtar H. Chemoprevention of prostate carcinogenesis by alpha-difluoromethylornithine in TRAMP mice. Cancer Res. 2000;60:5125–33.

5. Chung AC-K, Zhou S, Liao L, Tien JC-Y, Greenberg NM, Xu J. Genetic ablation of the amplified-in-breast cancer 1 inhibits spontaneous prostate cancer progression in mice. Cancer Res. 2007;67:5965–75.

6. Zhang Q, Liu S, Ge D, Zhang Q, Xue Y, Xiong Z, et al. Interleulin-17 Promotes Formation and Growth of Prostate Adenocarcinoma in Mouse Models. Cancer Res. 2012;72:2589–99.

7. Serra V, Markman B, Scaltriti M, Eichhorn PJ, Valero V, Guzman M, et al. NVP-BEZ235, a dual PI3K/mTOR inhibitor, prevents PI3K signaling and inhibits the growth of cancer cells with activating PI3K mutations. Cancer Res. 2008;68:8022–30.

8. Sun S, Sprenger CC, Vessella RL, Haugk K, Soriano K, Mostaghel EA, et al. Castration resistance in human prostate cancer is conferred by a frequently occurring androgen receptor splice variant. JClinInvest. 2010;120:2715–30.

9. Adeniji AO, Chen M, Penning TM. AKR1C3 as a target in castrate resistant prostate cancer. J Steroid Biochem Mol Biol. 2013;137:136–49.

7. Appendices

The published papers listed under “Reportable outcome/Manuscripts” are attached.

Cancer Treatment Reviews 40 (2014) 426–433

Contents lists available at ScienceDirect

Cancer Treatment Reviews

journal homepage: www.elsevierhealth.com/journals/ctrv

Laboratory-Clinic Interface

Castration-resistant prostate cancer: Adaptive responses in the androgen axis

Alison Egan [a], Yan Dong [b,e,f], Haitao Zhang [c,e], Yanfeng Qi [b,e], Steven P. Balk [g], Oliver Sartor [a,d,e,*]

[a] Department of Medicine, Tulane University School of Medicine, New Orleans, LA 70112, USA
[b] Department of Structural and Cellular Biology, Tulane University School of Medicine, New Orleans, LA 70112, USA
[c] Department of Pathology and Laboratory Medicine, Tulane University School of Medicine, New Orleans, LA 70112, USA
[d] Department of Urology, Tulane University School of Medicine, New Orleans, LA 70112, USA
[e] Department of Tulane Cancer Center, Tulane University School of Medicine, New Orleans, LA 70112, USA
[f] National Engineering Laboratory for AIDS Vaccine, Department of Medicine, Beth Israel Deaconess Medical Center and Harvard Medical School, 330 Brookline Avenue, Boston, MA 02215, USA
[g] College of Life Sciences, Jilin University, China and Hematology–Oncology Division, Department of Medicine, Beth Israel Deaconess Medical Center and Harvard Medical School, 330 Brookline Avenue, Boston, MA 02215, USA

ARTICLE INFO

Article history:
Received 1 July 2013
Accepted 6 September 2013

Keywords:
Androgen receptor
Prostate cancer
Castrate-resistance
Adaptive signaling

ABSTRACT

The androgen signaling axis in prostate cancer is associated with multiple adaptive mechanisms in response to castration. Herein we review these adaptations with an emphasis on recent molecular insights into the growth and development of castration resistant prostate cancer (CRPC). Alterations include both conventional and novel intracrine androgen synthesis pathways and androgen transport as well as androgen receptor (AR) overexpression, mutation, and splice variation. Each of these underlying mechanisms are potentially linked to post-castration growth, especially after treatment with newer hormonal agents such as abiraterone and enzalutamide. Post-translational AR modifications are well documented and these can affect receptor activity, stability, localization, and interaction with other proteins. Changes in recruitment of androgen receptor associated co-activators/repressors and a distinct AR-induced transcriptional program can dramatically alter proliferation, invasion, and metastasis in a ligand and context-dependent manner. Numerous previously uncharacterized non-coding RNAs, some of which are androgen regulated, may also have important biological function in this disease. Taken together, the view of CRPC has changed dramatically in the last several years. This has occurred not only within the setting of multiple treatment paradigm changes, but also as a multiplicity of potential molecular mechanisms underlying this disease state have been explored and discovered.

Introduction

Prostate cancer is by far the most common non-skin cancer and currently the second leading cause of cancer death in men in the United States. Both normal and malignant prostate epithelial cells depend on androgen dependent activation of the androgen receptor (AR) for prostate-specific antigen (PSA) production and survival. Androgen deprivation therapy (ADT) via surgical or medical castration remains the standard form of treatment, and has been so for the last 70 years for clinically advanced prostate cancer [1]. Disease progression after initial ADT, despite castration levels of testosterone, is termed castrate resistant prostate cancer (CRPC). This may either be metastatic or non-metastatic and the natural history is distinct. For men with metastatic disease, castration resistance as measured by PSA rise develops approximately 16 months after initial ADT [2]. This is markedly distinct from those with no metastases. For patients who start ADT for PSA only progression, time to castration resistance is in part dependent on PSA doubling time, but has been reported to be as long as 10 years [3].

Many studies have found that AR is present in both initially diagnosed prostate cancer cells and in the vast majority of cells in prostates from CRPC patients [4]. PSA, a known AR target gene, will eventually rise in most CRPC patients, serving as a marker that the androgen axis is still functional despite low circulating levels of serum androgens. Multiple mechanisms have been proposed for the continued activation of AR and the development of CRPC. Molecular studies dissecting the androgen signaling pathways in CRPC are ongoing with multiple new insights in the last several years. This review covers a broad review of these potential mechanisms (see Table 1).

* Corresponding author at: Tulane Cancer Center, Tulane University School of Medicine, New Orleans, LA 70112, USA. Tel.: +1 504 988 7869; fax: +1 504 988 5059.
E-mail address: osartor@tulane.edu (O. Sartor).

0305-7372/$ - see front matter © 2013 Elsevier Ltd. All rights reserved.
http://dx.doi.org/10.1016/j.ctrv.2013.09.011

Table 1
Proposed mechanisms for continued AR signaling in CRPC.

Intracrine synthesis of androgens
Amplification and/or overexpression of AR
Overexpression and/or polymorphism of steroid transporters
Mutation of the AR gene
Constitutively-active AR splice variants
Alteration in AR co-regulators
Crosstalk between AR and other signaling pathways
Post-translational modifications of AR
Distinct AR mediated transcriptional programs

Androgen receptor: overview

AR is a member of the steroid receptor superfamily that acts predominately as a ligand-dependent transcription factor after binding to various DNA binding sites. The AR gene is located on the X-chromosome (Xq12), made up of 8 exons [5]. AR consists of an N-terminal domain (NTD) which contains a transactivation domain (AF1) that serves as a primary transcription regulatory region (see Fig. 1). The central DNA binding domain (DBD) contains two zinc fingers that connect to the hinge region allowing DNA recognition, dimerization, and stabilization. The DBD is highly homologous with the DBD of the human glucocorticoid receptor and the human progesterone receptor. The hinge region contains a canonical nuclear localization signal that regulates the nuclear import of the receptor. The hinge region is also a target site for acetylation, ubiquitination, and methylation [6]. The C-terminal domain (CTD) contains the ligand binding domain (LBD) and the AF2 domain, a second transcriptional regulation domain. The NTD and CTD both contain transactivation domains (AF1/AF2), but AF1 is considered dominant in most AR signaling studies conducted under normal physiological conditions. This is particularly relevant in the study of AR splice variants (vide infra).

After synthesis of AR protein, a variety of conformational changes are required to generate a receptor with high-ligand-binding affinity. This requires a complex cascade of events initiated by a "foldosome" that includes complex interactions of a variety of chaperone proteins including HSP40, HSP90, and HSP23 [7]. Upon ligand binding, further conformational changes of AR occur, leading to intra-receptor NTD/CTD interaction followed by translocation of the ligand-bound receptor to the nucleus and homodimerization. Various studies now distinguish nuclear and cytoplasmic AR in both clinical specimens and pharmacological responses, with the nuclear AR contributing to androgen-axis signaling via transcriptional regulation [8].

In the nucleus, the ligand-bound AR homodimers recruit various co-activators and co-repressors, bind to androgen-response elements (ARE), and lead to a broad program of transcriptional activation in AR target genes such as PSA and TMPRSS2. AR-regulated target genes can be both up- or down-regulated and can vary according to ligand concentration. AR target genes vary in cells derived from hormone sensitive cancer as compared to cells derived from CRPC.

Intracrine synthesis of androgens

CRPC tissue exhibits persistent levels of androgens, despite ADT, albeit some androgen levels are lower compared to hormone-naïve tissue [9,10]. Studies have shown the upregulation of steroidogenic enzymes in both model CRPC systems and in tissue from CRPC patients suggesting increased intratumoral synthesis of androgens [11]. In metastases of CRPC patients, relative to primary tumors, there is increased expression of a number of genes involved in androgen metabolism including HSD3B2 (3 beta-hydroxysteroid dehydrogenase), AKR1C3 (also known as 17 hydroxysteroid dehydrogenase type 5 or hydroxysteroid 17-beta-dehydrogenase 5), AKR1C2 (3α-hydroxysteroid dehydrogenase), AKR1C1 (20 alpha-hydroxysteroid dehydrogenase), SRD5A1 (5-alpha reductase type 1), and UGT2B15 (UDP-glucuronosyltransferase 2B15). Of note, AKR1C3 is involved in the conversion of androstenedione to testosterone; SRD5A1/2 converts testosterone to DHT (see Fig. 2). Other investigators have reported variations on this theme [12–14] but taken together, from a functional perspective, these changes are compatible with the over-arching hypothesis that CRPC cells can synthesize potent androgens from various steroidal precursors.

The conventional mechanisms of androgen synthesis are emphasized by many but alternative mechanisms of testosterone and DHT synthesis are also demonstrated in CRPC (see Fig. 2). Androstenedione may be 17-keto reduced to testosterone, and/or

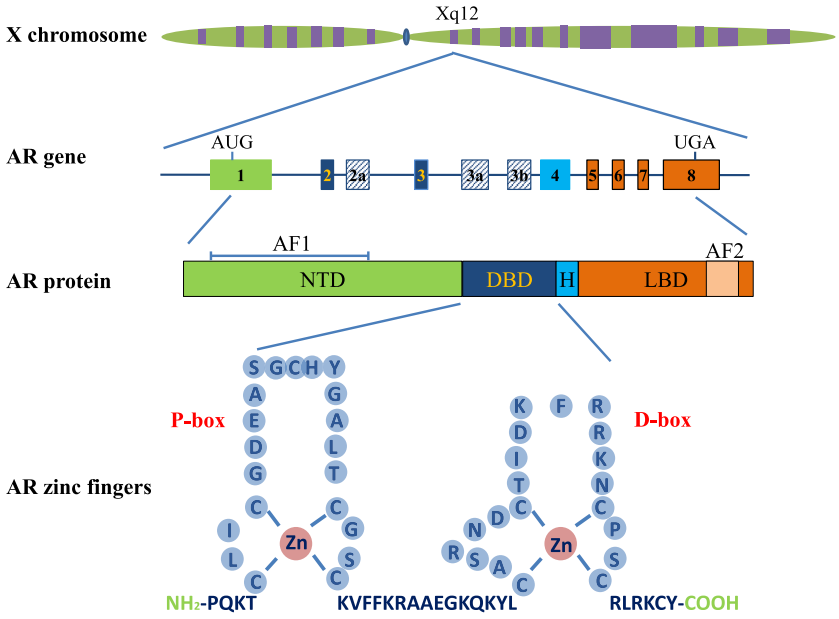

Fig. 1. Schematic representation of the structure of the AR gene, protein, and the two zinc fingers in AR DBD. H, hinge region; P-box mediates DNA recognition; D-box mediates AR DBD-dependent dimerization.

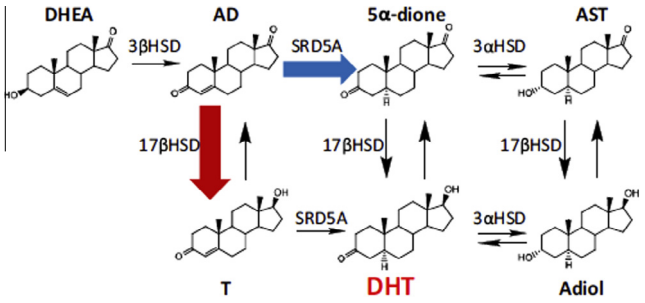

Fig. 2. Androstenedione (AD) can be converted to testosterone directly or it can be 5-alpha reduced to 5-alpha-dione. DHT (dihydrotestosterone) can then be synthesized directly (via 17-beta HSD) or indirectly as shown above. Other abbreviations include T (testosterone), DHT (dihydrotestosterone), DHEA (dehydroepiandrosterone), AD (androstenedione), AST (androsterone), 5α-dione (5α-androstenedione), and Adiol (5α-androstane-3α,17β-diol). Enzymes include 3αHSD or 3βHSD or 17βHSD (3α or 3β or 17β-hydroxysteroid dehydrogenases, respectively), or SRD5A (steroid-5α-reductase). Figure from K.H. Chang et al. [15].

5α reduced by to 5α-dione. In cell lines derived from CRPC patients, the reduction of androstenedione to 5α-dione occurs earlier and more rapidly than the 17-keto reduction to testosterone suggesting primary utilization of the pathway that synthesizes DHT from precursors other than testosterone. Assays in fresh tumor samples confirm the cell line findings [15]. The SRD5A1 enzyme is dominant over the SRD5A2 enzyme in this process [11,15]. 5α-Dione can be converted into DHT via two different mechanisms, either via the direct 17-keto reduction of 5α-dione by AKR1C3, or via conversion of 5α-dione to androsterone, and then conversion of 5α-androstane-3α,17β-diol to DHT. Interestingly in these experiments using CRPC cells, the dominant form of DHT synthesis does not appear to involve testosterone as precursor. "Back door" synthesis of DHT is also possible via 5α-reduction of either progesterone or 17α-hydroxy-progesterone [15]. These reductions are followed by a series of enzymatic conversions similar to the classic DHT steroidogenesis pathway except that conversion of testosterone to DHT is bypassed [15]. Whether or not the "back door" pathway is critical for CRPC development is not yet clear.

Steroid transporters

The efficiency of androgen transport has been shown to affect both efficacy of ADT and transition rate to CRPC. The solute carriers (SLCOs) are a complex family of genes that are involved in transport of organic molecules across cell membranes. The proteins derived from these genes are termed organic acid transporters (OATs). Several of these transporters, including those derived from the SLCO2B1 and SLCO1B3 genes, have significantly increased expression in metastatic CRPC tissues compared to primary cancers [16]. Certain single nucleotide polymorphism (SNP) variants of SLCO2B1 are associated with shorter responses to ADT (hence more rapid CRPC development). One of these SLCO2B1 risk SNPs is exonic, and two are intronic. There also appears to be a gene–gene interaction between the SLCO 2B1 SNPS in terms of time to progression post-ADT. Increasing the number of risk SNPs to 2 or more is associated with a shortened time to progression post-ADT compared to those with zero to one risk genotype [17]. There was an 18 month survival difference if 3 risk genotypes were present compared to none/one and a 12 month difference if 2 risk genotypes were present compared to none/one [17]. In a separate study of CRPC patients, individuals with SLCO1B3 334GG/699AA haplotype showed longer median survival and improved survival probability at 10 years than patients carrying TT/AA and TG/GA haplotypes [18].

The SLCO transporters are involved in various steroid hormonal uptakes in a complex fashion. SLCO2B1 is found in multiple tissues and is involved in transport of compounds including atorvastatin, DHEAS, and estrone-3 sulfate. One of the variants of SCLO2B1 associated with more rapid post-ADT progression is also associated with enhanced transport of dehydroepiandrosterone sulfate (DHEAS), increased AR expression, and increased PSA expression using an *in vitro* prostate cancer model [17]. SLCO1B3 is primarily found in liver and cancer cells and transports testosterone across membranes in a SNP dependent manner. One of the provocative aspects of the OATs is that they are potentially "druggable" targets. We note that atorvastatin strongly interacts with SLCO2B1 and that (hypothetically) this observation could have therapeutic implications.

AR overexpression

CRPC has been shown to express more AR than benign tissue and hormone naïve cancers [4,19]. Increased AR expression may sensitize the receptor to low levels of androgen [20]. Donovan et al. demonstrated that an increase in nuclear AR expression in advanced disease in either diagnostic biopsy or radical prostatectomy samples was associated with reduced time to prostate-cancer specific mortality [21].

One mechanism for AR protein overexpression is via AR genetic amplification, which has been reported in approximately 30% of CRPC cases [22]. An increase in AR mRNA levels without genomic amplification has also been well described [12]. A number of potential links between AR expression and other signaling pathways are postulated. AR signaling in normal prostate decreases AR gene transcription via lysine specific demethylase I recruitment and H3K4me1,2 demethylation of a specific enhancer in intron 2 of the AR gene [23,24]. Considerable data now suggest that "relief" from AR mediated repression of AR expression can increase AR mRNA in CRPC [23,24]. A link between retinoblastoma protein (RB1) loss and AR expression may be important as well. RB1 loss is frequently seen in transition to CRPC and is associated with poor clinical outcomes. By losing RB1, the transcription factor E2F1 is increased, driving AR overexpression via an increased transcription rate [25]. Micro-RNAs such as miR-let-7c may also serve as important regulator of AR expression. Down-regulation of Let-7c is inversely correlated with AR expression, whereas the expression of Lin28 (a repressor of let-7) is positively correlated [26]. These types of studies suggest potential new drug targets to decrease AR expression in selected patients.

AR mutations in CRPC

Loss-of-function, germline mutations of AR are frequently associated with androgen insensitivity syndrome but AR mutations in prostate cancer are almost exclusively somatic and often associated with gain-of-function [27]. In general, the frequency of AR mutation is lower in untreated, hormone-sensitive prostate cancer than in CRPC [28]. Employing exome sequencing, Grasso et al. [29] reported somatic AR mutations in 5 of 50 cases of lethal, heavily pre-treated CRPC, but none of 11 cases of untreated, localized prostate cancer.

The higher incidence of AR mutations in CRPC suggests an adaptive response and a "Darwinian" mutant-AR clonal selection in some cases [30,31]. This hypothesis is further supported by the observation that AR mutations are more frequent in patients treated with an anti-androgen/castration combination as compared to castration alone [31]. Mutations of the AR gene most frequently localize to exons that encode the LBD (~49%), followed by the N-terminal domain (~40%), the DBD (~7%), and the hinge domain

(2%). Mutations are rarely found in untranslated regions [27]. Mutations in the LBD could potentially affect the ligand specificity of AR, allowing it to be activated by non-androgenic steroids, or anti-androgens, in a promiscuous manner.

The T877A mutation, which has been described by multiple investigators, expands AR ligand binding to estrogen, progestin, selected corticosteroids, and selected anti-androgens [32]. Another mutation in the ligand-binding pocket, H874Y, was identified in CRPC patients treated with flutamide. This mutation also increases ligand promiscuity, allowing DHEA, estradiol, progesterone, and hydroxyflutamide to activate transcription in various model systems [33]. Mutations outside of the LBD could cause gain-of-function or loss-of-function of the receptor by influencing on nuclear localization, co-regulator binding, protein stability, and promoter selectivity [34]. Constitutively active mutants have been described in the regulatory NTD (G142V, M523V, G524D, and M537V) [35].

When certain steroid or steroid binding treatments are withdrawn (flutamide, bicalutamide, nilutamide, megestrol, cyproterone acetate, prednisone, or estramustine), there is potential for improvement in PSA and/or other parameters of disease progression [36]. Whether or not mutated AR is responsible for these withdrawal responses is not clear but laboratory-based experiments clearly uphold the feasibility of such a hypothesis.

Taken together, AR mutations in CRPC potentially allow for continued ligand dependent activation of AR by creating promiscuous ligand binding, altered binding of co-regulators, and/or alterations in genomic regulatory element binding. More studies are needed to assess the clinical impact of these mutations on disease progression. Better categorization of these mutants in patients may provide a greater degree of personalization of therapeutic selection.

AR splice variants

A large number of AR splice variants (AR-Vs) have been recently identified and characterized in CRPC patients (see Fig. 3). These variants have insertions of cryptic exons downstream of the sequences encoding the DBD or deletions of the exons encoding the AR-LBD, resulting in a disrupted AR open reading frame and the expression of truncated AR-V proteins devoid of the functional LBD [37–42]. The majority of the AR-Vs identified to date displays constitutive activity. Two major AR-Vs, AR-V7 (also named as AR3) and ARv567es, have been shown to be capable of regulating target gene expression in the absence of the full-length AR (AR-FL) signaling. Profiling of gene expression changes after knockdown or ectopic expression of AR-V7 or ARv567es suggests that AR-Vs and AR-FL regulate an overlapping yet distinctive set of target genes [43–45]. These studies are rapidly evolving and significant differences in the AR-V transcriptome have been identified in different studies, possibly due to the use of different model systems.

AR-Vs are prevalently upregulated in CRPC compared to hormone-naïve cancers, and can emerge as an adaptive response to therapies targeting the androgen signaling axis, especially new potent drugs such as abiraterone and enzalutamide [46,47]. It is important to recognize the existence of discrepancy between the abundance of AR-V mRNAs and that of AR-V proteins reported in clinical specimens. Although the levels of AR-V mRNAs have been reported to be relatively low, Western analyses of 13 CRPC bone metastases demonstrate that the levels of AR-V proteins could constitute a median of 32% of the AR-FL protein level [39]. In 38% of these CRPC bone metastases, the AR-V proteins are expressed at a level comparable to that of the AR-FL protein [39].

There is now intriguing evidence supporting the important contribution of the constitutively-active AR-Vs to the development of castration resistance. Ectopic expression of AR-V7 or ARv567es confers castration-resistant growth of LNCaP xenograft tumors [42], whereas specific knockdown of AR-V7 attenuates the growth of castration-resistant 22Rv1 xenograft tumors in castrated host [38]. In addition, AR-V7 or ARv567es expression level has been shown to be associated with adverse clinical outcomes. Higher expression of AR-V7 in hormone-naïve prostate tumors predicts increased risk of biochemical recurrence following radical prostatectomy [38,40]. Patients with high AR-V7 or detectable ARv567es expression have significantly shorter cancer-specific survival than other CRPC patients [39]. Thus, the extensive *in vitro* and xenograft literature on AR-V expression translates into clinically relevant observations.

In addition to the role of the constitutively-active AR-Vs in promoting castration-resistant progression after first-line ADT, their

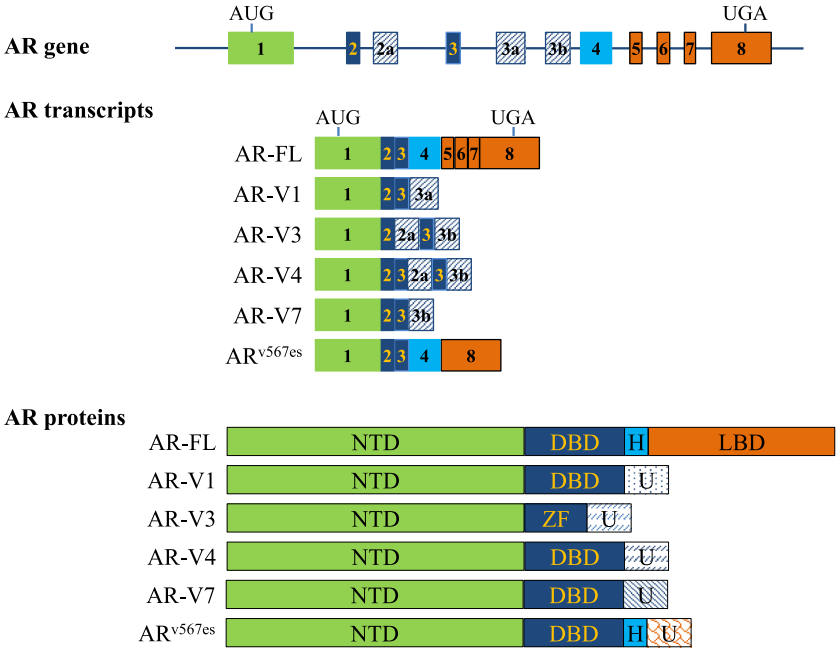

Fig. 3. Schematic representation of the structure of AR-FL and AR-V transcripts and proteins. H, hinge region; U, untranslated region; ZF, zinc finger.

lack of the functional LBD also predicts resistance to the new androgen-axis-targeting drugs, such as abiraterone and enzalutamide [46,47]. Several natural or synthetic compounds have been shown pre-clinically to inhibit AR-V actions [48–52]. Targeting the AR-Vs with these novel agents is an important concept in the therapeutic advances against CRPC, but all of these agents will require clinical trials for proof of action.

Alterations in AR co-regulators

Over 170 potential co-regulators of AR have been identified that bind to AR, stabilize the protein, and lead to either increased or decreased transcriptional activity by altering ligand specificity or allowing transactivation of AR in low levels of androgen [53]. This deregulated co-regulator expression affects AR activity and is repeatedly hypothesized to contribute to the development of CRPC [54,55].

Members of the steroid receptor co-activator family including SRC-1, SRC-2/TIF-2, and SRC-3, have been found to bind the AR NTD and activate AR transactivation via histone acetyltransferase activity as well as by recruiting additional co-activators including CBP/p300. Members of the SRC family are increased in prostate cancer; even higher levels are seen in CRPC [53,55]. SRC-2 has been frequently noted to be amplified as well [54]. These higher levels may lead to increased sensitivity of AR to weak agonists such as androstenedione and DHEA [55]. When phosphorylated by mitogen-activated kinase (MAPK) signaling pathways, SRC1 can activate AR in the absence of androgens to the same magnitude as potent androgens [56]. p300 can also acetylate AR [57], and this post-translational change can enhance co-activator and inhibit co-repressor binding to AR [58].

Co-activators ARA70 and ARA55 also affect ligand specificity of the receptor. ARA70 overexpression enhances AR activation in response to normal weak agonists or to enable antagonists to act as agonists [59]. ARA55 binds to AR leading to an increase in AR activity and altered specificity to binding ligands [58]. Some studies have shown increased expression is associated with shorter recurrence-free survival and overall survival in CRPC patients [60].

Recently, a member of the Snail family of transcription factors (Slug or SNAI2), has been implicated as an AR target gene that can both help upregulate AR and enhance AR-mediated signaling in both wild type, and splice variant, expressing systems [61]. Slug may be particularly important given it acts as a potential oncogene in other cancers and can trigger epithelial–mesenchymal transition (EMT), a frequently described attribute of advanced CRPC [62].

Research on AR co-regulators has focused on both co-activators and co-repressors [63]. SMRT and NCoR are particularly important co-repressors, and their recruitment may play a role in mediating the inhibition of androgen-axis signaling by anti-androgens. Thus alteration in the relative ratios of co-repressors/co-activators recruitment may play a role in the development of CRPC. The scope of this article prevents a full discussion of this area.

Crosstalk with growth factor and cytokine signaling pathways and post-translational AR modifications

Extracellular peptides, including cytokines and growth factors, along with their downstream intracellular signaling cascades, have been implicated in prostate cancer. In CRPC, the crosstalk between these signaling pathways and AR provides a ligand-independent mechanism to sustain AR activation and promote cell growth [6,53,56,64–66].

Post-translational modifications of nuclear receptors including AR effect receptor function, stability, localization, and interactions with other proteins. Phosphorylation, sumoylation, acetylation, and ubiquitination are potential reversible mechanisms behind these alterations.

AR phosphorylations have been described both at serine/threonine residues and various tyrosine residues. MAPK, AKT, protein kinase A, protein kinase C, src-family kinases and Ack1 kinases have all been implicated. In some cases these kinase pathways are thought to be driven by various cytokines and growth factors. Phosphorylation of the AR can localize the receptor to the nucleus and alter AR-dependent transcriptional activity [64–66].

Acetylation occurs at highly conserved lysine residues in AR due to a physiologic stimulus including DHT and the recruitment of co-activators such as p300, which contain intrinsic histone acetyltransferase activity [6,66,67]. Ligand induced AR function is enhanced by this acetyltransferase activity, and augments AR activity at promoter sites of cell cycle genes leading to increased cell proliferation. Mutations in the hinge region can lead to loss of acetylation and decreased DHT binding and signaling [6,66].

SUMOylation typically results in repression of AR. This process results in the attachment of small ubiquitin like modifiers (SUMO) to AR with reversal via SUMO specific proteases including SENP1. AR is modified by SUMO-1 in an androgen dependent manner leading to rapid reversal of AR function. Mutations at the site of SUMOylation within the NTD lead to decreased SUMO-1 binding and enhanced transcriptional activity of AR [6,66,68,69].

The ubiquitin E3 ligase, RNF6, induces AR ubiquitination and promotes AR transcriptional activity. RNF6 is overexpressed in CRPC tissues and has been linked to prostate cancer cell growth after androgen-depletion. Data suggest that RNF6-induced ubiquitination regulates both AR transcriptional activity and specificity by altering cofactor recruitment [66,68,70].

These mechanisms illustrate the effects of post-translational modifications and their impacts on AR activity. Further in vivo studies are needed to address their clinical significance and influence on disease progression, as well as their potential for developing novel prostate cancer specific therapies.

Altered gene expression in CRPC

Recent studies have shed considerable insight into how AR signaling assists cancer cells in adapting to the decline in androgen levels and how AR transcriptional networks are regulated in CRPC, as compared to androgen-dependent prostate cancer. A variety of studies reveal that AR can alter the transcription of a significant number of genes mediating androgen synthesis, DNA synthesis, and cell cycle progression. Chromatin immunoprecipitation coupled with sequencing (ChIP-seq) of DNA adjacent to histone marks H3K4me1 and H3K4me3 in CRPC tissue reveal significant overlapping binding sites with AR (26% of AR binding sites overlap with these H3K4 peaks in CRPC tissue) [71]. These and other studies emphasize the critical importance of histone methylation in regulating AR mediated transcription.

Urbanucci et al. demonstrate that, when AR-transfected LNCaP cells are exposed to low concentrations of androgens, even a modest overexpression of AR could lead to a significant increase in the number of binding sites in the AR cistrome, as well as the strength of AR binding [72]. Moreover, in these cells, receptor binding to chromatin can take place at a concentration of androgen that is 100-fold lower than that in control cells. The canonical androgen-response elements (AREs) and ARE half-sites are among the most significantly overrepresented motifs in this setting [73]. Additional data suggest that AR may be preferentially recruited to chromatin sites that lack the canonical AREs or ARE half-sites by tethering proteins [74].

Via gene expression profiling, a distinct set of genes are clearly upregulated in CRPC compared to the androgen-dependent state. Many AR driven promoters in CRPC tissue demonstrate preferential

co-occurrence of AR binding sites and histone mark H3K4me3. AR recruitment to chromatin associated with the H3K4me1 histone marks is more pronounced at enhancers rather than promoters [71,72]. A complex but distinct transcription program has been identified in CRPC resulting in cellular growth rather than differentiation [72]. In normal prostate cells, AR signaling primarily promotes a differentiation of cells. In CRPC, unlike androgen-dependent cells, AR directly promotes transcription of M-phase cell cycle regulatory genes such as CDC20, UBE2C, CDK1, and these alterations increase cellular proliferation in combination with various collaborating transcription factors (such as FoxA1) and co-activators (such as MED1).

As an example of re-directed gene expression in CRPC, the ubiquitin-conjugating enzyme E2C (UBE2C) may be particularly important as expression is critical for inactivation of the cell cycle M-phase checkpoint [72]. In CRPC models, two UBE2C gene enhancer sites contain H3K4me1 and H3K4me2. These epigenetic marks allow FoxA1 and MED1 binding, which then directs AR binding to the enhancer, thereby activating AR-dependent UBE2C transcription. Both the H3K4 marks and the "pioneer factor" FoxA1 are required for AR binding to occur. The critical role of UBE2C is suggested by silencing of UBE2C, which stops proliferation in CRPC models. Interestingly, though silencing of FOXA1 abolishes AR mediated UBE2C transcription in CRPC models, it has no effect on traditional AR target gene expression (PSA and TMPRSS2) in androgen dependent models, suggesting the critical importance of FoxA1 in unique CRPC transcription programs [72].

It is not appropriate to view AR-mediated CRPC gene reprogramming solely in terms of gene expression. Liganded AR has distinct effects on AR mediated transcription that are dependent on both ligand concentration and cellular context. One hypothesis suggests that androgen levels in CRPC cells are adequate to stimulate selected enhancer elements, but are not adequate to effectively recruit AR to suppressor elements that can negatively regulate cellular proliferation. Under these circumstances, both the concentration of ligand and the CRPC context are keys to understanding AR regulated gene expression [24].

Enhancer of zeste homolog 2 (EZH2), which is over-expressed in CRPC (and many other advanced cancers), can functionally switch from transcriptional repression in normal cells to gene activation in CRPC. EZH2 phosphorylation at Ser21, potentially an Akt mediated event in CRPC, promotes association with an AR-containing complex and dramatically alters expression of a large number of transcripts involved in cellular proliferation. Suppression of EZH2 decreases growth rates in various CRPC model systems suggesting potential as a drug target [75].

Another example of dramatic alterations in the AR cistrome involves the AR-regulated TMPRSS2:ERG fusion gene. Expression of the TMPRSS2:ERG fusion gene is restored in CRPC, in concert with activation of AR transcriptional activity, and a continued important role for ERG in CRPC has been postulated [23]. In CRPC cells, ERG over-expression redirects AR to a set of genes (including the potentially important SOX9) that are not normally androgen stimulated [76].

Taken together, AR gene expression signatures in CRPC are dynamic, context-dependent, and involve hundreds of transcripts (both coding and non-coding) that promote cell proliferation, motility, and invasion. Significant variations are noted between cell cultures and human samples [71], thus caution is advised in over-interpreting cell culture studies. Developing gene expression signatures with clinical relevance is an ongoing goal [71].

Non-AR mutations in CRPC

In a study of metastatic CRPC tissues derived from autopsy specimens, mutations were recurrently noted in a variety of exomes including those derived from p53, ZFHX3, RB1, PTEN, APC, MLL2, OR5L1 and CDK12 [29]. These appear to constitute adaptive responses that arise in CRPC but are distinct from those seen in the AR-axis. Next-generation sequencing promises to further elucidate further genomic alterations/mutations in both coding and non-coding regions of the genome. This area will rapidly progress in the near future. Whether clinically actionable mutations will arise from these analyses is unclear. Additional focus on this important arena is beyond the scope of this manuscript.

Non-coding RNAs

This complex arena is only now beginning to be explored. Recent studies of the human transcriptome indicate that the number of non-coding RNAs is in far excess of the number of protein coding genes. Non-coding RNAs vary tremendously in size. Thus far, microRNAs are among those best studied given their stability and annotation. Androgens can up- or down-regulate a number of microRNAs, with exact results being dependent on the model studied [77]. Androgen represses the miR-99a/let7c/125b-2 cluster [26]. Serum samples from metastatic CRPC patients exhibit distinct circulating microRNA signatures. miR-375, miR-378, and miR-141 are over-expressed in serum from CRPC patients compared with serum from low-risk localized patients, while miR-409-3p is under-expressed [78]. Among longer non-coding RNAs, approximately 120 are transcriptionally dysregulated in prostate cancer [79]. One of these, PCAT-1 has been potentially implicated in advanced disease [80]. Considerable evolution in this area is expected in the next several years.

Conclusion

Multiple adaptive mechanisms involve the androgen signaling axis in CRPC. Alterations in the AR-axis include altered ligand/receptor interactions, and/or altered transcriptional response to AR. Both AR hypersensitivity due to AR overexpression and intratumoral androgen synthesis have been shown to continue androgen dependent growth despite a relatively hormone-depleted environment. AR mutations are noted, especially in tumors treated with selected anti-androgens. AR splice variants can create a constitutively active receptor, alter recruitment of co-activators/repressors, and alter gene expression leading to sustained CRPC growth. Changes in co-regulator expression and various polymorphisms in androgen transporters have also been identified. Ligand independent activation of AR has been seen with cross talk between extracellular peptides, intracellular kinase pathways, co-regulatory proteins, and intrinsic activation of AR. Post-translational modifications can affect AR activity, stability, localization, and interaction with other proteins. A distinct AR-induced transcriptional program leading to proliferation, invasion, and metastasis provides an additional important mechanism for the development of CRPC. The exploration of numerous uncharacterized non-coding RNAs, some of which are androgen-regulated, may also have important biological functions in this disease. Non-AR-axis mutations are also increasingly being documented and their relevance to the growth of CRPC is currently being explored. In summary, CRPC development and progression is centered, in part, around adaptations of the androgen signaling, opening doors for continued research and potential development of novel therapeutic concepts.

Funding source

This work is supported by D.O.D. W81XWH-12-1-0112 (Y.D.) and W81XWH-12-1-0275 (H.Z.), Louisiana Board of Regents Grant LEQSF(2012-15)-RD-A-25 (H.Z.), Louisiana Cancer Research

Consortium Fund (Y.D. and H.Z.), and the Laborde endowed professorship (O.S.). The study sponsors had no involvement in the collection, analysis and interpretation of data, the writing of the manuscript, or the decision to submit the manuscript for publication.

Conflict of interest statement

There are no conflicts to declare.

References

[1] Huggins C, Hodges CV. Studies on prostatic cancer. I. The effect of castration, of estrogen and androgen injection on serum phosphatases in metastatic carcinoma of the prostate. Cancer Res 1941;1(4):293–7.
[2] Ross RW, Xie W, Regan MM, et al. Efficacy of androgen deprivation therapy (ADT) in patients with advanced prostate cancer: association between Gleason score, prostate-specific antigen level, and prior ADT exposure with duration of ADT effect. Cancer 2008;112(6):1247–53.
[3] Crook JM, O'Callaghan CJ, Duncan G, et al. Intermittent androgen suppression for rising PSA level after radiotherapy. N Engl J Med 2012;367(10):895–903.
[4] Ford III OH, Gregory CW, Kim D, Smitherman AB, Mohler JL. Androgen receptor gene amplification and protein expression in recurrent prostate cancer. J Urol 2003;170(5):1817–21.
[5] Dehm SM, Tindall DJ. Androgen receptor structural and functional elements: role and regulation in prostate cancer. Mol Endocrinol 2007;21(12):2855–63.
[6] Clinckemalie L, Vanderschueren D, Boonen S, Claessens F. The hinge region in androgen receptor control. Mol Cell Endocrinol 2012;358(1):1–8.
[7] Cano LQ, Lavery DN, Bevan CL. Mini-review: foldosome regulation of androgen receptor action in prostate cancer. Mol Cell Endocrinol 2013;369(1–2):52–62.
[8] Watson PA, Chen YF, Balbas MD, et al. Constitutively active androgen receptor splice variants expressed in castration-resistant prostate cancer require full-length androgen receptor. Proc Natl Acad Sci USA 2010;107(39):16759–65.
[9] Geller J, Albert JD, Nachtsheim DA, Loza D. Comparison of prostatic cancer tissue dihydrotestosterone levels at the time of relapse following orchiectomy or estrogen therapy. J Urol 1984;132(4):693–6.
[10] Mohler JL, Gregory CW, Ford III OH, et al. The androgen axis in recurrent prostate cancer. Clin Cancer Res 2004;10(2):440–8.
[11] Stanbrough M, Bubley GJ, Ross K, et al. Increased expression of genes converting adrenal androgens to testosterone in androgen-independent prostate cancer. Cancer Res 2006;66(5):2815–25.
[12] Holzbeierlein J, Lal P, LaTulippe E, et al. Gene expression analysis of human prostate carcinoma during hormonal therapy identifies androgen-responsive genes and mechanisms of therapy resistance. Am J Pathol 2004;164(1):217–27.
[13] Locke JA, Guns ES, Lubik AA, et al. Androgen levels increase by intratumoral de novo steroidogenesis during progression of castration-resistant prostate cancer. Cancer Res 2008;68(15):6407–15.
[14] Montgomery RB, Mostaghel EA, Vessella R, et al. Maintenance of intratumoral androgens in metastatic prostate cancer: a mechanism for castration-resistant tumor growth. Cancer Res 2008;68(11):4447–54.
[15] Chang KH, Li R, Papari-Zareei M, et al. Dihydrotestosterone synthesis bypasses testosterone to drive castration-resistant prostate cancer. Proc Natl Acad Sci USA 2011;108(33):13728–33.
[16] Wright JL, Kwon EM, Ostrander EA, et al. Expression of SLCO transport genes in castration-resistant prostate cancer and impact of genetic variation in SLCO1B3 and SLCO2B1 on prostate cancer outcomes. Cancer Epidemiol Biomarkers Prev 2011;20(4):619–27.
[17] Yang M, Xie W, Mostaghel E, et al. SLCO2B1 and SLCO1B3 may determine time to progression for patients receiving androgen deprivation therapy for prostate cancer. J Clin Oncol 2011;29(18):2565–73.
[18] Hamada A, Sissung T, Price DK, et al. Effect of SLCO1B3 haplotype on testosterone transport and clinical outcome in caucasian patients with androgen-independent prostatic cancer. Clin Cancer Res 2008;14(11):3312–8.
[19] Linja MJ, Savinainen KJ, Saramaki OR, Tammela TL, Vessella RL, Visakorpi T. Amplification and overexpression of androgen receptor gene in hormone-refractory prostate cancer. Cancer Res 2001;61(9):3550–5.
[20] Waltering KK, Helenius MA, Sahu B, et al. Increased expression of androgen receptor sensitizes prostate cancer cells to low levels of androgens. Cancer Res 2009;69(20):8141–9.
[21] Donovan MJ, Osman I, Khan FM, et al. Androgen receptor expression is associated with prostate cancer-specific survival in castrate patients with metastatic disease. BJU Int 2010;105(4):462–7.
[22] Visakorpi T, Hyytinen E, Koivisto P, et al. In vivo amplification of the androgen receptor gene and progression of human prostate cancer. Nat Genet 1995;9(4):401–6.
[23] Cai C, Wang H, Xu Y, Chen S, Balk SP. Reactivation of androgen receptor-regulated TMPRSS2: ERG gene expression in castration-resistant prostate cancer. Cancer Res 2009;69(15):6027–32.
[24] Cai C, He HH, Chen S, et al. Androgen receptor gene expression in prostate cancer is directly suppressed by the androgen receptor through recruitment of lysine-specific demethylase 1. Cancer Cell 2011;20(4):457–71.
[25] Sharma A, Yeow WS, Ertel A, et al. The retinoblastoma tumor suppressor controls androgen signaling and human prostate cancer progression. J Clin Invest 2010;120(12):4478–92.
[26] Sun D, Layer R, Mueller AC, et al. Regulation of several androgen-induced genes through the repression of the miR-99a/let-7c/miR-125b-2 miRNA cluster in prostate cancer cells. Oncogene 2013. http://dx.doi.org/10.1038/onc.2013.77 (Epub ahead of print)..
[27] Gottlieb B, Beitel LK, Nadarajah A, Paliouras M, Trifiro M. The androgen receptor gene mutations database: 2012 update. Hum Mutat 2012;33(5):887–94.
[28] Koochekpour S. Androgen receptor signaling and mutations in prostate cancer. Asian J Androl 2010;12(5):639–57.
[29] Grasso CS, Wu YM, Robinson DR, et al. The mutational landscape of lethal castration-resistant prostate cancer. Nature 2012;487(7406):239–43.
[30] Taplin ME, Bubley GJ, Shuster TD, et al. Mutation of the androgen-receptor gene in metastatic androgen-independent prostate cancer. N Engl J Med 1995;332(21):1393–8.
[31] Taplin ME, Bubley GJ, Ko YJ, et al. Selection for androgen receptor mutations in prostate cancers treated with androgen antagonist. Cancer Res 1999;59(11):2511–5.
[32] Veldscholte J, Voorhorst-Ogink MM, Bolt-de VJ, van Rooij HC, Trapman J, Mulder E. Unusual specificity of the androgen receptor in the human prostate tumor cell line LNCaP: high affinity for progestogenic and estrogenic steroids. Biochim Biophys Acta 1990;1052(1):187–94.
[33] Steketee K, Timmerman L, Ziel-van der Made AC, Doesburg P, Brinkmann AO, Trapman J. Broadened ligand responsiveness of androgen receptor mutants obtained by random amino acid substitution of H874 and mutation hot spot T877 in prostate cancer. Int J Cancer 2002;100(3):309–17.
[34] Steinkamp MP, O'Mahony OA, Brogley M, et al. Treatment-dependent androgen receptor mutations in prostate cancer exploit multiple mechanisms to evade therapy. Cancer Res 2009;69(10):4434–42.
[35] Hay CW, McEwan IJ. The impact of point mutations in the human androgen receptor: classification of mutations on the basis of transcriptional activity. PLoS One 2012;7(3):e32514.
[36] Kelly WK, Slovin S, Scher HI. Steroid hormone withdrawal syndromes. Pathophysiology and clinical significance. Urol Clin North Am 1997;24(2):421–31.
[37] Dehm SM, Schmidt LJ, Heemers HV, Vessella RL, Tindall DJ. Splicing of a novel androgen receptor exon generates a constitutively active androgen receptor that mediates prostate cancer therapy resistance. Cancer Res 2008;68(13):5469–77.
[38] Guo Z, Yang X, Sun F, et al. A novel androgen receptor splice variant is up-regulated during prostate cancer progression and promotes androgen depletion-resistant growth. Cancer Res 2009;69(6):2305–13.
[39] Hornberg E, Ylitalo EB, Crnalic S, et al. Expression of androgen receptor splice variants in prostate cancer bone metastases is associated with castration-resistance and short survival. PLoS One 2011;6(4):e19059.
[40] Hu R, Dunn TA, Wei S, et al. Ligand-independent androgen receptor variants derived from splicing of cryptic exons signify hormone-refractory prostate cancer. Cancer Res 2009;69(1):16–22.
[41] Sun S, Sprenger CC, Vessella RL, et al. Castration resistance in human prostate cancer is conferred by a frequently occurring androgen receptor splice variant. J Clin Invest 2010;120(8):2715–30.
[42] Zhang X, Morrissey C, Sun S, et al. Androgen receptor variants occur frequently in castration resistant prostate cancer metastases. PLoS One 2011;6(11):e27970.
[43] Chan SC, Li Y, Dehm SM. Androgen receptor splice variants activate androgen receptor target genes and support aberrant prostate cancer cell growth independent of canonical androgen receptor nuclear localization signal. J Biol Chem 2012;287(23):19736–49.
[44] Hu R, Isaacs WB, Luo J. A snapshot of the expression signature of androgen receptor splicing variants and their distinctive transcriptional activities. Prostate 2011;71(15):1656–67.
[45] Hu R, Lu C, Mostaghel EA, et al. Distinct transcriptional programs mediated by the ligand-dependent full-length androgen receptor and its splice variants in castration-resistant prostate cancer. Cancer Res 2012;72(14):3457–62.
[46] Li Y, Chan SC, Brand LJ, Hwang TH, Silverstein KA, Dehm SM. Androgen receptor splice variants mediate enzalutamide resistance in castration-resistant prostate cancer cell lines. Cancer Res 2013;73(2):483–9.
[47] Mostaghel EA, Marck BT, Plymate SR, et al. Resistance to CYP17A1 inhibition with abiraterone in castration-resistant prostate cancer: induction of steroidogenesis and androgen receptor splice variants. Clin Cancer Res 2011;17(18):5913–25.
[48] Andersen RJ, Mawji NR, Wang J, et al. Regression of castrate-recurrent prostate cancer by a small-molecule inhibitor of the amino-terminus domain of the androgen receptor. Cancer Cell 2010;17(6):535–46.
[49] Cao B, Liu X, Li J, et al. 20(S)-protopanaxadiol-aglycone downregulation of the full-length and splice variants of androgen receptor. Int J Cancer 2013;132(6):1277–87.
[50] Li J, Cao B, Liu X, et al. Berberine suppresses androgen receptor signaling in prostate cancer. Mol Cancer Ther 2011;10(8):1346–56.

[51] Li X, Liu Z, Xu X, et al. Kava components down-regulate expression of AR and AR splice variants and reduce growth in patient-derived prostate cancer xenografts in mice. PLoS One 2012;7(2):e31213.
[52] Mashima T, Okabe S, Seimiya H. Pharmacological targeting of constitutively active truncated androgen receptor by nigericin and suppression of hormone-refractory prostate cancer cell growth. Mol Pharmacol 2010;78(5):846–54.
[53] Heemers HV, Tindall DJ. Androgen receptor (AR) coregulators: a diversity of functions converging on and regulating the AR transcriptional complex. Endocr Rev 2007;28(7):778–808.
[54] Comuzzi B, Nemes C, Schmidt S, et al. The androgen receptor co-activator CBP is up-regulated following androgen withdrawal and is highly expressed in advanced prostate cancer. J Pathol 2004;204(2):159–66.
[55] Taylor BS, Schultz N, Hieronymus H, et al. Integrative genomic profiling of human prostate cancer. Cancer Cell 2010;18(1):11–22.
[56] Ueda T, Bruchovsky N, Sadar MD. Activation of the androgen receptor N-terminal domain by interleukin-6 via MAPK and STAT3 signal transduction pathways. J Biol Chem 2002;277(9):7076–85.
[57] Fu M, Wang C, Reutens AT, et al. P300 and p300/cAMP-response element-binding protein-associated factor acetylate the androgen receptor at sites governing hormone-dependent transactivation. J Biol Chem 2000;275(27):20853–60.
[58] Fu M, Rao M, Wang C, et al. Acetylation of androgen receptor enhances coactivator binding and promotes prostate cancer cell growth. Mol Cell Biol 2003;23(23):8563–75.
[59] Yeh S, Chang HC, Miyamoto H, et al. Differential induction of the androgen receptor transcriptional activity by selective androgen receptor coactivators. Keio J Med 1999;48(2):87–92.
[60] Miyoshi Y, Ishiguro H, Uemura H, et al. Expression of AR associated protein 55 (ARA55) and androgen receptor in prostate cancer. Prostate 2003;56(4):280–6.
[61] Wu K, Gore C, Yang L, et al. Slug, a unique androgen-regulated transcription factor, coordinates androgen receptor to facilitate castration resistance in prostate cancer. Mol Endocrinol 2012;26(9):1496–507.
[62] Alves CC, Carneiro F, Hoefler H, Becker KF. Role of the epithelial–mesenchymal transition regulator Slug in primary human cancers. Front Biosci 2009;14:3035–50.
[63] Godoy AS, Sotomayor PC, Villagran M, et al. Altered corepressor SMRT expression and recruitment to target genes as a mechanism that change the response to androgens in prostate cancer progression. Biochem Biophys Res Commun 2012;423(3):564–70.
[64] Chen S, Kesler CT, Paschal BM, Balk SP. Androgen receptor phosphorylation and activity are regulated by an association with protein phosphatase 1. J Biol Chem 2009;284(38):25576–84.
[65] Chen S, Gulla S, Cai C, Balk SP. Androgen receptor serine 81 phosphorylation mediates chromatin binding and transcriptional activation. J Biol Chem 2012;287(11):8571–83.
[66] Gioeli D, Paschal BM. Post-translational modification of the androgen receptor. Mol Cell Endocrinol 2012;352(1–2):70–8.
[67] Gong J, Zhu J, Goodman Jr OB, et al. Activation of p300 histone acetyltransferase activity and acetylation of the androgen receptor by bombesin in prostate cancer cells. Oncogene 2006;25(14):2011–21.
[68] Coffey K, Robson CN. Regulation of the androgen receptor by post-translational modifications. J Endocrinol 2012;215(2):221–37.
[69] Poukka H, Karvonen U, Janne OA, Palvimo JJ. Covalent modification of the androgen receptor by small ubiquitin-like modifier 1 (SUMO-1). Proc Natl Acad Sci USA 2000;97(26):14145–50.
[70] Xu K, Shimelis H, Linn DE, et al. Regulation of androgen receptor transcriptional activity and specificity by RNF6-induced ubiquitination. Cancer Cell 2009;15(4):270–82.
[71] Sharma NL, Massie CE, Ramos-Montoya A, et al. The androgen receptor induces a distinct transcriptional program in castration-resistant prostate cancer in man. Cancer Cell 2013;23(1):35–47.
[72] Wang Q, Li W, Zhang Y, et al. Androgen receptor regulates a distinct transcription program in androgen-independent prostate cancer. Cell 2009;138(2):245–56.
[73] Urbanucci A, Marttila S, Janne OA, Visakorpi T. Androgen receptor overexpression alters binding dynamics of the receptor to chromatin and chromatin structure. Prostate 2012;72(11):1223–32.
[74] Gonit M, Zhang J, Salazar M, et al. Hormone depletion-insensitivity of prostate cancer cells is supported by the AR without binding to classical response elements. Mol Endocrinol 2011;25(4):621–34.
[75] Xu K, Wu ZJ, Groner AC, et al. EZH2 oncogenic activity in castration-resistant prostate cancer cells is polycomb-independent. Science 2012;338(6113):1465–9.
[76] Cai C, Wang H, He HH, et al. ERG induces androgen receptor-mediated regulation of SOX9 in prostate cancer. J Clin Invest 2013;123(3):1109–22.
[77] Waltering KK, Porkka KP, Jalava SE, et al. Androgen regulation of micro-RNAs in prostate cancer. Prostate 2011;71(6):604–14.
[78] Nguyen HC, Xie W, Yang M, et al. Expression differences of circulating microRNAs in metastatic castration resistant prostate cancer and low-risk, localized prostate cancer. Prostate 2013;73(4):346–54.
[79] Prensner JR, Chinnaiyan AM. The emergence of lncRNAs in cancer biology. Cancer Discov 2011;1(5):391–407.
[80] Prensner JR, Iyer MK, Balbin OA, et al. Transcriptome sequencing across a prostate cancer cohort identifies PCAT-1, an unannotated lincRNA implicated in disease progression. Nat Biotechnol 2011;29(8):742–9.

Am J Clin Exp Urol 2013;1(1):18-24
www.ajceu.us /ISSN:2330-1910/AJCEU1312005

Review Article

Splicing variants of androgen receptor in prostate cancer

Haitao Zhang[1,5], Yang Zhan[2], Xichun Liu[1], Yanfeng Qi[2], Guanyi Zhang[1], Oliver Sartor[3,4,5], Yan Dong[2,5,6]

Departments of [1]Pathology and Laboratory Medicine, [2]Structural and Cellular Biology, [3]Urology, [4]Medicine, Tulane University School of Medicine, [5]Tulane Cancer Center, New Orleans, LA; [6]National Engineering Laboratory for AIDS Vaccine, College of Life Sciences, Jilin University, China

Received December 19, 2013; Accepted December 22, 2013; Epub December 25, 2013; Published December 30, 2013

Abstract: Significant advances in our understanding of continued androgen receptor (AR) signaling in castration-resistant prostate cancer have led to the development and FDA approval of two next-generation androgen-directed therapies, abiraterone and enzalutamide. These new therapies heralded a new era of prostate cancer therapy. However, disease progression during androgen-directed therapies remains the most critical challenge in the clinical management of prostate cancer. Accumulating evidence points to an important contribution of constitutively-active AR splice variants to AR-driven tumor progression during androgen-directed therapies. In this review, we will focus on the structure, activity, detection, clinical relevance, and mechanisms of production of AR splice variants.

Keywords: Androgen receptor, AR splice variants, castration resistance, prostate cancer

Introduction

Prostate cancer is the most common non-skin cancer and the second leading cause of cancer mortality in men in the United States. Androgen deprivation therapy, which disrupts androgen receptor (AR) signaling by reducing androgen levels through surgical or chemical castration, or by administration of anti-androgens that compete with androgens for binding to AR [2], is the first-line treatment for metastatic and locally advanced prostate cancer. While this regimen is effective initially, progression to the presently incurable and lethal stage, termed castration-resistant prostate cancer (CRPC), invariably occurs [1, 2]. With a median survival of ~16-18 months [3], CRPC accounts for the majority of disease-related mortality. Mounting evidence suggests that resurgent AR drives therapeutic failure and castration-resistant progression [1, 2]. A number of ligand-dependent and -independent mechanisms have been proposed to underlie AR reactivation during androgen deprivation therapy [1, 2]. While these mechanisms are thoroughly reviewed by many, this review is focused on the discussion of the role of constitutively-active AR splice variants that lack the functional ligand-binding domain (LBD) in AR-signaling reactivation.

Structure and activity of the AR splice variants

The canonical AR protein is 919 amino acids long, encoded by 8 exons on the X-chromosome (Xq12) [4]. Structurally, the full-length AR (AR-FL) resembles other members of the steroid receptor family, consisting of 4 domains (**Figure 1**). The N-terminal domain (NTD) contains an activation function 1 (AF1) domain that functions as a ligand-independent transcriptional activation domain. Another important function of NTD is recruitment of coregulators. The DNA-binding domain (DBD) contains two zinc fingers that are involved in DNA recognition, dimerization, and stabilization. The hinge domain (H) provides flexibility to the protein and regulates the nuclear translocation of the receptor through a canonical nuclear localization signal. The C-terminal LBD contains a ligand-binding pocket that mediates high affinity ligand-binding. A second activation function domain (AF2) is located in the LBD and regulates transcriptional activation in a ligand-dependent manner. All hormonal therapies currently accepted in

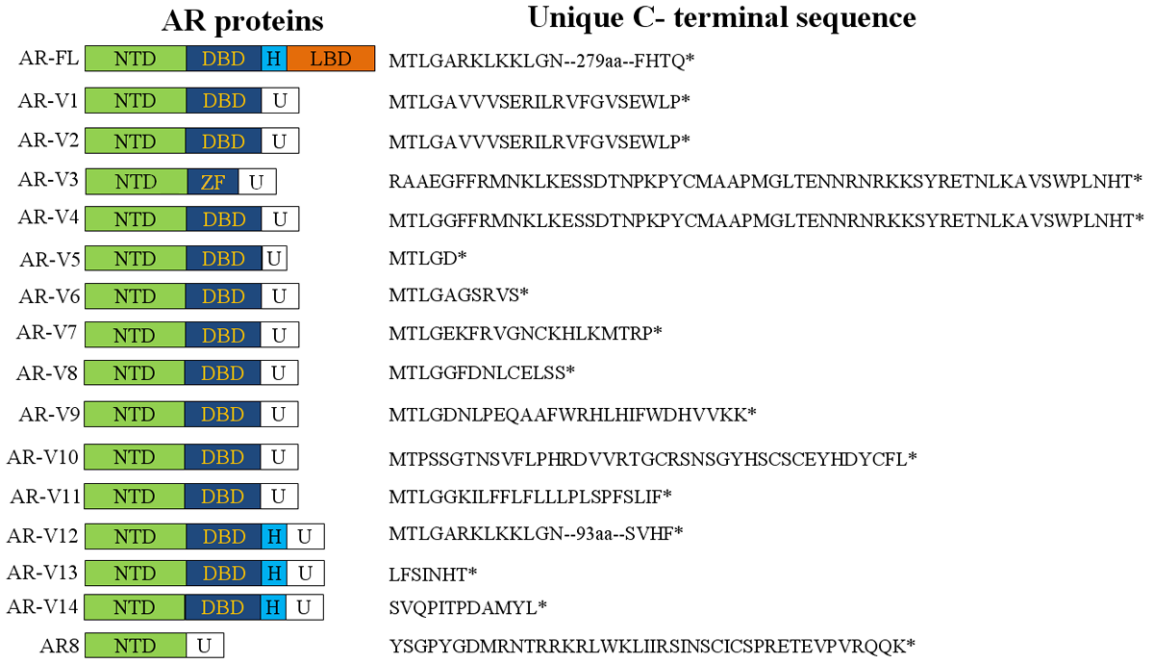

Figure 1. Schematic representation of the structure of AR-FL and AR-V proteins. U, unique sequence; ZF, zinc finger.

the clinic for treatment of prostate cancer, including the recent FDA-approved abiraterone [5] and enzalutamide [6], target the LBD *de facto*.

Recently, a cadre of AR splice variants (AR-Vs) that are devoid of a functional LBD have been identified (**Figure 1**). Structurally, these variants either have insertions of cryptic exons immediately downstream of the exons encoding the DBD or have deletions of the exons encoding the LBD, resulting in a disrupted AR open reading frame and the expression of truncated proteins [7-12]. Since the NTD and DBD remain intact in the majority of the AR-Vs identified to date, many variants display constitutive activity [7-12]. Others are considered conditionally active because these variants display ligand-independent activity only in certain cell models [12]. Two major AR-Vs, AR-V7 (also known as AR3) and AR^{v567es} (a.k.a. AR-V12), have been shown to be capable of regulating target gene expression in the absence of the AR-FL signaling [8-10, 13]. Gene expression profiling showed that AR-V7 and AR^{v567es} regulate the expression of both canonical androgen-responsive genes and a distinct set of targets enriched for cell-cycle function [9, 10, 13]. However, there exists significant difference in the AR-V transcriptome identified by different studies [8-10, 13], possibly due to the use of different model systems.

Notably, not all AR-Vs function as a transcription factor. For example, AR8 lacks a functional DBD, and has been shown to localize mainly to the plasma membrane [14]. AR8 may play a role in mediating Src kinase activation as well as AR-FL tyrosine phosphorylation and subsequent nuclear translocation in response to EGF treatment, possibly by forming a membrane-associated signaling complex that includes AR8, AR-FL, Src kinase, and EGFR [14]. Depletion of AR8 by RNA interference compromised EGF-induced Src activation and AR phosphorylation, as well as inhibited cell proliferation and induced cell death [14]. Thus, AR8 activates the AR signaling pathway and promotes cell survival via a nongenomic mechanism.

Potentiation of AR-FL activity is not limited to the transcriptionally inactive AR8. In cells co-expressing AR^{v567es} and AR-FL, AR^{v567es} could bind to AR-FL and facilitate the nuclear translocation of AR-FL in the absence of ligand [10]. Similarly, AR-V7 could also facilitate the nuclear translocation of AR-FL in an androgen depleted condition or in the presence of the potent AR antagonist enzalutamide (Cao *et al.*, manuscript under review).

Table 1. Isoform-specific PCR primers for detecting AR-Vs

AR-Vs	Alias	PCR Primers	Primer locations	Product size (bp)	Ref.
AR-V1	AR4	F: 5'-CCATCTTGTCGTCTTCGGAAATGTTATGAAGC-3' R: 5'-CTGTTGTGGATGAGCAGCTGAGAGTCT-3'	Exon 3 CE1	149	[8]
		F: 5'-CTACTCCGGACCTTACGGGGACATGCG-3' R: 5'-GATTCTTTCAGAAACAACAACAGCTGCT-3'	Exon 1 Exon 3/CE1	322	[9]
AR-V2		N/A			[8]
AR-V3	AR1/2/2b	N/A			[7, 8]
AR-V4	AR1/2/3/2b, AR5	F: 5'-CTACTCCGGACCTTACGGGGACATGCG-3' R: 5'-CTTTTAATTTGTTCATTCTGAAAAATCCTC-3'	Exon 1 CE2	323	[9]
AR-V5		N/A			[8]
AR-V6		N/A			[8]
AR-V7	AR3	F: 5'-CCATCTTGTCGTCTTCGGAAATGTTATGAAGC-3' F: 5'-TTTGAATGAGGCAAGTCAGCCTTTCT-3'	Exon 3 CE3	125	[8]
		F: 5'-CTACTCCGGACCTTACGGGGACATGCG-3' R: 5'-TGCCAACCCGGAATTTTTCTCCC-3'	Exon 1 Exon 3/CE3	314	[9]
AR-V8		N/A			[11]
AR-V9		F: 5'-CCATCTTGTCGTCTTCGGAAATGTTATGAAGC-3' R: 5'-TTAGTTCTACTTCTTAACAACGTGATCCCA-3'	Exon 3 CE5	128	[12]
AR-V10		N/A			[11]
AR-V11		N/A			[11]
AR-V12	AR^{v567es}	F: 5-GCCTTGCCTGATTGCGAG R: 5'-CATGTGTGACTTGATTAGCAGGTCAAA	Exons 4/8 Exon 8	64	[12]
		F: 5'-CCAAGGCCTTGCCTGATTGC-3' R: 5'-TTGGGCACTTGCACAGAGAT-3'	Exons 4/8 Exon 8	124	[10]
AR-V13		N/A			[12]
AR-V14		N/A			[12]
AR8		F: 5'-CGACTTCACCGCACCTGATG-3' R: 5'-CTCTTTCTTCGGGTATTTCGCATG-3'	Exon 1 Exons 1/3'	150	[14]

Detection of AR-V expression

The majority of AR-V transcripts can be detected by reverse transcription polymerase chain reaction (RT-PCR), taking advantage of their unique exon compositions and exon-exon junctions. A collation of published PCR primers for AR-Vs is presented in **Table 1**. Although RT-PCR provides a sensitive and specific assay for the mRNA, the results do not always correlate with protein expression. For example, the transcript, but not the protein product, of AR-V7 has been detected in the LNCaP cell line [15]. To date, isoform-specific antibodies have only been reported for AR-V7 [8, 9] and AR8 [14], and the only commercially available antibody is for AR-V7 (Precision Antibodies, Columbia, MD). To overcome this limitation, Zhang *et al.* developed an immunohistochemical assay to detect the expression of AR-Vs by using two antibodies recognizing the N- and C-terminus of AR, respectively [16]. A decrease of AR nuclear staining by the C-terminal antibody when compared to that by the N-terminal antibody was used to indicate the presence of LBD-truncated, transcriptionally active AR-Vs. The authors reported a significant loss in AR C-terminal nuclear immunoreactivity in CRPC specimens, but not in tissues from primary cancers, suggesting the prevalence of AR-Vs in CRPC. The results were further corroborated by RT-PCR [16]. Despite the demonstrated success, this approach requires significant efforts in assay optimization and standardization. There is a great demand for the development of additional isoform-specific antibodies for AR-Vs. The unique C-terminal peptide sequences of AR-Vs are presented in **Figure 1**.

Clinical relevance of AR-Vs

AR-Vs are prevalently upregulated in CRPC compared to hormone-naïve cancers, and may emerge as an adaptive response to therapies targeting the androgen signaling axis [8-11, 16, 17]. It is important to recognize the existence of discrepancy between the relative abundance of AR-V mRNAs and that of AR-V proteins in clinical specimens. Although the levels of AR-V mRNAs in metastatic CRPCs have been shown to constitute at most 7% of the AR-FL mRNA level [11, 17], Western analyses of 13 CRPC

bone metastases demonstrated that the levels of AR-V proteins could constitute a median of 32% of the AR-FL protein level (ranging from 0 to 95%) [17]. In fact, in 38% of these CRPC bone metastases, the AR-V proteins are expressed at a level comparable to that of the AR-FL protein [17]. The relative high abundance of AR-V proteins is also supported by data from immunohistochemistry analysis. With the use of an antibody specific to AR-V7, several groups show that AR-V7 is readily detectable in prostate cancer specimens [9, 13, 18]. Using the two-antibodies approach described above, Zhang and colleagues analyzed 50 primary prostate cancer and 162 metastatic CRPC tissues and found that 24% of these CRPC tissues display a staining pattern similar to that of the LuCaP86.2 xenograft, which predominantly expresses AR-V [16].

It is also important to recognize that the absolute levels of AR-Vs may not be as important as that of AR-FL for their respective activity. This is because AR-FL is located in the cytoplasm in the absence of ligand and translocates to the nucleus and activates target-gene expression upon ligand binding, whereas constitutively-active AR-Vs localize to the nucleus and activate target-gene expression in the absence of ligand [8-12, 19]. Strikingly, higher expression of AR-V7 in hormone-naïve prostate tumors predicts increased risk of biochemical recurrence following radical prostatectomy [8, 9], and patients with high levels of expression of AR-V7 or detectable expression of AR^{v567es} have a significantly shorter survival than other CRPC patients [17], indicating an association between AR-V expression and a more lethal form of prostate cancer. Collectively, the existing data support that AR-V proteins are expressed at a significant level in clinical specimens and should not be trivialized simply based on their relative low mRNA abundance.

Preclinical studies have pointed to an important role of AR-Vs in mediating castration resistance. Ectopic expression of AR-V7 or AR^{v567es} confers castration-resistant growth of LNCaP xenograft tumors [9-11]. Conversely, knockdown of AR-V7 attenuates the growth of castration-resistant 22Rv1 xenograft tumors [9]. Targeted expression of AR^{v567es} in prostate epithelium induces *de novo* prostate cancer development and promotes castration-resistant progression of the tumors in transgenic mice [20]. Although only prostatic intraepithelial neoplasia lesions are observed in AR-V7 transgenic mice, the majority of AR-V7-positive cells in castrated AR-V7 transgenic mice are ck5+/ck8+ intermediate cells, indicating a role of AR-V7 in maintaining or expanding prostate progenitor cell population during androgen deprivation [21].

AR-Vs have also been indicated to confer resistance to abiraterone and enzalutamide in preclinical studies. AR-Vs are increased in CRPC xenografts that recurred after abiraterone [22] or enzalutamide treatment (Cao *et al.*, manuscript under review). Knockdown of AR-Vs sensitizes 22Rv1 cells and NFκB p52-transfected LNCaP cells to enzalutamide inhibition of growth [23, 24]. Reducing AR-V levels with small-molecule drugs improves enzalutamide efficacy against the growth of 22Rv1 cells and xenografts [25]. Intriguingly, ectopic expression of AR-V7 in AR-FL-overexpressing LNCaP xenografts does not affect the growth inhibitory efficacy of enzalutamide [11]. A plausible explanation for the discrepancy is that, in the context of AR overexpression, the growth of LNCaP tumors may be driven mainly by the AR-FL signaling, making enzalutamide highly effective irrespective of AR-V expression. Nonetheless, our data showed that, when the ectopically-expressed AR-FL is lost in these xenografts, they can become resistant to enzalutamide, and the resistance is accompanied by increased expression of AR-Vs (Cao *et al.*, manuscript under review). Thus, prostate cancers may evade all androgen-directed therapies through shifting towards AR-V-mediated signaling.

Mechanisms of AR-V production

Two mechanisms have been proposed for AR-V production, AR gene rearrangement [26, 27] and increased pre-mRNA splicing [35]. Modeling gene rearrangement in prostate cancer cells showed expression of AR^{v567es} without AR-FL in clonally selected cells [27]. While AR gene rearrangement could contribute to AR-V production in a subset of prostate cancers, AR-V production at the expense of AR-FL appears to be inconsistent with the tight correlation between AR-V and AR-FL mRNAs observed in individual clinical specimens and in xenograft [11, 17] or co-expression of AR-FL and AR-V7 in CRPC specimens, as indicated by overlapping AR-FL and AR-V7 immunohistochemistry staining of

adjacent tumor sections [13]. Moreover, while a clonal selection process is required for gene-rearrangement-mediated AR-V production to be manifested at the level of tumor tissues, change in AR-V levels in response to androgen deprivation was rather rapid in xenograft tumors [10, 11]. Further, different AR-Vs can be expressed in the same tissues. Clonal expansion of cells with one type of gene arrangement could lead to expression of one specific AR-V but may not be able to account for the expression of different AR-Vs. Compared to gene arrangement, increased splicing appears to be more generalizable. RNA splicing is closely coupled with gene transcription [36]. Androgen deprivation was shown to enhance the rate of AR-gene transcription and thereby indirectly contribute to increased AR pre-mRNA splicing to produce both AR-FL and AR-V7 [35]. A comprehension of the mechanisms of AR-V production is paramount for developing effective means to suppress AR-V expression.

Conclusion

AR signaling is active in CRPC although the cancer is no longer responsive to androgen deprivation therapy. LBD-truncated AR splice variants not only may play a role in maintaining the canonical AR transcriptome in a genuine ligand-independent manner, but may also regulate a unique subset of target genes. Accumulating clinical and preclinical data suggest that AR-Vs are critically involved in the treatment failure of first- and second-line hormonal therapies. Therefore, targeting the AR-Vs appears to an important concept and a fruitful direction of therapeutic development. To this end, several natural or synthetic compounds have been shown pre-clinically to inhibit AR-V actions [18, 29-34], and proof of efficacy in clinical trials is keenly awaited. Furthermore, the expression of constitutively active AR-Vs could serve as a prognostic and response biomarker to guide treatment decisions.

Acknowledgements

We are grateful to Dr. Stephen Plymate for in-depth discussions and communications on this subject. This work was supported by the following grants: DOD W81XWH-12-1-0112, National Natural Science Foundation of China 81272851 (Y.D.) W81XWH-12-1-0275, Louisiana Board of Regents Grant LEQSF (2012-15)-RD-A-25 (H.Z.), Louisiana Cancer Research Consortium Fund (Y.D. and H.Z.), and the Laborde endowed professorship (O.S.).

Address correspondence to: Haitao Zhang, 1430 Tulane Avenue SL-79, New Orleans, LA 70112. Tel: 504-988-7696; Fax: 504-988-7389; E-mail: hzhang@tulane.edu; Yan Dong, 1430 Tulane Avenue SL-49, New Orleans, LA 70112. Tel: 504-988-4761; Fax: 504-988-0468; E-mail: ydong@tulane.edu

References

[1] Egan A, Dong Y, Zhang H, Qi Y, Balk SP, Sartor O. Castration-resistant prostate cancer: Adaptive responses in the androgen axis. Cancer Treat Rev 2013 Sep 14; [Epub ahead of print]. Available at: http://www.sciencedirect.com/science/article/pii/S0305737213002004.

[2] Knudsen KE, Scher HI. Starving the addiction: new opportunities for durable suppression of AR signaling in prostate cancer. Clin Cancer Res 2009; 15: 4792-8.

[3] Pienta KJ, Bradley D. Mechanisms underlying the development of androgen-independent prostate cancer. Clin Cancer Res 2006; 12: 1665-71.

[4] Bennett NC, Gardiner RA, Hooper JD, Johnson DW, Gobe GC. Molecular cell biology of androgen receptor signalling. Int J Biochem Cell Biol 2010; 42: 813-27.

[5] de Bono JS, Logothetis CJ, Molina A, Fizazi K, North S, Chu L, Chi KN, Jones RJ, Goodman OB Jr, Saad F, Staffurth JN, Mainwaring P, Harland S, Flaig TW, Hutson TE, Cheng T, Patterson H, Hainsworth JD, Ryan CJ, Sternberg CN, Ellard SL, Fléchon A, Saleh M, Scholz M, Efstathiou E, Zivi A, Bianchini D, Loriot Y, Chieffo N, Kheoh T, Haqq CM, Scher HI; COU-AA-301 Investigators. Abiraterone and increased survival in metastatic prostate cancer. N Engl J Med 2011; 364: 1995-2005.

[6] Scher HI, Fizazi K, Saad F, Taplin ME, Sternberg CN, Miller K, de Wit R, Mulders P, Chi KN, Shore ND, Armstrong AJ, Flaig TW, Fléchon A, Mainwaring P, Fleming M, Hainsworth JD, Hirmand M, Selby B, Seely L, de Bono JS; AFFIRM Investigators. Increased survival with enzalutamide in prostate cancer after chemotherapy. N Engl J Med 2012; 367: 1187-97.

[7] Dehm SM, Schmidt LJ, Heemers HV, Vessella RL, Tindall DJ. Splicing of a novel androgen receptor exon generates a constitutively active androgen receptor that mediates prostate cancer therapy resistance. Cancer Res 2008; 68: 5469-77.

[8] Hu R, Dunn TA, Wei S, Isharwal S, Veltri RW, Humphreys E, Han M, Partin AW, Vessella RL,

Isaacs WB, Bova GS, Luo J. Ligand-independent androgen receptor variants derived from splicing of cryptic exons signify hormone-refractory prostate cancer. Cancer Res 2009; 69: 16-22.

[9] Guo Z, Yang X, Sun F, Jiang R, Linn DE, Chen H, Chen H, Kong X, Melamed J, Tepper CG, Kung HJ, Brodie AM, Edwards J, Qiu Y. A novel androgen receptor splice variant is up-regulated during prostate cancer progression and promotes androgen depletion-resistant growth. Cancer Res 2009; 69: 2305-13.

[10] Sun S, Sprenger CC, Vessella RL, Haugk K, Soriano K, Mostaghel EA, Page ST, Coleman IM, Nguyen HM, Sun H, Nelson PS, Plymate SR. Castration resistance in human prostate cancer is conferred by a frequently occurring androgen receptor splice variant. J Clin Invest 2010; 120: 2715-30.

[11] Watson PA, Chen YF, Balbas MD, Wongvipat J, Socci ND, Viale A, Kim K, Sawyers CL. Constitutively active androgen receptor splice variants expressed in castration-resistant prostate cancer require full-length androgen receptor. Proc Natl Acad Sci U S A 2010; 107: 16759-65.

[12] Hu R, Isaacs WB, Luo J. A snapshot of the expression signature of androgen receptor splicing variants and their distinctive transcriptional activities. Prostate 2011; 71: 1656-67.

[13] Hu R, Lu C, Mostaghel EA, Yegnasubramanian S, Gurel M, Tannahill C, Edwards J, Isaacs WB, Nelson PS, Bluemn E, Plymate SR, Luo J. Distinct transcriptional programs mediated by the ligand-dependent full-length androgen receptor and its splice variants in castration-resistant prostate cancer. Cancer Res 2012; 72: 3457-62.

[14] Yang X, Guo Z, Sun F, Li W, Alfano A, Shimelis H, Chen M, Brodie AM, Chen H, Xiao Z, Veenstra TD, Qiu Y. Novel membrane-associated androgen receptor splice variant potentiates proliferative and survival responses in prostate cancer cells. J Biol Chem 2011; 286: 36152-60.

[15] Haile S, Sadar MD. Androgen receptor and its splice variants in prostate cancer. Cell Mol Life Sci 2011; 68: 3971-81.

[16] Zhang X, Morrissey C, Sun S, Ketchandji M, Nelson PS, True LD, Vakar-Lopez F, Vessella RL, Plymate SR. Androgen Receptor Variants Occur Frequently in Castration Resistant Prostate Cancer Metastases. PLoS One 2011; 6: e27970.

[17] Hörnberg E, Ylitalo EB, Crnalic S, Antti H, Stattin P, Widmark A, Bergh A, Wikström P. Expression of androgen receptor splice variants in prostate cancer bone metastases is associated with castration-resistance and short survival. PLoS One 2011; 6: e19059.

[18] Yamashita S, Lai KP, Chuang KL, Xu D, Miyamoto H, Tochigi T, Pang ST, Li L, Arai Y, Kung HJ, Yeh S, Chang C. ASC-J9 Suppresses Castration-Resistant Prostate Cancer Growth through Degradation of Full-length and Splice Variant Androgen Receptors. Neoplasia 2012; 14: 74-83.

[19] Chan SC, Li Y, Dehm SM. Androgen Receptor Splice Variants Activate Androgen Receptor Target Genes and Support Aberrant Prostate Cancer Cell Growth Independent of Canonical Androgen Receptor Nuclear Localization Signal. J Biol Chem 2012; 287: 19736-49.

[20] Liu G, Sprenger C, Sun S, Epilepsia KS, Haugk K, Zhang X, Coleman I, Nelson PS, Plymate S. AR variant ARv567es induces carcinogenesis in a novel transgenic mouse model of prostate cancer. Neoplasia 2013; 15: 1009-17.

[21] Sun F, Chen HG, Li W, Yang X, Wang X, Jiang R, Guo Z, Chen H, Huang J, Borowsky AD, Qiu Y. Androgen receptor splice variant AR3 promotes prostate cancer via modulating expression of autocrine/paracrine factors. J Biol Chem 2013 Dec 2; [Epub ahead of print].

[22] Mostaghel EA, Marck BT, Plymate SR, Vessella RL, Balk S, Matsumoto AM, Nelson PS, Montgomery RB. Resistance to CYP17A1 inhibition with abiraterone in castration resistant prostate cancer: Induction of steroidogenesis and androgen receptor splice variants. Clin Cancer Res 2011; 17: 5913-25.

[23] Li Y, Chan SC, Brand LJ, Hwang TH, Silverstein KAT, Dehm SM. Androgen Receptor Splice Variants Mediate Enzalutamide Resistance in Castration-Resistant Prostate Cancer Cell Lines. Cancer Res 2013; 73: 483-9.

[24] Nadiminty N, Tummala R, Liu C, Yang J, Lou W, Evans CP, Gao AC. NF-κB2/p52 Induces Resistance to Enzalutamide in Prostate Cancer: Role of Androgen Receptor and Its Variants. Mol Cancer Ther 2013; 12: 1629-37.

[25] Zhan Y, Cao B, Qi Y, Liu S, Zhang Q, Zhou W, Xu D, Lu H, Sartor O, Kong W, Zhang H, Dong Y. Methylselenol prodrug enhances MDV3100 efficacy for treatment of castration-resistant prostate cancer. Int J Cancer 2013; 133: 2225-33.

[26] Li Y, Hwang TH, Oseth LA, Hauge A, Vessella RL, Schmechel SC, Hirsch B, Beckman KB, Silverstein KA, Dehm SM. AR intragenic deletions linked to androgen receptor splice variant expression and activity in models of prostate cancer progression. Oncogene 2012; 31: 4759-67.

[27] Nyquist MD, Li Y, Hwang TH, Manlove LS, Vessella RL, Silverstein KA, Voytas DF, Dehm SM. TALEN-engineered AR gene rearrangements reveal endocrine uncoupling of androgen receptor in prostate cancer. Proc Natl Acad Sci U S A 2013; 110: 17492-7.

[28] Edwards J, Krishna NS, Grigor KM, Bartlett JMS. Androgen receptor gene amplification and protein expression in hormone refractory prostate cancer. Br J Cancer 2003; 89: 552-6.
[29] Andersen RJ, Mawji NR, Wang J, Wang G, Haile S, Myung JK, Watt K, Tam T, Yang YC, Bañuelos CA, Williams DE, McEwan IJ, Wang Y, Sadar MD. Regression of castrate-recurrent prostate cancer by a small-molecule inhibitor of the amino-terminus domain of the androgen receptor. Cancer Cell 2010; 17: 535-46.
[30] Li J, Cao B, Liu X, Fu X, Xiong Z, Chen L, Sartor O, Dong Y, Zhang H. Berberine suppresses androgen receptor signaling in prostate cancer. Mol Cancer Ther 2011; 10: 1346-56.
[31] Cao B, Liu X, Li J, Liu S, Qi Y, Xiong Z, Zhang A, Wiese T, Fu X, Gu J, Rennie PS, Sartor O, Lee BR, Ip C, Zhao L, Zhang H, Dong Y. 20(S)-protopanaxadiol-aglycone downregulation of the full-length and splice variants of androgen receptor. J Int Cancer 2013; 132: 1277-87.
[32] Li X, Liu Z, Xu X, Blair CA, Sun Z, Xie J, Lilly MB, Zi X. Kava components down-regulate expression of AR and AR splice variants and reduce growth in patient-derived prostate cancer xenografts in mice. PLoS One 2012; 7: e31213.
[33] Mashima T, Okabe S, Seimiya H. Pharmacological targeting of constitutively active truncated androgen receptor by nigericin and suppression of hormone-refractory prostate cancer cell growth. Mol Pharmacol 2010; 78: 46-54.
[34] Narizhneva NV, Tararova ND, Ryabokon P, Shyshynova I, Prokvolit A, Komarov PG, Purmal AA, Gudkov AV, Gurova KV. Small molecule screening reveals a transcription-independent prosurvival function of androgen receptor in castration-resistant prostate cancer. Cell Cycle 2009; 8: 4155-67.
[35] Liu LL, Xie N, Sun S, Plymate S, Mostaghel E and Dong X. Mechanisms of the androgen receptor splicing in prostate cancer cells. Oncogene 2013; [Epub ahead of print].
[36] Kornblihtt AR. Coupling transcription and alternative splicing. Adv Exp Med Biol 2007; 623: 175-89.

Androgen receptor splice variants activating the full-length receptor in mediating resistance to androgen-directed therapy

Bo Cao[1,2,*], Yanfeng Qi[1,*], Guanyi Zhang[2,3], Duo Xu[1,2], Yang Zhan[1], Xavier Alvarez[4], Zhiyong Guo[5], Xueqi Fu[2], Stephen R. Plymate[6,7], Oliver Sartor[8,9], Haitao Zhang[2,3], and Yan Dong[1,10]

[1] Department of Structural and Cellular Biology, Tulane University School of Medicine, Tulane Cancer Center, New Orleans, LA

[2] College of Life Sciences, Jilin University, China

[3] Department of Pathology and Laboratory Medicine, Tulane University School of Medicine, Tulane Cancer Center, New Orleans, LA

[4] Tulane National Primate Research Center, Covington, LA

[5] Department of Pharmacology, University of Maryland School of Medicine, Baltimore, MD

[6] Departments of Medicine, University of Washington School of Medicine, Seattle, WA

[7] Department of Urology, University of Washington School of Medicine, Seattle, WA

[8] Department of Urology, Tulane University School of Medicine, Tulane Cancer Center, New Orleans, LA

[9] Department of Medicine, Tulane University School of Medicine, Tulane Cancer Center, New Orleans, LA

[10] National Engineering Laboratory for AIDS Vaccine, College of Life Sciences, Jilin University, China

[*] These authors contributed equally; in alphabetical order

Correspondence to: *Yan Dong,* ***email***: *ydong@tulane.edu; Haitao Zhang,* ***email***: *hzhang@tulane.edu*

Keywords: androgen receptor, splice variant, prostate cancer, castration resistance, enzalutamide

Received: *February 18, 2014* ***Accepted***: *March 2, 2014* ***Published***: *March 4, 2014*

ABSTRACT:

Upregulation of constitutively-active androgen receptor splice variants (AR-Vs) has been implicated in AR-driven tumor progression in castration-resistant prostate cancer. To date, functional studies of AR-Vs have been focused mainly on their ability to regulate gene expression independent of the full-length AR (AR-FL). Here, we showed that AR-V7 and AR^{v567es}, two major AR-Vs, both facilitated AR-FL nuclear localization in the absence of androgen and mitigated the ability of the antiandrogen enzalutamide to inhibit AR-FL nuclear trafficking. AR-V bound to the promoter of its specific target without AR-FL, but co-occupied the promoter of canonical AR target with AR-FL in a mutually-dependent manner. AR-V expression attenuated both androgen and enzalutamide modulation of AR-FL activity/cell growth, and mitigated the *in vivo* antitumor efficacy of enzalutamide. Furthermore, AR^{v567es} levels were upregulated in xenograft tumors that had acquired enzalutamide resistance. Collectively, this study highlights a dual function of AR-Vs in mediating castration resistance. In addition to trans-activating target genes independent of AR-FL, AR-Vs can serve as a "rheostat" to control the degree of response of AR-FL to androgen-directed therapy via activating AR-FL in an androgen-independent manner. The findings shed new insights into the mechanisms of AR-V-mediated castration resistance and have significant therapeutic implications.

INTRODUCTION

Androgen deprivation therapy, which disrupts androgen receptor (AR) signaling through androgen ablation or AR antagonists, is the first-line treatment for disseminated prostate cancer. While this regimen is effective initially, progression to the presently incurable and lethal stage, termed castration-resistant prostate

cancer (CRPC), invariably occurs [1,2]. Resurgent AR activity is an established driver of therapeutic failure and castration-resistant progression [1,2]. A number of ligand-dependent and –independent mechanisms have been proposed to underlie AR reactivation after androgen-directed therapies [1,2]. For example, overexpression of the full-length AR (AR-FL) was shown to convert prostate cancer growth from a castration-sensitive to a castration-resistant stage [3]. In addition, CRPC tissues were shown to exhibit persistent levels of androgens despite androgen deprivation [1,2]. These led to the development of the potent AR antagonist enzalutamide (MDV3100) and the androgen biosynthesis inhibitor abiraterone for treatment of metastatic CRPC [4,5]. They heralded a new era of prostate cancer therapy. However, many patients presented with therapy-resistant disease, and most initial responders developed acquired resistance within months of therapy initiation, again accompanied by increased prostate-specific antigen (PSA), indicating reactivated AR signaling [4,5]. Emerging evidences indicate that prostate tumors can adapt to these androgen-directed therapies, including the new agents, by signaling through constitutively-active AR splice variants (AR-Vs) that lack the functional ligand-binding domain [6-16].

AR-Vs are upregulated in most CRPCs compared to hormone-naïve cancers [6,7,13-17]. Intriguingly, there is a significant discrepancy between the relative abundance of AR-V mRNAs and that of AR-V proteins in clinical specimens. While the level of AR-V mRNAs is low relative to that of the AR-FL, the AR-V proteins are expressed at a level comparable to that of AR-FL in a considerable portion of metastatic CRPC tissues [6,16]. In addition, the absolute levels of AR-Vs may not be as important as that of AR-FL for their respective activity. This is because AR-FL is located in the cytoplasm in the absence of ligand and translocates to the nucleus and activates target-gene expression upon ligand binding, whereas constitutively-active AR-Vs localize to the nucleus and activate target-gene expression in the absence of ligand [13-15,18-20]. AR-V7 (aka AR3) and AR^{v567es} are two major AR-Vs expressed in clinical specimens [6,7,13-15]. Strikingly, patients with high levels of expression of AR-V7 or detectable expression of AR^{v567es} have a significantly shorter survival than other CRPC patients [6], indicating an association between AR-V expression and a more lethal form of prostate cancer.

Preclinical studies have pointed to an important role of AR-Vs in mediating castration resistance. Ectopic expression of AR-V7 or AR^{v567es} confers castration-resistant growth of LNCaP xenograft tumors [13,15,20]. Conversely, knockdown of AR-V7 attenuates the growth of castration-resistant 22Rv1 xenograft tumors [13]. AR-Vs have also been shown to confer resistance to enzalutamide in preclinical studies. Knockdown of AR-Vs sensitizes 22Rv1 cells and NFκB p52-transfected LNCaP cells to enzalutamide inhibition of growth [8,11]. Reducing AR-V levels with small-molecule drugs improves enzalutamide efficacy against the growth of 22Rv1 cells and xenografts [21]. Thus, AR-V upregulation appears to be a mechanism for prostate cancer cells to evade androgen-directed therapies. A comprehension of mechanisms of AR-V action is paramount for developing effective means to suppress AR-V signaling.

Gene expression profiling showed that AR-Vs regulate the expression of both canonical androgen-responsive genes and a distinct set of targets enriched for cell-cycle function [7,13,15]. The ability of AR-Vs to regulate target-gene expression has been attributed largely to their AR-FL-independent activity [7,8,12-15,19]. However, AR-FL and AR-V7 immunohistochemistry staining of adjacent sections of CRPC specimens showed that AR-V is often co-expressed with AR-FL [7]. We reason that, in addition to binding to chromatin sites and regulating gene expression independent of AR-FL, AR-Vs may bind to chromatin as a complex with AR-FL. Combined, these two activities may account for the expanded AR-V transcriptome. In fact, AR^{v567es} has been shown to coimmunoprecipitate with AR-FL and facilitate AR-FL nuclear localization in the absence of androgen [15]. In the present study, we dissected the interplay between AR-Vs and AR-FL in regulating gene expression and mediating resistance to androgen-directed therapies.

RESULTS

AR-V mitigates enzalutamide inhibition of AR-FL nuclear localization

Both AR^{v567es} and AR-V7 can reside constitutively in the nucleus [14,15,18], and AR^{v567es} has been shown to facilitate AR-FL nuclear localization in the absence of androgen [15]. Enzalutamide is known to attenuate androgen-induced AR-FL nuclear localization in cells expressing AR-FL alone [22]. To assess the effect of AR-V7 on AR-FL subcellular localization and the impact of AR-Vs on enzalutamide modulation of AR-FL localization, we expressed AR-FL-green-fluorescent-protein (AR-FL-GFP) with or without AR-V7-turbo-red-fluorescent-protein (AR-V7-TurboFP) or AR^{v567es}-TurboFP in the AR-null COS-7 cells. Consistent with previous reports [14,15,18], as shown in Figure 1A, both AR-Vs were found primarily in the nucleus, whereas AR-FL localized predominantly in the cytoplasm in androgen-deprived conditions. Enzalutamide caused ~50% reduction of androgen-induced AR-FL nuclear localization, but had no effect on AR-V localization or AR-FL localization in the absence of androgen.

When co-expressed with AR-V7 or AR^{v567es} (Figure 1B), AR-FL could localize to the nucleus in the absence of androgen. The nuclear localization was unaffected by

enzalutamide. Strikingly, although addition of androgen further induced AR-FL nuclear localization, enzalutamide could not retain AR-FL in the cytoplasm when AR-V was present. Moreover, AR-V localization was not affected by androgen or enzalutamide even when co-expressed with AR-FL. A similar result was obtained in the PC-3 prostate cancer cells (Supplementary Figure 1). Taken together, the data suggest that AR-Vs facilitate AR-FL nuclear localization in the absence of androgen and mitigate the ability of enzalutamide to inhibit androgen-induced AR-FL nuclear localization.

AR-V and AR-FL co-occupy the target-gene promoter

Although AR-V-mediated AR-FL nuclear localization may not necessarily entail a physical interaction between AR-V and AR-FL, AR^{v567es} has been shown to coimmunoprecipitate with AR-FL, indicating AR-V can form a complex with AR-FL [15]. To find out whether they bind to target promoters as a complex, we performed sequential chromatin immunoprecipitation (Re-ChIP) analysis with an AR-V7 antibody followed by an AR-FL antibody in 22Rv1 cells, which express endogenous AR-V7 and are in part driven by AR-V7 [23]. We had to limit the analysis to AR-V7 because it is the only AR-V to which a specific antibody has been developed. As shown in Figure 2A, we detected co-occupancy of AR-V7 and AR-FL on the promoter of the PSA gene, and the co-occupancy was unaffected by androgen or enzalutamide treatment. In contrast, the promoter of ubiquitin-conjugating enzyme E2C (UBE2C) is only bound by AR-V7 (Figure 2A and 2B), and ChIP assay showed that AR-FL knockdown (shFL) did not significantly affect the binding (Figure 2B). This is consistent with UBE2C as an AR-V-specific target [6,7]. We then conducted a ChIP assay on the PSA promoter in 22Rv1 cells with or without specific knockdown of AR-FL or AR-V7 in androgen-deprived condition. As shown in Figure 2C, AR-FL knockdown diminished AR-V7 binding to the PSA promoter. Similarly, AR-V7 knockdown (shV7) reduced androgen-independent AR-FL binding to the promoter (Figure 2D). Collectively, the data indicate that,

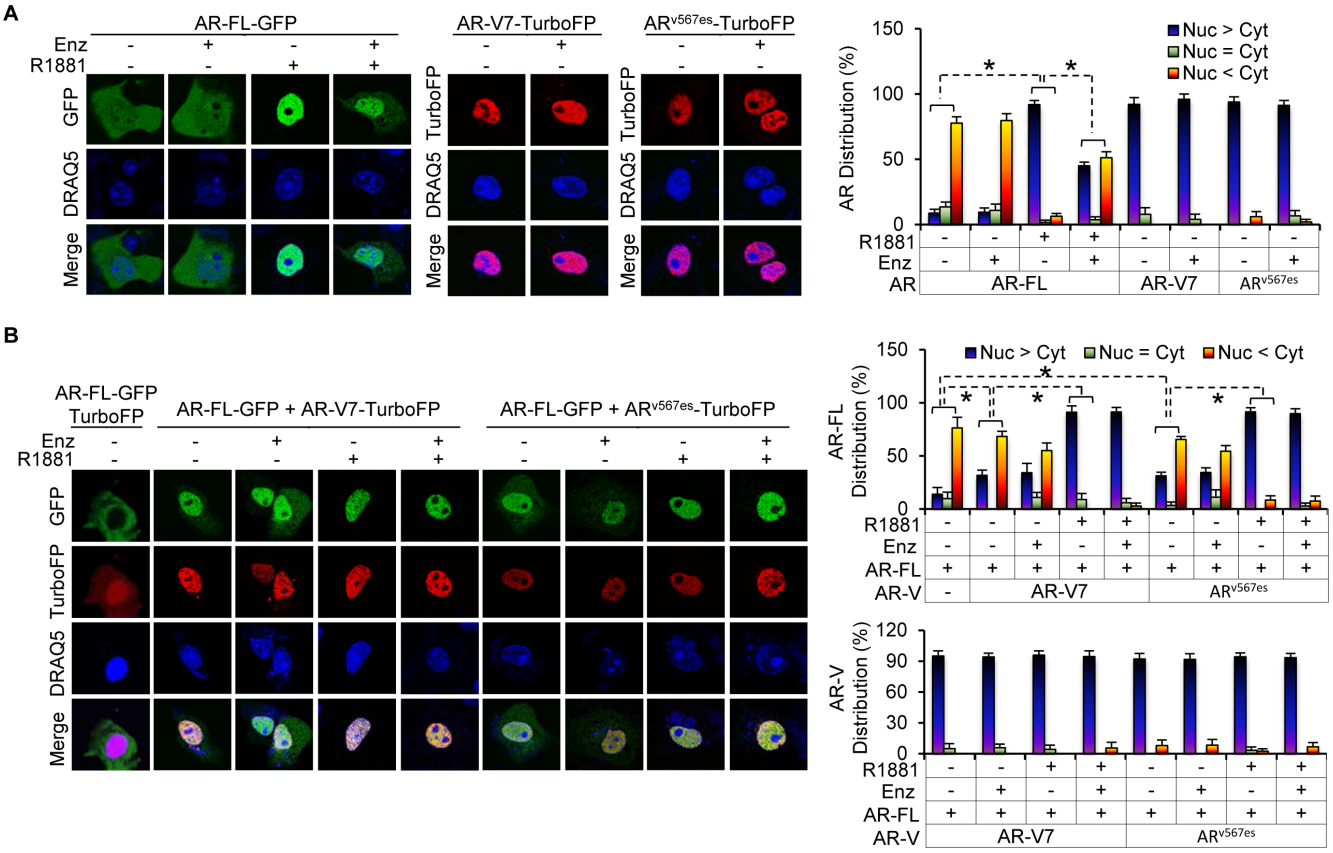

Figure 1: AR-V facilitates AR-FL nuclear localization in the absence of androgen and mitigates enzalutamide inhibition of androgen-induced AR-FL nuclear localization. A & B. Confocal fluorescence microscopy of AR-FL and AR-V subcellular localization when expressed alone (A) or when co-expressed with AR-V (B) in COS-7 cells. Right panels, quantitation of % of cells with predominantly nuclear, equally nuclear and cytoplasmic, or predominantly cytoplasmic expression. DRAQ5, nuclear stain. Cells cultured in androgen-deprived condition were pre-treated with 10 μM enzalutamide (Enz) for 2 hr, followed by treatment with or without 1 nM R1881 for 3 hr. *, $P < 0.05$.

in the absence of androgen, AR-V and AR-FL co-occupy the promoter of canonical androgen-responsive gene, but not AR-V-specific target, in a mutually-dependent manner.

AR-V attenuates androgen-induced AR-FL transactivation

To determine the impact of promoter co-occupancy on target gene expression, we measured the mRNA levels of both canonical androgen-responsive genes (PSA and TMPRSS2) and AR-V-specific targets (CCNA2 and UBE2C) in 22Rv1 cells in response to AR-FL or AR-V7 knockdown (Figure 3A). While knockdown of AR-FL and AR-V7 both reduced androgen-independent expression of PSA and TMPRSS2, only AR-V7 knockdown downregulated CCNA2 and UBE2C. Notably, although AR-V7 knockdown diminished basal PSA and TMPRSS2 levels, the levels after androgen stimulation were essentially the same in control and AR-V7-knockdown cells. AR-V7 knockdown thus led to a higher magnitude of androgen induction of PSA (2.7-fold *vs*. 1.7-fold) and TMPRSS2 (2.6-fold *vs*. 1.4-fold), and enzalutamide was very effective in blocking the induction. Conversely, ectopic expression of AR-V7 or AR^{v567es} in LNCaP cells dose-dependently induced basal PSA and TMPRSS2 expression and diminished the degree of response of PSA and TMPRSS2 to androgen (Figure 3B and Supplementary Figure 2). Taken together, the data indicate that, in addition to *trans*-activating a distinct set of genes, AR-Vs activate AR-FL in an androgen-independent manner to induce the expression of their shared targets. In doing so, AR-Vs could serve as "rheostats" to control the degree of response of AR-FL to androgen and to androgen-directed therapy. Interestingly, while ectopic co-expression of AR-V7 or AR^{v567es} rendered enzalutamide ineffective against androgen-induced AR-FL nuclear localization (Figure 1B), the presence of AR-V7 did not affect the ability of enzalutamide to inhibit androgen-dependent expression of PSA and TMPRSS2 (Figure 3A and Supplementary Figure 2). Collectively, these results suggest that AR-Vs could facilitate the nuclear localization of AR-FL in the presence of enzalutamide, but are unable to overcome the suppression of ligand-activated AR-FL transactivation by enzalutamide.

AR-V mitigates androgen and enzalutamide modulation of cell growth

We proceeded to characterize the effect of AR-V7 knockdown on androgen and enzalutamide modulation

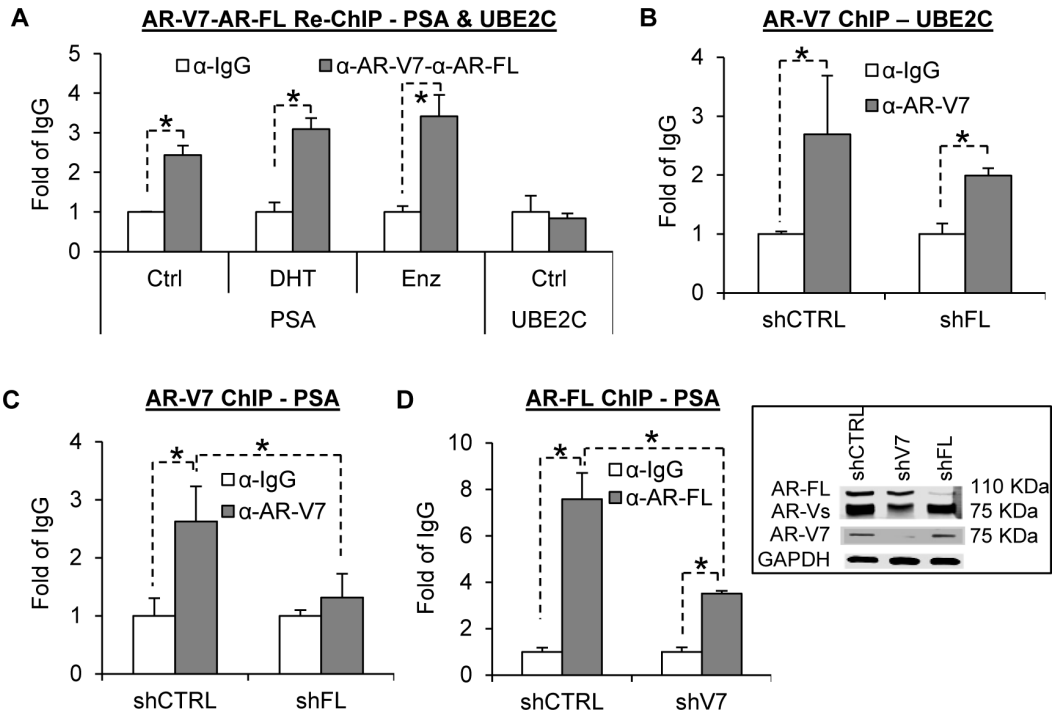

Figure 2: AR-V7 and AR-FL co-occupy the PSA, but not UBE2C, promoter in a mutually dependent manner. A. Sequential ChIP analysis in 22Rv1 cells with an AR-V7 antibody followed by an AR-FL antibody showing co-occupancy of the PSA, but not UBE2C, promoter by AR-V7 and AR-FL. Enzalutamide (Enz), 10 μM. DHT, 1 nM. B. AR-V7 ChIP analysis in 22Rv1 cells showing AR-V7 binding to the UBE2C promoter. C. AR-V7 ChIP analysis in 22Rv1 cells showing AR-FL knockdown diminishes AR-V7 binding to the PSA promoter. D. AR-FL ChIP analysis in 22Rv1 cells showing AR-V7 knockdown reduces AR-FL binding to the PSA promoter. The values of the IgG samples are set as 1, and the ChIP results are presented as relative fold of IgG. *, $P < 0.05$. Western blots showed the knockdown efficacy of AR-FL and AR-V7.

of the growth of 22Rv1 cells. Congruent with the mRNA data, after AR-V7 knockdown, the cells became more sensitive to DHT induction of growth (Figure 4A; ~2-fold in AR-V7-knockdown cells *vs.* 1.3-fold in control cells). Consequently, the knockdown cells were more responsive to enzalutamide growth inhibition than the control cells. We next inoculated AR-V7-knockdown cells or control cells in nude mice, and characterized the response of the ensuing tumors to enzalutamide. As shown in Figure 4B, growth inhibition by enzalutamide was more pronounced after AR-V7 knockdown (the tumor growth curves are presented in Supplementary Figure 3). Collectively, the data suggest that AR-V may contribute to enzalutamide resistance by dampening the response of the cells to androgen induction of growth.

Increased AR-Vs in tumors that had developed acquired resistance to enzalutamide

Enzalutamide has been demonstrated to be very effective against the growth of castration-resistant AR-FL-overexpressing LNCaP xenografts [22]. As shown in Figure 5A, we observed the same phenomenon in xenografts established by inoculating LNCaP cells that were transduced with wild-type-AR-FL-encoding lentivirus into castrated nude mice. Some tumors resumed growth with prolonged treatment (after 7-17 weeks) (Figure 5B). We serially passaged the relapsed Tumor #1 and #2 (Figure 5B) in castrated mice treated with enzalutamide, and considered tumors from the second to fourth passages as enzalutamide resistant. RNA-seq analysis of four enzalutamide-sensitive tumors and six enzalutamide-resistant tumors showed that none of the tumors carried the AR F876L missense mutation (Figure 5C), which was identified in enzalutamide-resistant LNCaP cells and shown to confer agonist activity to enzalutamide [24-26]. Instead, the transcripts of AR^{v567es} and AR-V7 (trending toward significance) were upregulated in enzalutamide-resistant tumors, while the levels of AR-V4 or AR-FL transcript did not differ (Figure 6A-D). The upregulation of AR-V was also reflected at the protein level (Figure 6E). Interestingly, all the enzalutamide-resistant tumors that showed higher AR-V protein expression also express increased levels of glucocorticoid receptor (Supplementary Figure 4), the upregulation of which has been shown to be a mechanism of acquired resistance to enzalutamide [27]. The data indicate that these tumors may use multiple mechanisms to evade enzalutamide treatment.

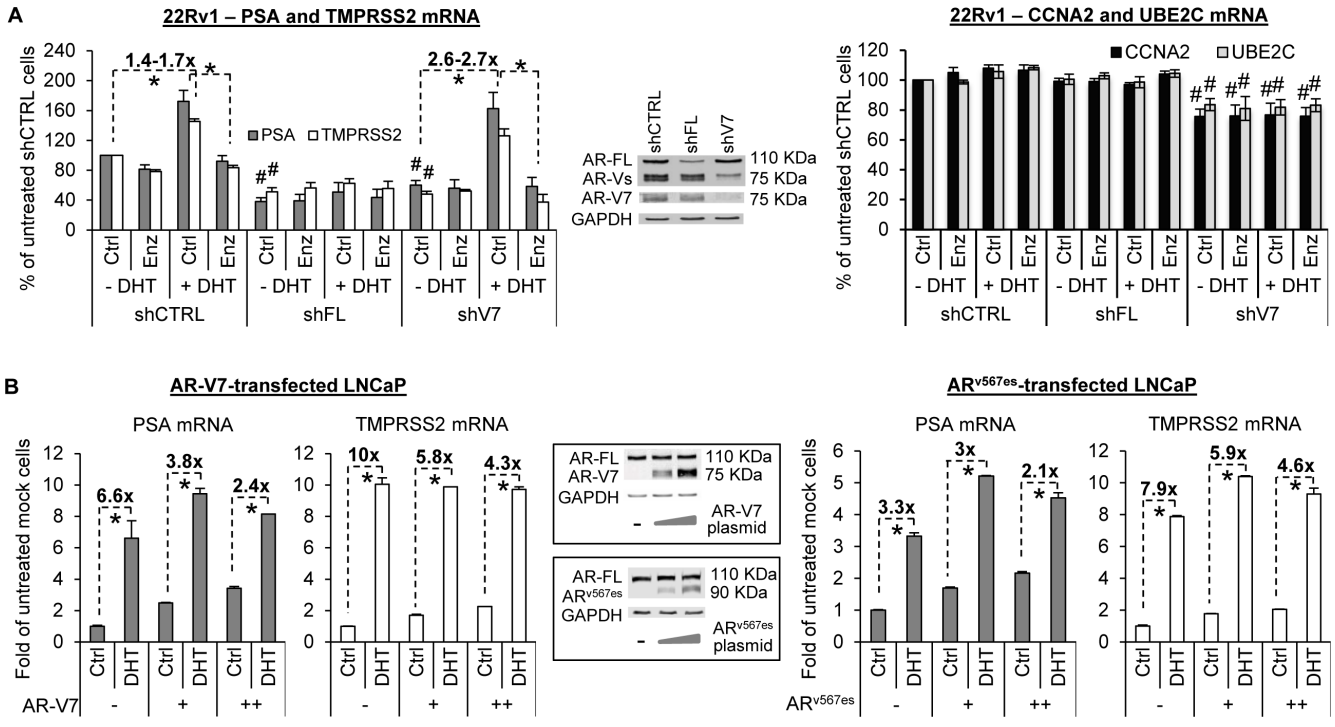

Figure 3: AR-V attenuates androgen and enzalutamide modulation of AR-target expression. A. qRT-PCR analysis showing reduced androgen-independent expression of PSA and TMPRSS2 after knockdown of either AR-FL or AR-V7 (left panel) and reduced expression of CCNA2 and UBE2C only after AR-V7 knockdown (right panel). AR-V7 knockdown also renders 22Rv1 cells more sensitive to DHT and enzalutamide modulation of PSA and TMPRSS2 expression. B. qRT-PCR analysis showing that AR-V transfection dose-dependently attenuates DHT induction of PSA and TMPRSS2 in LNCaP cells. Treatment duration, 8 hr (A); 4 hr (B). Enzalutamide (Enz), 10 μM. DHT, 1 nM. *, $P < 0.05$. #, $P < 0.05$ from untreated control-shRNA cells.

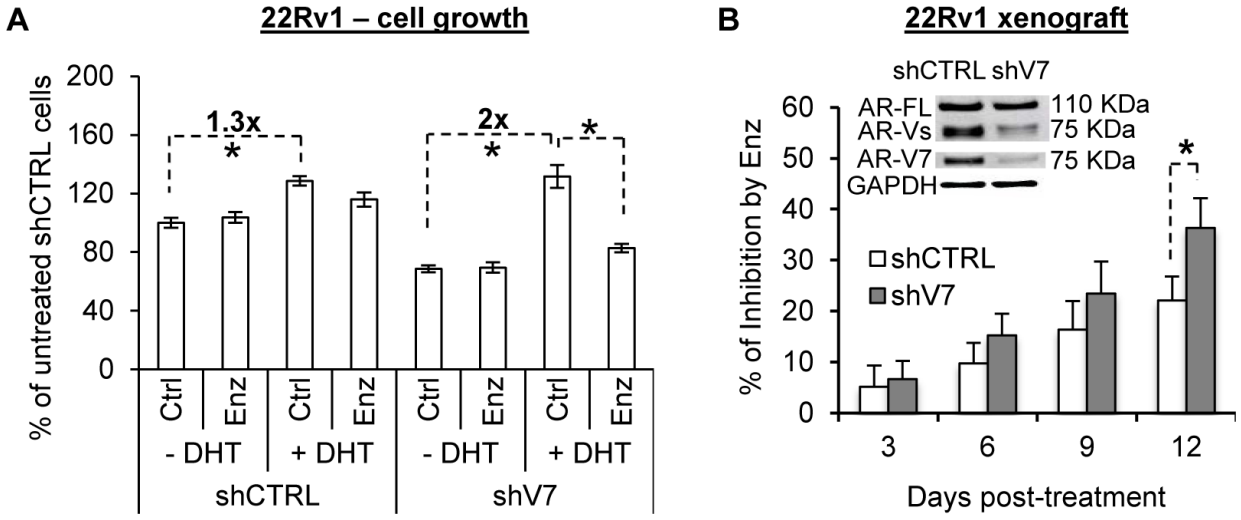

Figure 4: AR-V attenuates androgen and enzalutamide modulation of cell growth. A. AR-V7 knockdown enhances the response of 22Rv1 cells to androgen and enzalutamide modulation of cell growth. B. Enzalutamide inhibition of 22Rv1 tumor growth becomes more pronounced after AR-V7 knockdown. Data are expressed as % of inhibition by enzalutamide. *, $P < 0.05$. Enzalutamide (Enz), 10 mg/kg/day. n = 8.

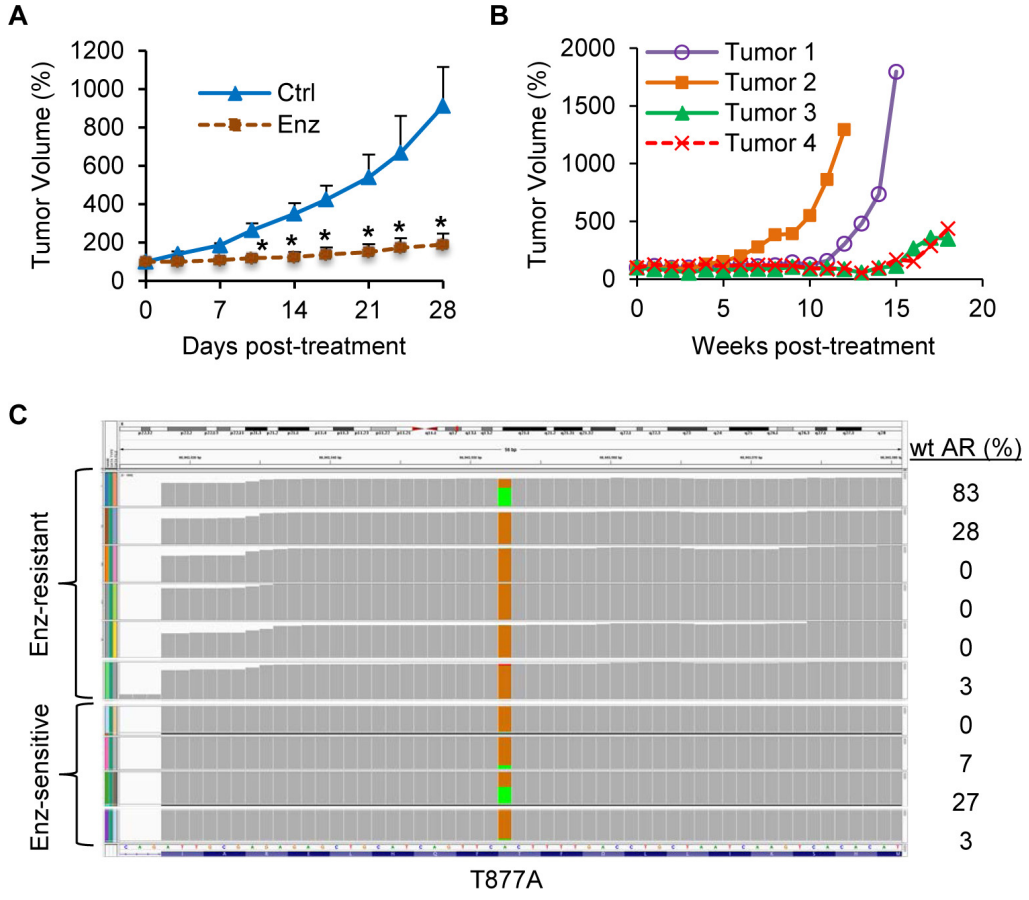

Figure 5: Absence of AR F876L mutation in LNCaP tumors that have developed acquired resistance to enzalutamide. A. Enzalutamide (Enz) inhibits the growth of castration-resistant LNCaP tumors initially. LNCaP cells were transduced with lentivirus encoding wild-type (wt) AR-FL before inoculated into castrated mice. *, $P < 0.05$ from the control group. n = 5. B. LNCaP tumors resume growth after 7-17 weeks of enzalutamide treatment. The mean tumor volumes were presented as % of original tumor size at Day 0 of treatment. C. Integrative Genomics Viewer (IGV) plot of RNA-seq data showing no detection of F876L mutation in the AR gene in enzalutamide-sensitive and –resistant LNCaP tumors. The brown boxes represent the relative frequencies of T877A-mutated AR that is present in the LNCaP tumors. The relative frequencies of the transduced wt AR remained in the tumors are denoted by the green boxes and tabled on the right. Allele frequency threshold was set at 0.01.

DISCUSSION

To date, the ability of AR-Vs to contribute to castration resistance has been attributed largely to their AR-FL-independent constitutive activity in regulating gene expression. Here, we identified what we believe to be a novel mechanism of AR-V action. We showed that AR-V7 and AR^{v567es}, two major AR-Vs, not only facilitate AR-FL nuclear localization in the absence of androgen but also mitigate the ability of the antiandrogen enzalutamide to inhibit androgen-induced AR-FL nuclear localization. In the nucleus, AR-V7 binds to the promoter of its specific target without AR-FL, but co-occupies the promoter of canonical androgen-responsive gene with AR-FL in a mutually-dependent manner. The co-occupancy is not affected by androgen or enzalutamide. Concordantly, knockdown of AR-FL and AR-V7 both result in reduced androgen-independent expression of canonical androgen-responsive genes, but only AR-V7 knockdown downregulates AR-V-specific targets. Notably, although basal levels of canonical androgen-responsive genes are diminished after AR-V7 knockdown, or elevated after AR-V7 or AR^{v567es} overexpression, the levels after androgen stimulation are unaffected. Thus, AR-Vs appear to repress the degree of response of AR-FL to androgen by activating AR-FL to induce target expression in an androgen-independent manner. This is further supported by the improved sensitivity of the cells to androgen induction of cell growth and enzalutamide inhibition of cell growth after AR-V7 knockdown. These collective findings suggest that, in addition to AR-FL-independent constitutive transactivation, AR-Vs may serve as "rheostats" to control the degree of response of AR-FL to androgen and to androgen-directed therapy.

In the present study, we also showed that enzalutamide becomes more potent in thwarting the growth of 22Rv1 xenograft tumors after AR-V7 knockdown, indicating that targeting both AR-Vs and AR-FL is needed to achieve complete AR blockade. While corroborating the *in vitro* observations from Li *et al*. [8] and Nadiminty *et al.* [11], the data contrast the finding from Watson *et al.* that ectopic expression of AR-V7 in AR-FL-overexpressing LNCaP xenograft tumors does not affect the growth inhibitory efficacy of enzalutamide [20]. A plausible explanation for the discrepancy is that, in the context of AR overexpression, the growth of LNCaP tumors may be driven mainly by the AR-FL signaling, making enzalutamide highly effective irrespective of AR-V expression. Nonetheless, we showed that, when the ectopically-expressed AR-FL is lost in these tumors, they can become resistant to enzalutamide. The resistance is

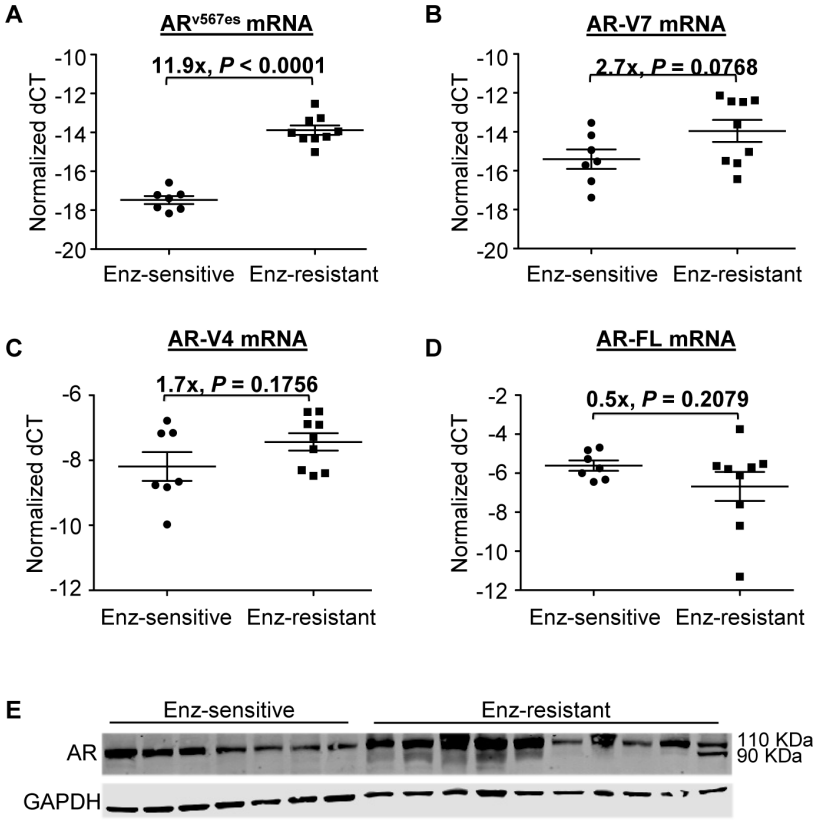

Figure 6: Increased AR-V expression in LNCaP tumors that have developed acquired resistance to enzalutamide. A-D. qRT-PCR analysis of the levels of AR-V transcripts. Fold changes are calculated from the difference in mean ΔC_T between the enzalutamide-sensitive and enzalutamide-resistant groups ($2^{\Delta\Delta CT}$). E. Western blot analysis of the levels of AR-FL and AR-V proteins.

accompanied by increased expression of AR^{v567es}. Thus, these tumors may also evade enzalutamide treatment through shifting towards AR-V-mediated signaling.

The significance of our finding that AR-Vs activate AR-FL to induce target-gene expression in an androgen-independent manner is based on the premise that AR-Vs and AR-FL are often co-expressed in biological contexts. This is supported by overlapping AR-FL and AR-V7 immunohistochemistry staining of adjacent sections of CRPC specimens [7]. This is also supported by the finding that androgen deprivation coordinately increases AR-FL and AR-V mRNAs by inducing the transcription of the AR gene and thereby increasing the recruitment of splicing factors to AR pre-mRNA to splice both AR-FL and AR-V mRNAs [9]. AR-V expression may also be a result of AR gene rearrangements [28,29], and gene-arrangement-caused AR-V production appears to occur at the expense of AR-FL [29]. However, a clonal selection process is required for gene-rearrangement-mediated AR-V production to be manifested at the level of tumor tissues. This appears to be in contrast to the rather rapid change of AR-V levels observed in xenograft tumors after androgen ablation or androgen replacement [15,20]. Further, different AR-Vs can be expressed in the same tissues. Clonal expansion of cells with one type of gene arrangement could lead to expression of one specific AR-V but may not be able to account for the expression of different AR-Vs. Finally, our data showing co-occupancy of AR-V7 and AR-FL on the PSA promoter in a mutually-dependent manner and increased response of AR-FL to androgen after AR-V7 knockdown provided further support to the co-expression of AR-FL and AR-V in the same cells. Thus, the ability of AR-Vs to activate AR-FL in an androgen-independent manner could be as important as their AR-FL-independent *trans*-activating activity in mediating castration resistance.

Our finding of AR-V and AR-FL co-regulating the expression of canonical androgen-responsive genes in androgen-deprived condition is reminiscent of the transcriptome data from Hu *et al*. that knockout of AR-FL in AR-V-transfected LNCaP cells almost completely abolishes the expression of at least a subset of canonical androgen-responsive genes [7]. In addition to regulating canonical androgen-responsive genes, AR-Vs have also been shown to regulate a distinct set of targets enriched for cell-cycle function [6,7,13]. This is further corroborated by our ChIP data showing the promoter of UBE2C is bound by AR-V7 but not AR-FL. Receptor dimerization is a crucial step of AR-FL activation [30]. AR^{v567es} has been shown to co-immunoprecipitate with AR-FL [15]. Here, we showed that AR-V7 and AR-FL co-reside on the promoter of their shared target. AR-V7 and AR^{v567es} can localize constitutively to the nucleus, and facilitate AR-FL nuclear localization in the absence of androgen. It is therefore possible that AR-V7 and AR^{v567es} dimerize with AR-FL in the cytoplasm in an androgen-independent manner, and the heterodimer translocates to the nucleus and binds to regulatory elements of their shared targets to regulate the transcription of these targets. It remains unknown as to whether dimerization is required for AR-Vs to regulate their specific targets. Future studies are needed to define the dimeric nature of AR-Vs in regulating gene expression.

In summary, our study provides further evidence to support AR-V upregulation as a means for prostate cancer cells to evade all androgen-directed therapies currently accepted in the clinic. Mechanistically, we identified a novel mechanism by which AR-Vs mediate castration-resistant progression. We showed that AR-Vs can activate AR-FL to induce target expression in an androgen-independent manner. By doing so, AR-Vs may serve as "rheostats" to control the degree of response of AR-FL to androgen and to androgen-directed therapy. Since AR-Vs are often co-expressed with AR-FL in biological contexts, this mechanism of AR-V action may be equally important as its AR-FL-independent activity to castration resistance. These findings underscore a critical need to develop effective means to target both AR-Vs and AR-FL to achieve complete AR blockade for more effective combat of these clinically challenging tumors. Several natural or synthetic compounds have been shown pre-clinically to inhibit AR-V and AR-FL actions [17,21,31-35]. Proof of efficacy in clinical trials is keenly awaited.

METHODS

Cell Lines and Reagents

LNCaP, 22Rv1, COS-7, and PC-3 cells were obtained from American Type Culture Collection at Passage 4. Cells used in this study were within 20 passages (~3 months of non-continuous culturing). All cell lines were tested and authenticated by the method of short tandem repeat profiling. Enzalutamide was purchased from Selleck Chemicals (Houston, TX), and the purity of >99% was confirmed by Nuclear Magnetic Resonance. The following antibodies were used in Western blot analysis: anti-glyceraldehyde-3-phosphate dehydrogenase (GAPDH, Millipore), anti-AR (N-terminus-directed; PG-21, Millipore), and anti-AR-V7 (Precision Antibody). Cell growth was determined by the Sulforhodamine assay.

Subcellular Localization

AR subcellular localization is detected by confocal fluorescence microscopy. The pTurboFP-AR-V7 and pTurboFP-AR^{v567es} plasmids were generated by cloning the cDNA fragments for AR-V7 and AR^{v567es}, respectively, into the pCMV-TurboFP635 vector. COS-7 or PC-3 cells were transfected with indicated plasmids and cultured in phenol

red-free RPMI-1640 supplemented with 10% charcoal-stripped fetal bovine serum. At 40 hr after transfection, cells were pre-treated with or without 10 μM enzalutamide for 2 hr, followed by treatment with or without 1 nM R1881 for 3 hr. The COS-7 cells were then fixed with 2% paraformaldehyde, and the nuclei stained with 2.5 μM DRAQ5 (Cell Signaling). The PC-3 cells were then fixed with 70% ethanol, and the nuclei stained with DAPI. Confocal images were obtained by using a Leica TCS SP2 system with a 63X oil-immersion objective on a Z-stage, and an average of 6 fields with ~10 cells per field was captured for each group. Data quantitation was performed as described [18].

qRT-PCR

qRT-PCR was performed as described [36]. The qPCR primer-probe sets for PSA, transmembrane protease, serine 2 (TMPRSS2), cyclin A2 (CCNA2), and UBE2C were from IDT. The primer sequences for AR isoforms were as described [13].

ChIP and Re-ChIP

ChIP and Re-ChIP were performed as described [37]. The following antibodies were used: mouse IgG2a (ab18413, abcam), rabbit IgG (ab46540, abcam), AR-FL-specific antibody (C-terminus-directed; C-19, sc-815 x, Santa Cruz Biotech), AR-V7-specific antibody (AG10008, Precision Antibody). The PSA promoter P2-ARE primers described by Guo *et al*. [13] and the UBE2C promoter primers described by Wang *et al*. [38] were used for qPCR analysis of ChIP or re-ChIP DNA. The RPL30 exon 3 control region (Cell Signaling) was used as a negative control.

Tumor Xenografts

Xenograft studies were conducted essentially as described [22,32]. LNCaP cells ($4x10^6$) infected with lentivirus encoding AR-FL or 22Rv1 cells infected with lentivirus encoding control shRNA or AR-V7 shRNA were inoculated into castrated or intact nude mice (Charles River), respectively. The cells were mixed with 50% Matrigel and inoculated subcutaneously on the right dorsal flank. Tumor volume was calculated as $0.524 \times width^2 \times length$ [39]. When the tumor size reached ~100 mm^3, the mice were randomized to daily treatment with vehicle or 10 mg/kg/day enzalutamide through oral gavage as described [22].

For the development of enzalutamide-resistant tumors, two LNCaP tumors that relapsed after enzalutamide treatment were resected, and ~20 mm^3 pieces of the tumors were transplanted into castrated nude mice. When the tumor bits grew to 100~200 mm^3, the mice started to receive 10 mg/kg/day enzalutamide through oral gavage. The tumors were harvested when they reached ~800 mm^3 and serially passaged in castrated nude mice following the same protocol. The second to fourth passages of tumors were considered as enzalutamide-resistant. All animal procedures were approved by the Tulane University Institutional Animal Care and Use Committee.

Statistical Analysis

The *Student's* two-tailed t test was used to determine the mean differences between two groups. $P < 0.05$ is considered significant. Data are presented as mean ± SEM.

ACKNOWLEDGEMENTS

We are grateful to Dr. Yun Qiu for AR-FL and AR-V7 cDNA and shRNA constructs, and Drs. Jun Luo, and Sanjiv Gambhir for pEGFP-AR and pCMV-TurboFP635 constructs, respectively. This work was supported by the following grants: NCI K01CA114252, ACS RSG-07-218-01-TBE, DOD W81XWH-12-1-0112 and W81XWH-12-1-0275, Louisiana Board-of-Regents Grant LEQSF(2012-15)-RD-A-25, Louisiana Cancer Research Consortium Fund, National Natural Science Foundation of China 81272851. S.R.P. was funded by P01-CA163227-01A1, DOD-W81XWH-13-2-0093, 2 P50 CA 097186-12, and Veterans Affairs Research Service.

Editorial note:

This paper has been accepted based in part on peer-review conducted by another journal and the authors' response and revisions as well as expedited peer-review in Oncotarget

REFERENCES

1. Egan A, Dong Y, Zhang H, Qi Y, Balk SP, Sartor O. Castration-resistant prostate cancer: Adaptive responses in the androgen axis. Cancer Treat.Rev. 2014; 40: 426-33.
2. Knudsen KE, Scher HI. Starving the addiction: new opportunities for durable suppression of AR signaling in prostate cancer. Clin.Cancer Res. 2009; 15: 4792-8.
3. Chen CD, Welsbie DS, Tran C, Baek SH, Chen R, Vessella R, Rosenfeld MG, Sawyers CL. Molecular determinants of resistance to antiandrogen therapy. Nat.Med. 2004; 10: 33-9.
4. Fizazi K, Scher HI, Molina A, Logothetis CJ, Chi KN, Jones RJ, Staffurth JN, North S, Vogelzang NJ, Saad F, Mainwaring P, Harland S, Goodman OB, Jr., Sternberg CN, Li JH, Kheoh T et al. Abiraterone acetate for treatment of

metastatic castration-resistant prostate cancer: final overall survival analysis of the COU-AA-301 randomised, double-blind, placebo-controlled phase 3 study. Lancet Oncol. 2012; 13: 983-92.

5. Scher HI, Fizazi K, Saad F, Taplin ME, Sternberg CN, Miller K, de WR, Mulders P, Chi KN, Shore ND, Armstrong AJ, Flaig TW, Flechon A, Mainwaring P, Fleming M, Hainsworth JD et al. Increased survival with enzalutamide in prostate cancer after chemotherapy. N.Engl.J.Med. 2012; 367: 1187-97.
6. Hornberg E, Ylitalo EB, Crnalic S, Antti H, Stattin P, Widmark A, Bergh A, Wikstrom P. Expression of androgen receptor splice variants in prostate cancer bone metastases is associated with castration-resistance and short survival. PLoS One. 2011; 6: e19059.
7. Hu R, Lu C, Mostaghel EA, Yegnasubramanian S, Gurel M, Tannahill C, Edwards J, Isaacs WB, Nelson PS, Bluemn E, Plymate SR, Luo J. Distinct transcriptional programs mediated by the ligand-dependent full-length androgen receptor and its splice variants in castration-resistant prostate cancer. Cancer Res. 2012; 72: 3457-62.
8. Li Y, Chan SC, Brand LJ, Hwang TH, Silverstein KA, Dehm SM. Androgen receptor splice variants mediate enzalutamide resistance in castration-resistant prostate cancer cell lines. Cancer Res. 2012; 73: 483-9.
9. Liu LL, Xie N, Sun S, Plymate S, Mostaghel E, Dong X. Mechanisms of the androgen receptor splicing in prostate cancer cells. Oncogene. 2013 Jul 15; [Epub ahead of print].
10. Mostaghel EA, Marck BT, Plymate SR, Vessella RL, Balk S, Matsumoto AM, Nelson PS, Montgomery RB. Resistance to CYP17A1 Inhibition with Abiraterone in Castration-Resistant Prostate Cancer: Induction of Steroidogenesis and Androgen Receptor Splice Variants. Clinical Cancer Research. 2011; 17: 5913-25.
11. Nadiminty N, Tummala R, Liu C, Yang J, Lou W, Evans CP, Gao AC. NF-kappaB2/p52 Induces Resistance to Enzalutamide in Prostate Cancer: Role of Androgen Receptor and Its Variants. Mol.Cancer Ther. 2013; 12: 1629-37.
12. Dehm SM, Schmidt LJ, Heemers HV, Vessella RL, Tindall DJ. Splicing of a novel androgen receptor exon generates a constitutively active androgen receptor that mediates prostate cancer therapy resistance. Cancer Res. 2008; 68: 5469-77.
13. Guo Z, Yang X, Sun F, Jiang R, Linn DE, Chen H, Chen H, Kong X, Melamed J, Tepper CG, Kung HJ, Brodie AM, Edwards J, Qiu Y. A novel androgen receptor splice variant is up-regulated during prostate cancer progression and promotes androgen depletion-resistant growth. Cancer Res. 2009; 69: 2305-13.
14. Hu R, Dunn TA, Wei S, Isharwal S, Veltri RW, Humphreys E, Han M, Partin AW, Vessella RL, Isaacs WB, Bova GS, Luo J. Ligand-independent androgen receptor variants derived from splicing of cryptic exons signify hormone-refractory prostate cancer. Cancer Res. 2009; 69: 16-22.
15. Sun S, Sprenger CC, Vessella RL, Haugk K, Soriano K, Mostaghel EA, Page ST, Coleman IM, Nguyen HM, Sun H, Nelson PS, Plymate SR. Castration resistance in human prostate cancer is conferred by a frequently occurring androgen receptor splice variant. J.Clin.Invest. 2010; 120: 2715-30.
16. Zhang X, Morrissey C, Sun S, Ketchandji M, Nelson PS, True LD, Vakar-Lopez F, Vessella RL, Plymate SR. Androgen receptor variants occur frequently in castration resistant prostate cancer metastases. PLoS One. 2011; 6: e27970.
17. Yamashita S, Lai KP, Chuang KL, Xu D, Miyamoto H, Tochigi T, Pang ST, Li L, Arai Y, Kung HJ, Yeh S, Chang C. ASC-J9 suppresses castration-resistant prostate cancer growth through degradation of full-length and splice variant androgen receptors. Neoplasia. 2012; 14: 74-83.
18. Chan SC, Li Y, Dehm SM. Androgen receptor splice variants activate androgen receptor target genes and support aberrant prostate cancer cell growth independent of canonical androgen receptor nuclear localization signal. J.Biol.Chem. 2012; 287: 19736-49.
19. Hu R, Isaacs WB, Luo J. A snapshot of the expression signature of androgen receptor splicing variants and their distinctive transcriptional activities. Prostate. 2011; 71: 1656-67.
20. Watson PA, Chen YF, Balbas MD, Wongvipat J, Socci ND, Viale A, Kim K, Sawyers CL. Constitutively active androgen receptor splice variants expressed in castration-resistant prostate cancer require full-length androgen receptor. Proc.Natl.Acad.Sci.U.S.A. 2010; 107: 16759-65.
21. Zhan Y, Cao B, Qi Y, Liu S, Zhang Q, Zhou W, Xu D, Lu H, Sartor O, Kong W, Zhang H, Dong Y. Methylselenol prodrug enhances MDV3100 efficacy for treatment of castration-resistant prostate cancer. Int.J.Cancer. 2013; 133: 2225-33.
22. Tran C, Ouk S, Clegg NJ, Chen Y, Watson PA, Arora V, Wongvipat J, Smith-Jones PM, Yoo D, Kwon A, Wasielewska T, Welsbie D, Chen CD, Higano CS, Beer TM, Hung DT et al. Development of a second-generation antiandrogen for treatment of advanced prostate cancer. Science. 2009; 324: 787-90.
23. Guo Z, Qiu Y. A new trick of an old molecule: androgen receptor splice variants taking the stage?! Int.J.Biol.Sci. 2011; 7: 815-22.
24. Balbas MD, Evans MJ, Hosfield DJ, Wongvipat J, Arora VK, Watson PA, Chen Y, Greene GL, Shen Y, Sawyers CL. Overcoming mutation-based resistance to antiandrogens with rational drug design. Elife. 2013; 2: e00499.
25. Korpal M, Korn JM, Gao X, Rakiec DP, Ruddy DA, Doshi S, Yuan J, Kovats SG, Kim S, Cooke VG, Monahan JE, Stegmeier F, Roberts TM, Sellers WR, Zhou W, Zhu P. An F876L Mutation in Androgen Receptor Confers Genetic and Phenotypic Resistance to MDV3100 (Enzalutamide). Cancer Discov. 2013; 3: 1030-43.

26. Joseph JD, Lu N, Qian J, Sensintaffar J, Shao G, Brigham D, Moon M, Maneval EC, Chen I, Darimont B, Hager JH. A Clinically Relevant Androgen Receptor Mutation Confers Resistance to Second-Generation Antiandrogens Enzalutamide and ARN-509. Cancer Discov. 2013; 3: 1020-9.

27. Arora VK, Schenkein E, Murali R, Subudhi SK, Wongvipat J, Balbas MD, Shah N, Cai L, Efstathiou E, Logothetis C, Zheng D, Sawyers CL. Glucocorticoid receptor confers resistance to antiandrogens by bypassing androgen receptor blockade. Cell. 2013; 155: 1309-22.

28. Li Y, Hwang TH, Oseth LA, Hauge A, Vessella RL, Schmechel SC, Hirsch B, Beckman KB, Silverstein KA, Dehm SM. AR intragenic deletions linked to androgen receptor splice variant expression and activity in models of prostate cancer progression. Oncogene. 2012; 31: 4759-67.

29. Nyquist MD, Li Y, Hwang TH, Manlove LS, Vessella RL, Silverstein KA, Voytas DF, Dehm SM. TALEN-engineered AR gene rearrangements reveal endocrine uncoupling of androgen receptor in prostate cancer. Proc.Natl.Acad. Sci.U.S.A. 2013; 110: 17492-7.

30. Centenera MM, Harris JM, Tilley WD, Butler LM. Minireview: The Contribution of Different Androgen Receptor Domains to Receptor Dimerization and Signaling. Mol Endocrinol. 2008; 22: 2373-82.

31. Andersen RJ, Mawji NR, Wang J, Wang G, Haile S, Myung JK, Watt K, Tam T, Yang YC, Banuelos CA, Williams DE, McEwan IJ, Wang Y, Sadar MD. Regression of Castrate-Recurrent Prostate Cancer by a Small-Molecule Inhibitor of the Amino-Terminus Domain of the Androgen Receptor. Cancer Cell. 2010; 17: 535-46.

32. Cao B, Liu X, Li J, Liu S, Qi Y, Xiong Z, Zhang A, Wiese T, Fu X, Gu J, Rennie PS, Sartor O, Lee BR, Ip C, Zhao L, Zhang H et al. 20(S)-protopanaxadiol-aglycone downregulation of the full-length and splice variants of androgen receptor. Int.J.Cancer. 2013; 132: 1277-87.

33. Li J, Cao B, Liu X, Fu X, Xiong Z, Chen L, Sartor O, Dong Y, Zhang H. Berberine Suppresses Androgen Receptor Signaling in Prostate Cancer. Molecular Cancer Therapeutics. 2011; 10: 1346-56.

34. Li X, Liu Z, Xu X, Blair CA, Sun Z, Xie J, Lilly MB, Zi X. Kava components down-regulate expression of AR and AR splice variants and reduce growth in patient-derived prostate cancer xenografts in mice. PLoS One. 2012; 7: e31213.

35. Mashima T, Okabe S, Seimiya H. Pharmacological targeting of constitutively active truncated androgen receptor by nigericin and suppression of hormone-refractory prostate cancer cell growth. Mol.Pharmacol. 2010; 78: 846-54.

36. Dong Y, Lee SO, Zhang H, Marshall J, Gao AC, Ip C. Prostate specific antigen expression is down-regulated by selenium through disruption of androgen receptor signaling. Cancer Res. 2004; 64: 19-22.

37. Furlan-Magaril M, Rincón-Arano Hc, Recillas-Targa F. Sequential Chromatin Immunoprecipitation Protocol: ChIP-reChIP. DNA-Protein Interactions (543 edition) 2008: 253-66.

38. Wang Q, Li W, Zhang Y, Yuan X, Xu K, Yu J, Chen Z, Beroukhim R, Wang H, Lupien M, Wu T, Regan MM, Meyer CA, Carroll JS, Manrai AK, Janne OA et al. Androgen receptor regulates a distinct transcription program in androgen-independent prostate cancer. Cell. 2009; 138: 245-56.

39. Gleave ME, Hsieh JT, Wu HC, von Eschenbach AC, Chung LW. Serum prostate specific antigen levels in mice bearing human prostate LNCaP tumors are determined by tumor volume and endocrine and growth factors. Cancer Res. 1992; 52: 1598-605.

Androgen receptor splice variants circumvent AR blockade by microtubule-targeting agents

Guanyi Zhang[1,2,6], Xichun Liu[2,6], Jianzhuo Li[1,2,6], Elisa Ledet[4,5,6], Xavier Alvarez[7], Yanfeng Qi[3,6], Xueqi Fu[1], Oliver Sartor[4,5,6], Yan Dong[1,3,6], Haitao Zhang[2,6]

[1]College of Life Sciences, Jilin University, Changchun, P.R. China

[2]Department of Pathology, Tulane University School of Medicine, New Orleans, Louisiana, USA

[3]Department of Structural and Cellular Biology, Tulane University School of Medicine, New Orleans, Louisiana, USA

[4]Department of Medicine, Tulane University School of Medicine, New Orleans, Louisiana, USA

[5]Department of Urology, Tulane University School of Medicine, New Orleans, Louisiana, USA

[6]Tulane Cancer Center, Tulane University School of Medicine, New Orleans, Louisiana, USA

[7]Division of Comparative Pathology, Tulane National Primate Research Center, Covington, Louisiana, USA

Correspondence to:
Haitao Zhang, **e-mail:** hzhang@tulane.edu

Keywords: *androgen receptor, splice variants, prostate cancer, taxane chemotherapy, microtubule*

Received: *April 24, 2015* ***Accepted:*** *June 09, 2015* ***Published:*** *June 22, 2015*

ABSTRACT

Docetaxel-based chemotherapy is established as a first-line treatment and standard of care for patients with metastatic castration-resistant prostate cancer. However, half of the patients do not respond to treatment and those do respond eventually become refractory. A better understanding of the resistance mechanisms to taxane chemotherapy is both urgent and clinical significant, as taxanes (docetaxel and cabazitaxel) are being used in various clinical settings. Sustained signaling through the androgen receptor (AR) has been established as a hallmark of CRPC. Recently, splicing variants of AR (AR-Vs) that lack the ligand-binding domain (LBD) have been identified. These variants are constitutively active and drive prostate cancer growth in a castration-resistant manner. In taxane-resistant cell lines, we found the expression of a major variant, AR-V7, was upregulated. Furthermore, ectopic expression of two clinically relevant AR-Vs (AR-V7 and AR^{V567es}), but not the full-length AR (AR-FL), reduced the sensitivities to taxanes in LNCaP cells. Treatment with taxanes inhibited the transcriptional activity of AR-FL, but not those of AR-Vs. This could be explained, at least in part, due to the inability of taxanes to block the nuclear translocation of AR-Vs. Through a series of deletion constructs, the microtubule-binding activity was mapped to the LBD of AR. Finally, taxane-induced cytoplasm sequestration of AR-FL was alleviated when AR-Vs were present. These findings provide evidence that constitutively active AR-Vs maintain the AR signaling axis by evading the inhibitory effects of microtubule-targeting agents, suggesting that these AR-Vs play a role in resistance to taxane chemotherapy.

INTRODUCTION

Prostate cancer is the most common non-skin cancer and the second leading cause of cancer mortality in men in the United States. Androgen deprivation therapy, which disrupts androgen receptor (AR) signaling by reducing androgen levels through surgical or chemical castration, or by administration of anti-androgens that compete with androgens for binding to AR [1], is the first-line treatment for metastatic and locally advanced prostate cancer. While this regimen is effective initially, progression to the presently incurable and lethal stage, termed castration-resistant prostate cancer (CRPC), invariably occurs. In 2004, docetaxel-based chemotherapy is established as a first-line treatment and standard of care for patients with metastatic CRPC [2]. However, about half of the patients

do not respond to treatment and those do respond become refractory within one year. Several new treatments, including the new taxane cabazitaxel [3], the CYP17A1 inhibitor abiraterone [4], and the potent antiandrogen enzalutamide [5], have received FDA approval as second-line treatments for metastatic CRPC in recent years. However, the survival benefits are relatively small (< = 5 months) and patients eventually become refractory to treatments. Therefore, breakthroughs in the treatment of prostate cancer hinge upon better understandings of the mechanisms of therapeutic resistance of CRPC.

Paclitaxel, docetaxel, and cabazitaxel belong to the taxane family of chemotherapeutic agents. Taxanes bind to the microtubules and prevent their disassembly, thereby suppressing microtubule dynamics, leading to mitotic arrest and apoptosis [6]. This was believed to be the mechanism of action of taxanes in prostate cancer until recently when it was demonstrated by several groups that taxanes in fact inhibit the AR signaling pathway in prostate cancer. Taxanes have been shown to block the nuclear translocation of AR and inhibit the expression of AR-regulated genes [7, 8]. Additionally, Gan et al. showed that taxanes inhibit the transcriptional activity of AR by inducing FOXO1, a transcriptional repressor of AR [9]. It is well-established that CRPC cells remain addicted to AR signaling; therefore, the inhibitory effect on AR, rather than the antimitotic activity, could possibly be the predominant mechanism of action for taxanes in prostate cancer.

Sustained signaling through AR has been established as a hallmark of CRPC. Recently, alternative splicing variants of AR (AR-Vs) that lack the ligand-binding domain (LBD) have been identified [10–13]. These splice variants remain transcriptionally active in the absence of androgens and drive prostate cancer growth in a castration-resistant manner. In addition, these variants are reported to be prevalently upregulated in CRPC compared to hormone-naïve prostate cancer [10–13]. AR-Vs can regulate the expression of canonical androgen-responsive genes, as well as a unique set of target genes [12, 14]. In a significant portion of metastatic CRPC tissues, the variants proteins are expressed at a level comparable to that of the canonical, full-length AR (AR-FL) [15, 16]. Patients with high expression of two major AR-Vs, AR-V7 (also known as AR3) and AR^{v567es}, have shorter cancer-specific survival than other CRPC patients [15]. In addition, recent studies have provided strong support for a critical role of these AR-Vs in resistance to hormonal therapies, including enzalutamide and abiraterone [17–20].

Recently, laboratory and clinical studies have suggested the existence of a cross-resistance mechanism between taxane-based chemotherapy and second-line hormonal therapies [21–25]. In this study, we set out to test the potential roles of AR-Vs in modulating the response to taxane-based chemotherapy.

RESULTS

Taxane-resistant prostate cancer cell lines express higher levels of AR-V7

We first established taxane-resistant 22Rv1 and LNCaP95 lines by culturing cells in escalating doses of paclitaxel and docetaxel over a period of 2 months. The response to taxanes were determined by the MTT assay (Fig. 1, A–C). Western blotting analyses showed that the expression of AR-FL was reduced, whereas the expression of AR-V7 was robustly induced, in the 22Rv1 resistant lines in comparison with the passage-matched parental line (Fig. 1D). A similar, albeit less pronounced, induction of AR-V7 was observed in the LNCaP95 docetaxel-resistant line (Fig. 1E). These results suggest that the constitutive active AR-V7 was selectively up-regulated in taxane-resistant prostate cancer cells.

Expression of constitutively active AR-Vs impairs the cytotoxicity of taxanes

To directly test the roles of constitutively active AR-Vs in resistance to taxanes, we transfected AR-V7 and AR^{v567es} into the AR-V-null LNCaP cells, and measured the responses to taxanes. As shown in Fig. 2A, cell viability after docetaxel treatment was markedly higher in cells expressing AR-V7 or AR^{v567es}, but not in those overexpressing AR-FL, than in vector-transfected cells. Similar observations were made with paclitaxel and cabazitaxel (Supplementary Figure S1). In LNCaP95 cells, when the expression of AR-V7 was silenced by a V7-specific shRNA, cells became more sensitive to docetaxal and cabazitaxel (Fig. 2B). Taken together, these results suggest the expression of constitutively active AR-Vs negatively impacts the efficacies of taxanes in prostate cancer cells.

Transcriptional activities of the constitutively active AR-Vs are refractory to the taxanes

To understand the difference between AR-V7/AR^{v567es} and the AR-FL in cytoprotection against the taxanes, we investigated the influence of taxane treatment on the transactivation activities of these AR isoforms. COS-7, which does not express any AR proteins, was chosen in this experiment to avoid interference from the endogenous AR. As shown in Fig. 3, treatment with docetaxel or paclitaxel dose-dependently inhibited the ligand-dependent transcriptional activity of AR-FL, but neither drug was able to inhibit the constitutive activities of AR-V7 and AR^{v567es}. This disparity can't be attributed to the down-regulation of AR-FL expression, as all AR proteins were not affected by the treatments (Supplementary Figure S2). These results suggest that the transcriptional activities of the AR variants are refractory to the inhibitory effects of taxanes.

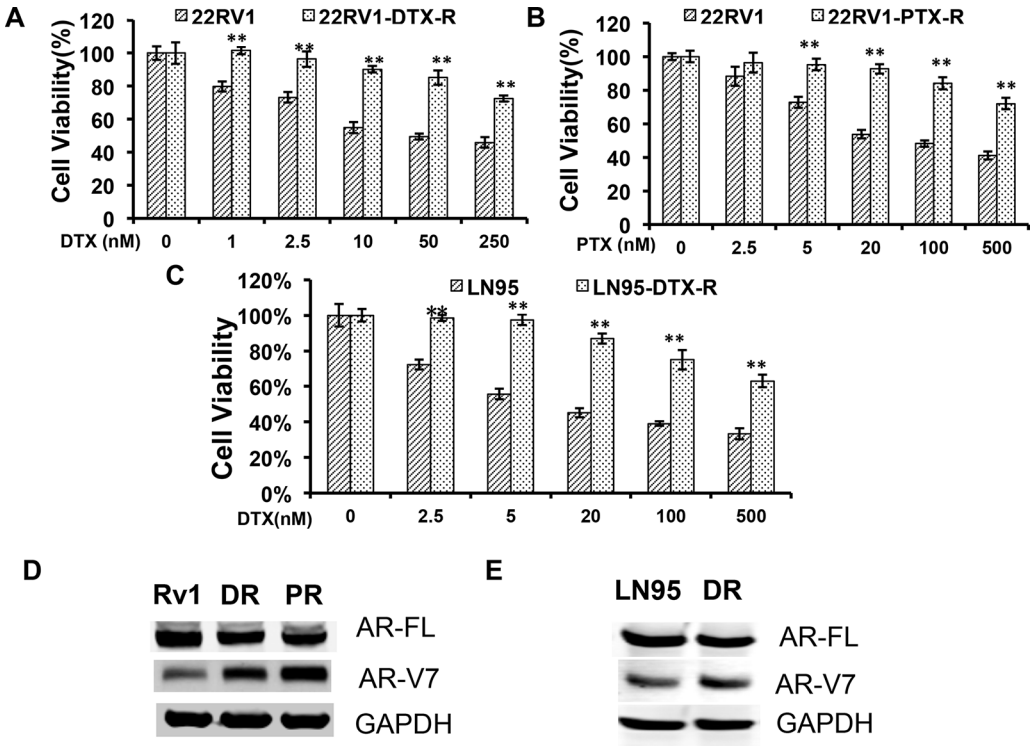

Figure 1: Upregulation of AR-V7 in taxane-resistant prostate cancer cells. A. and **B.** 22Rv1 with acquired resistance to taxanes were established by culturing in escalating doses of docetaxel (DTX) or paclitaxel (PTX). MTT assays were performed in passage-matched 22Rv1 or 22Rv1 resistant cells to determine the responses to taxanes. **C.** The response of DTX-resistant LNCaP95 to docetaxel treatment. **D.** and **E.** Western blotting using an anti-N terminal antibody or an AR-V7-specific antibody in 22Rv1 (D) or LNCaP95 (E) resistant cells. Rv1/LN95, passage-matched parental line; DR, docetaxel-resistant; PR, paclitaxel-resistant. The *P* values were determined by the *Student's t*-tests, ** denotes $P < 0.01$. The results presented are mean ± SEM from three experiments.

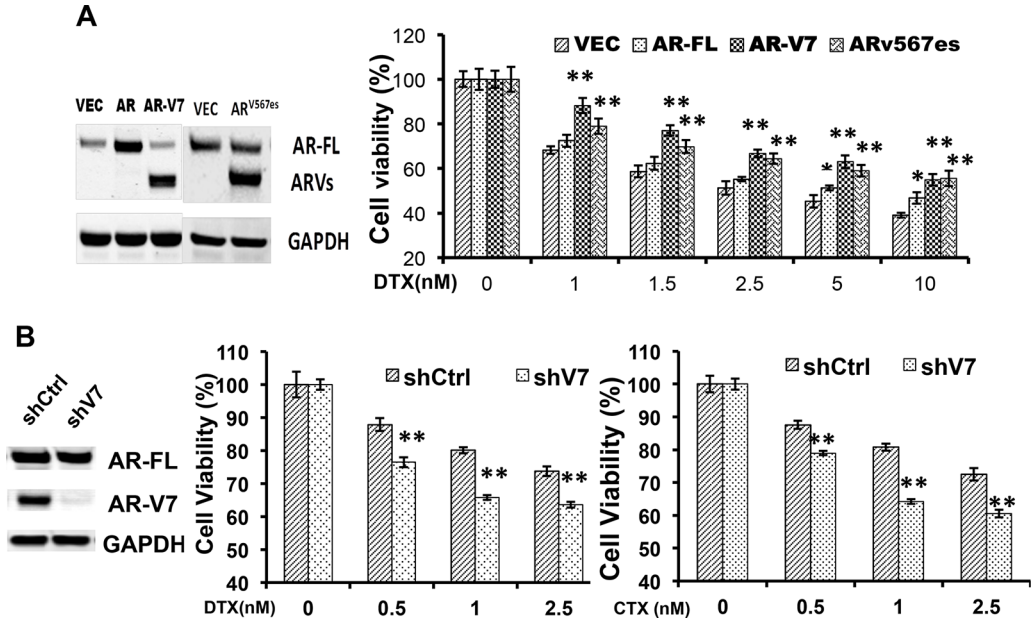

Figure 2: Expression of constitutively active AR-Vs negatively impact the cytotoxicities of taxanes. A. LNCaP cells were transfected with vector, AR-FL, AR-V7, or AR^{v567es}, and cell viability was determined by the MTT assay after 48 h of treatment with docetaxel. Western analysis was performed with an antibody recognizes the N-terminus of AR. The *P* values were determined by the *Student's t*-tests. *$P < 0.05$; **$P < 0.01$ vs vector. **B.** LNCaP95 cells were cultured in an androgen-depleted condition, and transfected with a control or an AR-V7-specific shRNA. **$P < 0.01$. CTX, cabazitaxel. The results presented are mean ± SEM.

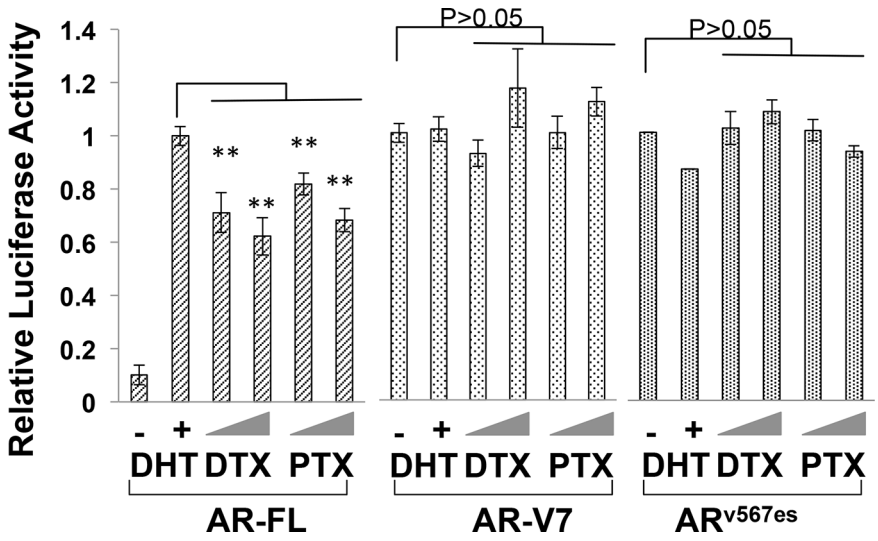

Figure 3: Transcriptional activities of constitutively active AR-Vs are refractory to taxane treatment. COS-7 cells were transfected with the ARR3-luc reporter plasmid along with a plasmid encoding AR-FL, AR-V7, or AR^{v567es}. The luciferase reporter assay was performed after 24 h treatment. The *P* values were determined by the *Student's t*-tests. $^{**}P < 0.01$ vs untreated. Doses: DTX, 1 and 2.5 nM; PTX, 2.5 and 5 nM. The results presented are mean ± SEM from three experiments.

Nuclear imports of constitutively active AR-Vs are microtubule-independent

Next, we investigated the influence of the taxanes on nuclear translocation of AR-V7 and AR^{v567es}, as these agents have been shown to block that of AR-FL [7, 8]. Enhanced green fluorescent protein (EGFP)-tagged AR-FL and AR-V7 were expressed in COS-7 cells and the localization of the fusion proteins was analyzed by fluorescence microscopy. Unlike EGFP-AR-FL, which required androgen stimulation for nuclear import, EGFP-AR-V7 spontaneously translocated to the nucleus (Supplementary Figure S3). When docetaxel and paclitaxel were added to the culture medium following androgen stimulation, accumulation of AR-FL in the cytoplasm was observed after 24 h of treatment (Supplementary Figure S3). However, treatment with the taxanes had no effect on the subcellular distribution of AR-V7.

To validate the results above, we performed fluorescence recovery after photobleaching (FRAP) assays in COS-7 cells expressing fluorescence-tagged AR proteins. Following treatment with docetaxel, selected nuclei were photobleached and the cells were imaged at regular intervals. Nuclear translocation is indicated by recovery of the nuclear to cytoplasmic fluorescence ratio (Fn/c). As indicated by the confocal images (Fig. 4A) and the fractional recovery plots (Fig. 4B), nuclear import of AR-FL was greatly deterred by docetaxel. In contrast, the nuclear translocations of AR-V7 and AR^{v567es} were not affected by docetaxel, evidenced by similar Fn/c recovery curves in control and treated cells (Fig. 4B). To substantiate these findings, we performed FRAP assays with additional microtubule inhibitors. KX-01 is a novel peptidomimetic inhibitor of Src family of kinases, but also inhibits tubulin polymerization [26], and nocodazole causes microtubule disassembly [27]. Once again, these drugs inhibited the nuclear import of AR-FL, but not that of AR-V7 or AR^{v567es} (Fig. 4B). Collectively, these results suggest the nuclear translocation of AR-V7 or AR^{v567es} are not mediated by the microtubules.

AR associates with the microtubules through the LBD

Proteins that use the microtubule pathway for nuclear import are known to bind to the microtubules [28, 29]. To test whether AR binds to the microtubules, we conducted *in vivo* microtubule-binding assays in COS-7 cells ectopically expressing AR. Under the condition in which the microtubules were stabilized, the majority of AR-FL co-precipitated with the microtubules and was found in the pellet (Fig. 5). Importin β was used as a negative control as previously described [29], and p53, which is known to be a microtubule-binding protein [30], was used as the positive control. The microtubule-binding activity was quantitated by the pellet to supernatant (P/S) ratio [29]. In contrast, when nocodazole, $CaCl_2$, or low temperature was employed to disrupt microtubule integrity, AR-FL shifted from the pellet to the supernatant, leading to marked decreases of the P/S ratios. These results suggest the AR-FL is a microtubule-associated protein.

To map the region responsible for microtubule-binding on AR, we generated a series of deletion constructs encompassing different domains of AR (Fig. 6, left panel). These constructs were analyzed by the microtubule binding assay. As shown in

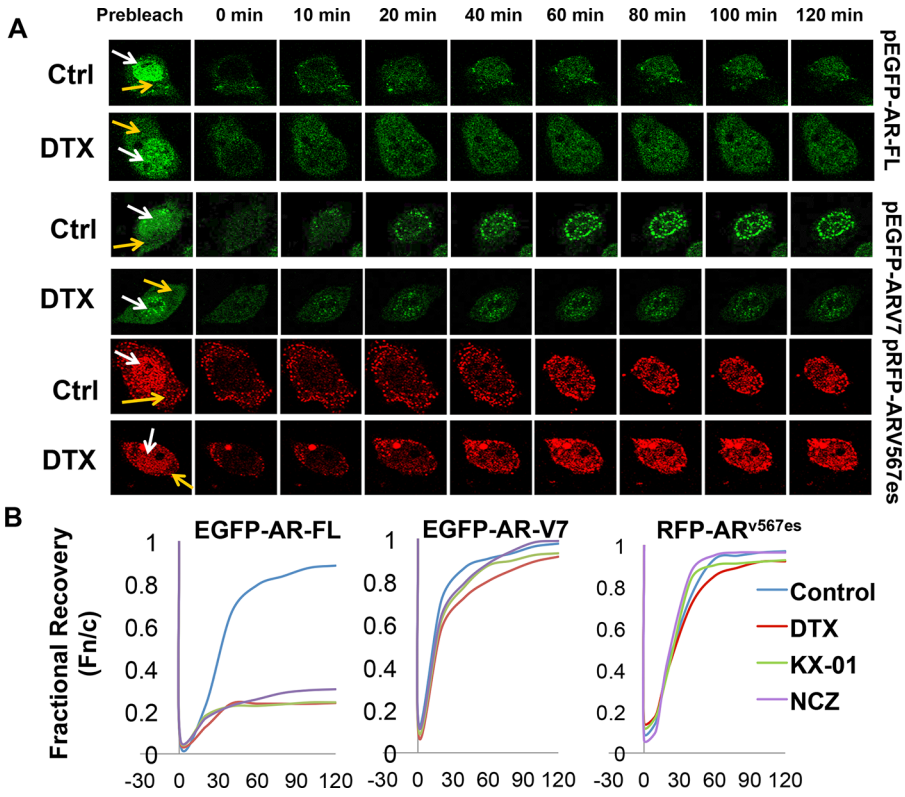

Figure 4: Nuclear imports of constitutively active AR-Vs are microtubule-independent. FRAP assays were performed in COS-7 cells expressing different fluorescence-tagged AR proteins. Cells transfected with EGFP-AR-FL were cultured in the presence of androgen. Cells were treated with 20 nM docetaxel for 2 h before photobleaching. **A.** Confocal images taken at different intervals after photobleaching of the nuclei. White and yellow arrows indicate the nucleus and the cytoplasm, respectively. **B.** Recovery plot of the nuclear:cytoplamic fluorescence ratio (Fn/c) over time in cells treated with different microtubule inhibitors. Fn/c ratios are expressed as fractions of the pre-photobleach Fn/c. Nocodazole (NCZ) was used at 5 μg/ml and KX-01 was at 100 nM. FRAP images for NCZ and KX-01 are in Supplementary Figure S4.

Supplementary Figure S4A and Figure 6 (right panel), all constructs lacking the LBD have poor microtubule-binding activities. In contrast, those retaining the LBD have similar binding activities as that of AR-FL (Supplementary Figure S4B and Figure 6). These results indicate that microtubule association is mediated by the LBD. Consistent with this finding, we found that the LBD-truncated AR-V7 and AR^{v567es} both bind poorly to the microtubules (Fig. 7).

AR-Vs interfere with docetaxel-mediated AR-FL cytoplasmic retention

It has been previously shown that both AR-V7 and AR^{v567es} facilitate AR-FL nuclear translocation in the absence of androgen [13, 19]. To investigate whether AR-Vs mitigate the inhibitory effect of AR-FL nuclear translocation by docetaxel, we expressed EGFP-AR-FL with or without TurboFP635-tagged AR-V7 or AR^{v567es} in the AR-null COS-7 cells. When co-expressed with TurboFP635, EGFP-AR-FL was retained in the cytoplasm following docetaxel treatment (Fig. 8A). However, in the presence of AR-V7-TurboFP635 or AR^{v567es}-TurboFP635, the inhibitory effect of docetaxel was significantly attenuated (Fig. 8A & 8B).

To further understand how AR-Vs circumvent docetaxel-mediated cytoplasmic sequestration of AR-FL, we conducted the microtubule-binding assay in COS-7 cells co-transfected with AR-FL and an AR-V. As shown in Fig. 8C, the binding of AR-FL to the microtubules was markedly reduced when it was co-expressed with AR-V7 or AR^{v567es}. Taken together, these results suggest that the constitutively active AR-V7 or AR^{v567es} could divert AR away from the microtubules, and facilitate its nuclear translocation in a microtubule-independent manner.

Nuclear import of AR-Vs is blocked by an importin β inhibitor

As an initial attempt to elucidate the nuclear translocation mechanisms of AR-V7 and AR^{v567es}, we investigated the involvement of the importin α/β machinery. FRAP assay was conducted in COS-7 transfected with EGFP-AR-V7 and treated with importazole, a specific inhibitor of importin β [31] . As shown by Fig. 9A & 9B, treatment with importazole

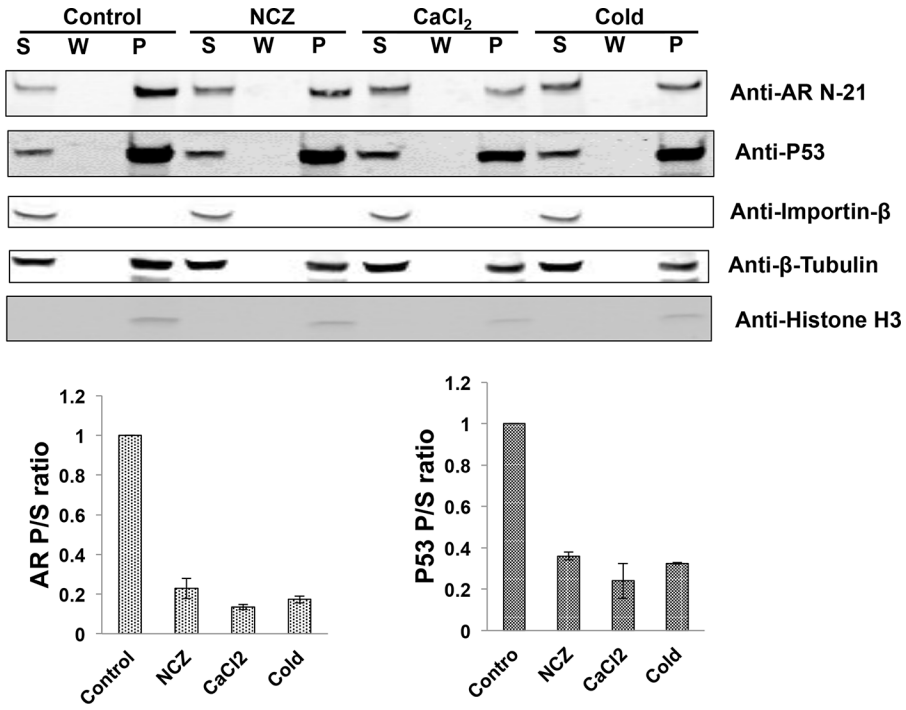

Figure 5: The full-length AR associates with the microtubules. COS-7 cells were transfected with an expression vector for AR-FL and *in vivo* microtubule binding assay was performed with a commercial kit (Cytoskeleton, BK038). Nocodazole (NCZ), $CaCl_2$, and low temperature (cold) were used to disrupt microtubule integrity. Assembled microtubules were precipitated by ultracentrifugation and the pellet was resuspended and analyzed by Western blot (Top). Importin β and p53 were used as negative and positive controls, respectively, and histone H3 was used to detect nuclear contamination. P, pellet; W, wash; S, supernatant. Bottom, the microtubule-binding activities for AR and p53 were quantitated by the P/S ratios. The results presented are mean ± SEM from three experiments.

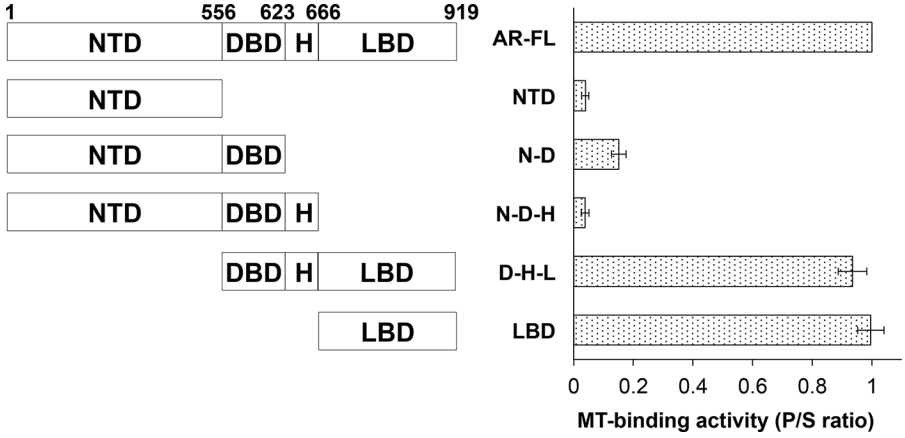

Figure 6: Microtubule-binding activity is mapped to the ligand-binding domain of AR. Left panel, a series of deletion constructs encompassing different domains of AR were generated and expressed in COS-7 cells. Right panel, the microtubule-binding activities of these constructs were analyzed by the *in vivo* microtubule binding assay and the Western blots (Supplementary Figure S5) were quantitated to calculate the P/S ratios. The results presented are mean ± SEM from three experiments. MT, microtubule.

significantly reduced the recovery of AR-V7 in the nucleus. Consistently, AR-V7 was found to accumulate in the cytoplasm following importazole treatment (Fig. 9C). FRAP assay showed a similar inhibition by importazole on the nuclear recovery of TurboFP635-tagged AR^{v567es} (Fig. 9D & 9E), suggesting that both variants are imported to the nucleus by the importin α/β machinery.

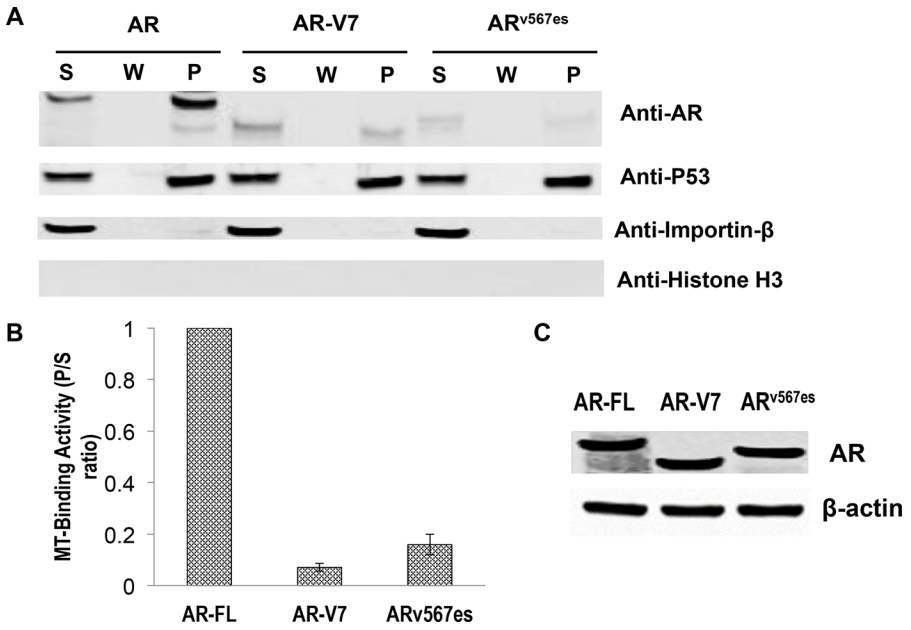

Figure 7: Poor microtubule-binding activities of the AR-Vs. COS-7 cells were transfected with an expression vector for AR-FL, AR-V7, and AR^{v567es} and cultured in an androgen-deprived condition. **A.** *In vivo* MT-binding assays. **B.** quantitation of the results in A. The results presented are mean ± SEM from three experiments. **C.** Western blot showing that the proteins were expressed at similar levels after transfection.

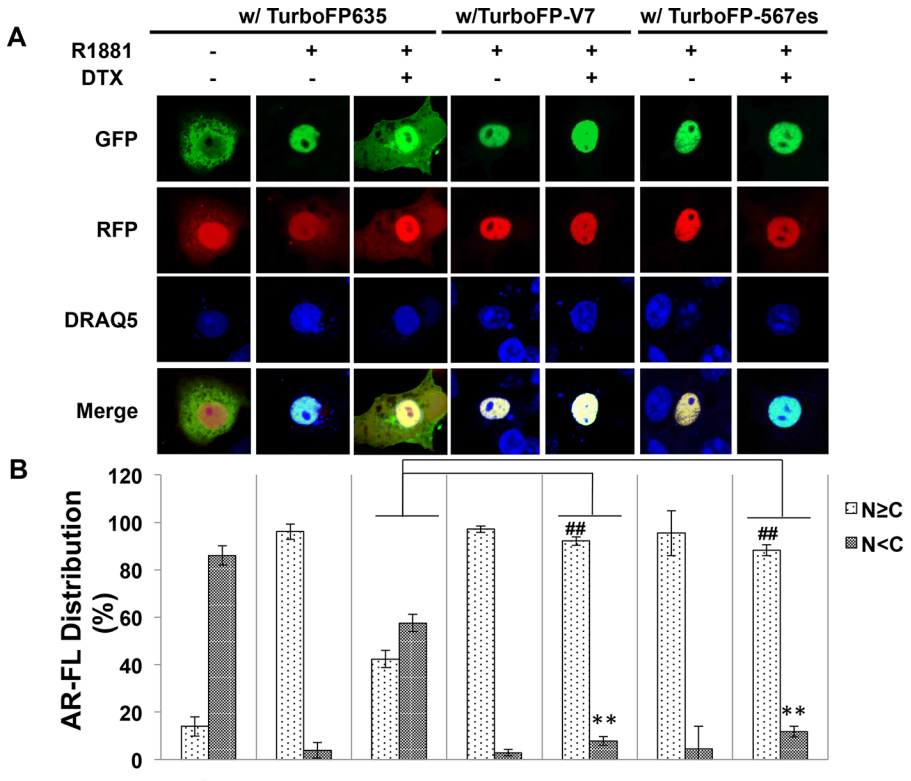

Figure 8: Cytoplasmic sequestration of AR-FL by docetaxel is attenuated by AR-V7 and AR^{v567es}. A. Confocal fluorescence microscopy of EGFP-AR-FL subcellular localization when it was expressed with TurboFP or with a TurboFP-tagged AR-V in COS-7 cells. **B.** Based on distribution of the green fluorescence signal, cells were categorized into cytoplasmic (N < C), or nuclear and equally nuclear and cytoplasmic (N ≥ C).% of cells in each category were quantified. DRAQ5 was used to stain the nuclei. Cells cultured in an androgen-deprived condition were pre-treated with 10 nM docetaxel for 6 hr, followed by treatment with 1 nM R1881 for 4 hr. ** and ## $P < 0.01$.

(*continued*)

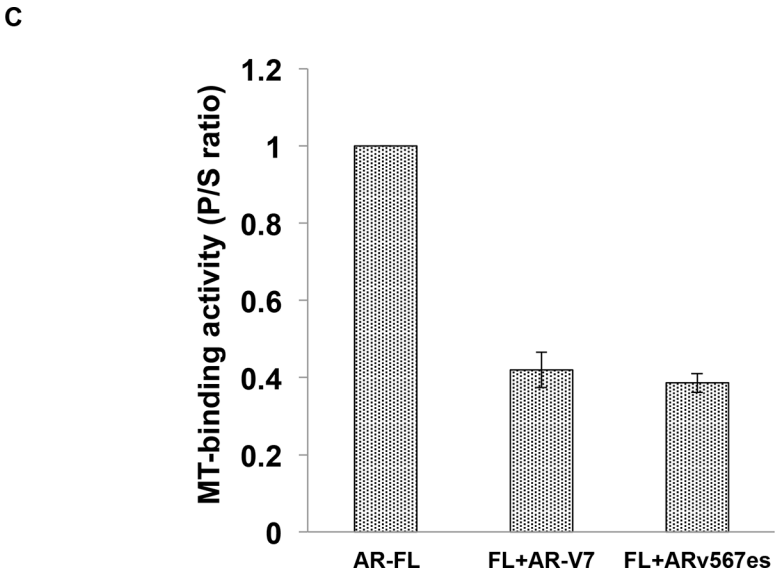

Figure 8: C. (*Continued*) *In vivo* MT-binding assay in COS-7 cells expressing AR-FL alone, or with AR-V7 or AR^{v567es}.

DISCUSSION

To date, docetaxel and cabazitaxel are the only chemotherapeutic agents that have been shown to offer survival benefits for patients with mCRPC. Even in today's rapidly evolving landscape of treatment options for mCRPC, taxane-based chemotherapy continues to be an important component of the treatment regimens. Recently, a randomized phase III trial supports the expansion of the indications of taxanes to earlier disease stages. The CHARRTED trial demonstrated that the addition of docetaxel to ADT in patients with high-volume, metastatic, hormonal-sensitive disease improves overall survival by 17 months (49.2 vs 32.2, $P = 0.0013$) than ADT alone [32]. With taxane chemotherapy projected to remain a mainstay in the treatment of prostate cancer, it is imperative to derive a better understanding of the mechanisms underlying the inherent and acquired taxane resistances, both of which are commonly observed in the clinic.

Resistance to taxanes could be multifactorial, involving general mechanisms of chemoresistance as well as mechanisms intrinsic to prostate cancer [33]. Existing literature focuses primarily on mechanisms common to many cancer types, including unfavorable tumor microenvironment, expression of drug efflux proteins, alterations in microtubule structure and/or function, expression of anti-apoptotic and cytoprotective proteins [34]. However, mechanisms that are specific to prostate cancer remain poorly understood. Recent clinical observations provided evidence for a cross-resistance of CRPC to hormonal therapy and taxane-based chemotherapy [21–25], suggesting a common culprit may underlie such a cross-resistance phenotype.

Our study represents a step forward in this direction. Herein, we present evidence that expression of constitutively active AR-Vs, but not over-expression of the canonical full-length receptor, protects prostate cancer cells from the cytotoxic effects of taxanes. We further show that taxane treatment selectively inhibits androgen-induced nuclear translocation and transactivation activity of AR-FL, while exerting no such inhibitory effects on the AR-Vs. These results reveal a fundamental difference in the nuclear translocation mechanisms of AR-FL and AR-Vs. AR-FL, as shown by this and other studies, utilizes a microtubule-facilitated pathway for nuclear translocation. This trafficking mechanism is shared by several nuclear proteins including glucocorticoid receptor (GR), p53, Rb, and parathyroid hormone-related protein (PTHrP) [29]. On the other hand, the nuclear import of AR-V7 and AR^{v567es} is not mediated by the microtubule pathway. The independence of the microtubule pathway enables the variants to evade taxane-induced cytoplasmic retention. Finally, we show that sequestration of AR-FL in the cytoplasm by taxanes is alleviated when AR-V7 or AR^{v567es} is present. This is likely caused by AR-V steering AR-FL away from the microtubules, as shown by reduced binding to the microtubules when AR-Vs are co-expressed. As an initial attempt to unveil the nuclear translocation mechanisms of the AR-Vs, we found that nuclear import of AR-V7 and AR^{v567es} is possibly mediated by the importin α/β machinery. Elucidation of the upstream events will likely lead to opportunities to design novel strategies to target this variant.

The clinical relevance of AR-Vs has been demonstrated by a myriad of studies. Higher expression of AR-V7 in hormone-naïve prostate tumors predicts increased risk of biochemical recurrence following radical

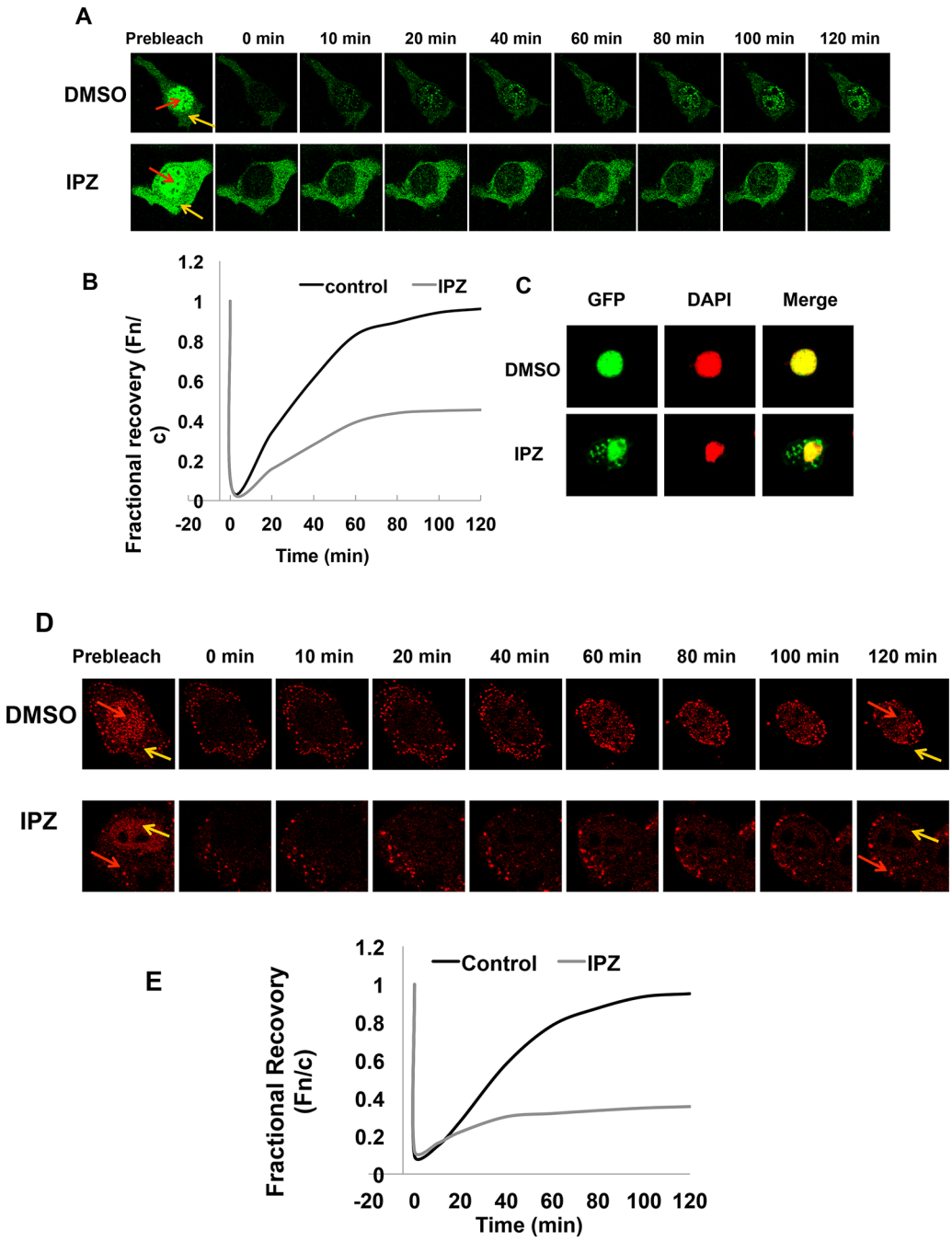

Figure 9: Nuclear translocation of AR-Vs is importin β-dependent. A. FRAP assays were performed in COS-7 cells expressing EGFP-tagged AR-V7. Cells were treated with DMSO or 50 μM importazole (IPZ) for 2 h before photobleaching. Confocal images taken at different intervals after photobleaching of the nuclei. Red and yellow arrows indicate nucleus and cytoplasm, respectively. **B.** Fn/c recovery plot for EGFP-AR-V7. **C.** COS-7 cells transfected with pEGFP-AR-V7 were treated with DMSO or 10 μM importazole for 48 h. DAPI was used for staining the nuclei. **D.** & **E.** confocal images (D) and Fn/c recovery plot (E) of FRAP assays in COS-7 cells expressing TurboFP635-tagged AR^{v567es} and treated with IPZ.

prostatectomy [11, 12], and patients with high levels of expression of AR-V7 or detectable expression of AR^{v567es} have a significantly shorter survival than other CRPC patients [15], indicating an association between AR-Vs expression and a more lethal form of prostate cancer. Studies have indicated that AR-Vs play important roles in resistance to androgen-directed therapies [17–19]. Particularly, a recent groundbreaking study by Antonarakis et al. showed that

patients positive for AR-V7 expression in circulating tumor cells have significantly worse responses to enzalutamide or abiraterone than AR-V7-negative patients [20].

While the roles of AR-Vs are well recognized in resistance to hormonal therapies, evidence has just started to accumulate to support their involvement in resistance to taxane chemotherapy. Thadani-Mulero and colleagues are the first to show evidence supporting a role of AR-V7 in resistance to taxane chemotherapy [35]. In addition, the study by Martin et al. [36] showed that in cells harboring AR-Vs, targeting the AR N-terminal domain of with a small molecule inhibitor enhances the therapeutic response to docetaxel [36]. A clinical study by Steinestel et al. showed expression of AR-V7 in circulating cancer cells significantly correlates with prior treatment with docetaxel [37]. Very recently, a clinical study presented at the American Society of Clinical Oncology Genitourinary Cancers Symposium investigated the responses to taxane chemotherapy in mCRPC patients with different AR-V7 status in circulating tumor cells [38]. Although all the clinical outcomes are worse in patients in the AR-V7(+) arm, the differences are not statistically significant [38]. The insignificant differences could result from the small sample size or due to a "threshold effect" of AR-V7. In other words, the influence of AR-V7 on taxane response may be manifested only when it is expressed above a certain level. Hence, the association of AR-Vs and sensitivity to taxane chemotherapy warrants further investigation in a larger cohort.

The main disparity between our study and that of Thadani-Mulero et al. [35] is on whether AR^{v567es} is inhibited by the taxanes. In contrast to the data present herein, Thadani-Mulero and colleagues showed that AR^{v567es} associates with the microtubules and that the nuclear translocation of AR^{v567es} is inhibited by taxanes. In addition, the microtubule-binding activity is mapped to the DNA-binding and hinge domains of AR [35]. One possible explanation for these discrepancies is the use of different assays. Thadani-Mulero et al. performed *in vitro* assays in which cell lysates containing AR proteins tagged by GFP or hemagglutinin were incubated with purified tubulin in a cell-free system to allow microtubule polymerization and association. In contrast, we conducted *in vivo* microtubule-binding assays in which the microtubules and associated proteins were extracted from cells expressing untagged AR isoforms. Another major difference between the two studies is the dosage of taxanes. Docetaxel was applied at a concentration of 1 μM in the cell culture studies by Thadani-Mulero et al., in contrast to the clinically attainable [39] nanomolar concentrations used in our studies. We demonstrated that treatment with taxanes, at the low nanomolar concentrations, fail to inhibit the transcriptional activity or nuclear import of AR^{v567es}.

The canonical AR nuclear localization signal (NLS) is located in the hinge domain, encoded by exons 3 and 4. Sequence analysis predicted that this NLS is truncated in AR-V7. However, the study by Chan et al. demonstrated that splicing of exon 3 with cryptic exon 3 in AR-V7 reconstitutes this bipartite NLS, which mediates the nuclear import of AR-V7 [40]. In addition, expression of a dominant negative mutant of Ran protein (RanQ69L) which causes premature dissociation of the importin/cargo complex, reduced nuclear localization of AR-V7 and AR^{v567es}. These findings are consistent with our importazole data, suggesting that the nuclear import of the AR-Vs is mediated by the importin α/β pathway. They also found that unlike AR-FL, the nuclear localization of AR-V7 and AR^{v567es} is not affected by an inhibitor for heat shock protein 90. Together, this study and our data present herein suggest a fundamental difference between AR-FL and AR-Vs in the events upstream of importin α/β-mediated nuclear entry.

In summary, our study provides support for the involvement of AR-V7 and AR^{v567es} in attenuating the response to taxane-based chemotherapy. Mechanistically, we demonstrated that both variants translocate to the nucleus in a microtubule-independent manner. Additionally, these variants can reduce the microtubule-binding activity of AR-FL, thus circumventing its cytoplasm sequestration triggered by taxanes. These findings have important clinical implications. The expression status of these AR variants could potentially be used as a biomarker to aid treatment selection and sequencing. More importantly, targeting AR-Vs could be a fruitful direction to pursue to enhance the efficacy of taxane chemotherapy. To this end, several small molecule inhibitors at various stages of clinical development have shown promises against AR-Vs [41–43], opening doors for novel therapeutic strategies.

MATERIALS AND METHODS

Cell lines and reagents

LNCaP, 22Rv1, and COS-7 cells were obtained from American Type Culture Collection. With the exception of drug-resistant lines, cells used in this study were within 20 passages (~3 months of non-continuous culturing). All cell lines were tested and authenticated by the method of short tandem repeat profiling. Docetaxel, cabazitaxel, and paclitaxel were purchased from Selleck Chemicals (Houston, TX). Nocodazole was from Sigma Aldrich, and KX-01 was provided by Kinex Pharmaceuticals. The following antibodies were used in Western blot analysis: anti-GAPDH, anti-AR (N-terminus-directed, PG-21; Millipore), anti-importin β1, anti-β-actin (Santa Cruz), anti-p53 (Calbiochem), anti-histone H3 (Cell Signaling), and anti-AR-V7 (Precision Antibody).

Selection of taxane resistant cell lines

22Rv1 cells were initially treated with 10 nM paclitaxel for 72 hours and the surviving cells were re-seeded and allowed to recover for 1 week.

Paclitaxel-resistant cells were developed over a period of 2 months by stepwise increasing concentrations of paclitaxel (5–50 nM). Age-matched parental cells which did not receive treatments were maintained in parallel. Docetaxel-resistant 22Rv1 and LNCaP95 lines were generated in a similar manner, but with different doses of docetaxel (5 nM initially, 2.5–20 nM for selection). The resistant cells were continuously maintained in the highest concentration of the taxane in which they selected.

Western blotting

Cells were washed with ice-cold phosphate-buffered saline (PBS) and lysed with 2X Cell Lysis Buffer (Cell Signaling) containing a phosphatase inhibitor and the protease inhibitor cocktail (Sigma). After incubating the cells on ice for 30 min, lysates were collected by centrifugation at 10, 000 rpm for 10 minutes. Protein concentrations were determined by the BCA Protein Assay kit (Pierce). The samples were separated on 10% SDS-polyacrylamide gels and transferred onto polyvinylidene fluoride (PVDF) membranes. After blocking in TBS buffer (150 mM NaCl, 10 mM Tris, pH 7.4) containing 5% nonfat milk, the blots were incubated with a primary antibody overnight at 4°C and a fluorescent-labeled secondary antibody for 1 h at room temperature. The fluorescent signals were obtained by the Odyssey Infrared Imaging System (LI-COR Bioscience).

Transient transfection and reporter gene assay

COS-7 cells were seeded in 10-cm dishes at a density to reach 80–90% confluency at time of transfection. Transient transfection was performed by using the Lipofectamine and Plus reagents following the manufacturer's instructions (Invitrogen). Cells were co-transfected with ARR3-luc luciferase reporter contruct and pRL-TK, along with a plasmid encoding for AR-FL, AR-V7 or AR^{v567es}. After incubating with the transfection mixture for 4 h, cells were re-plated in RPMI 1640 containing 10% charcoal-stripped fetal bovine serum (cs-FBS). Cells were allowed to recover overnight before treated with DTX (1 and 2.5 nM) or PTX (2.5 or 5 nM) in the presence or absence of 10 nM DHT. Dual-luciferase assay was performed at 24 h post treatment using the Dual-luciferase Reporter Assay System (Promega). The renilla luciferase activity was used to normalize that of firefly luciferase.

Confocal fluorescence microscopy

Subcellular localization of AR proteins was analyzed by confocal fluorescence microscopy. The pTurboFP635-AR-V7 and pTurboFP635-AR^{v567es} plasmids were generated by cloning the cDNA fragments for AR-V7 and AR^{v567es}, respectively, into the pCMV-TurboFP635 vector. COS-7 cells were transfected with indicated plasmids and cultured in phenol red-free RPMI-1640 supplemented with 10% cs-FBS. At 40 hr after transfection, cells were pre-treated with or without 10 nM docetaxel for 6 hr, followed by treatment with or without 1 nM R1881 for 4 hr. COS-7 cells were subsequently fixed with 2% paraformaldehyde, and the nuclei were stained with 2.5 μM DRAQ5 (Cell Signaling). Confocal images were obtained by using a Leica TCS SP2 system with a 63X oil-immersion objective on a Z-stage, and an average of 6 fields with ~10 cells per field were captured for each group. Data quantitation was performed as described [44].

Fluorescence recovery after photobleaching (FRAP) assay

FRAP assay was performed using a Leica TCS SP2 microscope equipped with 20X, 40X and 63X oil immersion lenses (Nikon) in combination with a heated stage (Delta T Open Dish System, Bioptechs), as described by Roth et al. [45] with modifications. Briefly, three images were obtained before photobleaching using 10% of total laser power with excitation at 488 nm, scanning at a rate of 8 μs/pixel. Photobleaching was performed by scanning an area covering the entire nucleus 10 times at a rate of 12.5 μs/pixel, applying 100% of the laser power. After bleaching, the recovery of fluorescence was monitored by scanning the cells at 1 minute intervals for up to 2 hours, using detector and laser settings identical to those prior to photobleaching. Image analysis was carried out by using the NIH Image J Software to quantitate the nuclear (Fn) and cytoplasmic (Fc) fluorescence signals. The ratios of Fn to Fc (Fn/c) were calculated and the extent of recovery was determined by fractional recovery of Fn/c, which is the Fn/c at each time point divided by the prebleach Fn/c. The data were fitted exponentially to generate the fractional recovery plot.

In vivo microtubule binding assay

The AR deletion constructs were generated by inserting PCR products of the corresponding cDNA regions into the pcDNA3.1(-) vector. The resulting plasmids were sequenced to confirm sequence accuracy and in-frame reading. COS-7 cells were transfected with indicated plasmids and cultured in RPMI 1640 medium supplemented with 10% cs-FBS. Microtubule-binding assay was performed by using the Microtubule/Tubulin *In Vivo* Assay Kit (Cytoskeleton Inc., Cat.# BK038) following the manufacturer's instructions. Briefly, 3×10^6 cells were lysed in 4 mL pre-warmed (37°C) Lysis and Microtubule Stabilization 2 (LMS2) buffer (100 mM PIPES, pH 6.9, 5 mM $MgCl_2$, 1mM EGTA, 30% (v/v) glycerol, 0.1% Nonidet P40, 0.1% Triton X-100, 0.1% Tween 20, 0.1% β-mercaptoethanol, 0.001% Antifoam, 100 μM GTP, 1 mM ATP, 1 × protease inhibitors cocktail) in a 10-cm cell culture dish. The lysates were collected

and spun at 2,000 g for 10 min at 37°C to remove nuclei and unbroken cells. The supernatants were then subjected to ultracentrifugation at 100, 000 g for 30 min at 37°C to separate the microtubules from the soluble, unpolymerized tubulin. The pellet was washed with pre-warmed LMS2 buffer and centrifuged at 100, 000 g for 30 min at 37°C. For microtubule destabilization conditions, LMS2 buffer containing nocodazole (5 μg/ml) or $CaCl_2$ (2 mM), or ice-cold LMS2 buffer were used in the above procedure. The pellets were resuspended in ice-cold 2 mM $CaCl_2$ and incubated in room temperature for 15 min to depolymerize microtubules. The supernatant (S), wash solution (W), and resuspended pellet (P) were adjusted to equal volumes and analyzed by Western blotting.

Statistical analysis

Statistical analysis was performed using Microsoft Excel. The *Student's* two-tailed *t*-test was used to determine the difference in means between two groups. $P < 0.05$ is considered significant. Data are presented as mean ± standard error of men (SEM).

ACKNOWLEDGMENTS

We are indebted to Dr. Yun Qiu for providing the AR-FL and AR-V7 cDNA constructs, to Dr. Stephen R. Plymate for the AR^{v567es} cDNA construct, to Dr. Jun Luo for the EGFP-AR-FL and EGFP-AR-V7 expression vectors, and to Dr. Rebecca Heald for providing importazole.

GRANT SUPPORT

This work was supported by the following grants: ACS RSG-07-218-01-TBE, DOD W81XWH-12-1-0275 and W81XWH-14-1-0480, NIH/NCI R01CA188609, Louisiana Board of Regents LEQSF(2012-15)-RD-A-25, NIH/NIGMS 5P20GM103518-10, Louisiana Cancer Research Consortium Fund, Oliver Sartor Prostate Cancer Research Fund, National Natural Science Foundation of China Projects 81272851 and 81430087.

CONFLICTS OF INTEREST

No conflicts of interest to declare.

REFERENCES

1. Harris WP, Mostaghel EA, Nelson PS, Montgomery B. Androgen deprivation therapy: progress in understanding mechanisms of resistance and optimizing androgen depletion. Nat Clin Pract Urol. 2009; 6:76–85.
2. Tannock IF, de WR, Berry WR, Horti J, Pluzanska A, Chi KN, Oudard S, Theodore C, James ND, Turesson I, Rosenthal MA, Eisenberger MA. Docetaxel plus prednisone or mitoxantrone plus prednisone for advanced prostate cancer. N Engl J Med. 2004; 351:1502–1512.
3. De Bono JS, Oudard S, Ozguroglu M, Hansen S, Machiels JP, Kocak I, Gravis G, Bodrogi I, Mackenzie MJ, Shen L, Roessner M, Gupta S, Sartor AO. Prednisone plus cabazitaxel or mitoxantrone for metastatic castration-resistant prostate cancer progressing after docetaxel treatment: a randomised open-label trial. Lancet. 2010; 376:1147–1154.
4. De Bono JS, Logothetis CJ, Molina A, Fizazi K, North S, Chu L, Chi KN, Jones RJ, Goodman OB, Saad F, Staffurth JN, Mainwaring P, Harland S, Flaig TW, Hutson TE, Cheng T, Patterson H, Hainsworth JD, Ryan CJ, Sternberg CN, Ellard SL, Flechon A, Saleh M, Scholz M, Efstathiou E, Zivi A, Bianchini D, Loriot Y, Chieffo N, Kheoh T, Haqq CM, Scher HI. Abiraterone and increased survival in metastatic prostate cancer. N Engl J Med. 2011; 364:1995–2005.
5. Scher HI, Fizazi K, Saad F, Taplin M-E, Sternberg CN, Miller K, de Wit R, Mulders P, Chi KN, Shore ND, Armstrong AJ, Flaig TW, Fléchon A, Mainwaring P, Fleming M, Hainsworth JD, Hirmand M, Selby B, Seely L, de Bono JS. Increased survival with enzalutamide in prostate cancer after chemotherapy. N Engl J Med. 2012; 367:1187–1197.
6. Jordan MA, Wilson L. Microtubules as a target for anticancer drugs. Nat Rev Cancer. 2004; 4:253–265.
7. Zhu ML, Horbinski CM, Garzotto M, Qian DZ, Beer TM, Kyprianou N. Tubulin-targeting chemotherapy impairs androgen receptor activity in prostate cancer. Cancer Res. 2010; 70:7992–8002.
8. Darshan MS, Loftus MS, Thadani-Mulero M, Levy BP, Escuin D, Zhou XK, Gjyrezi A, Chanel-Vos C, Shen R, Tagawa ST, Bander NH, Nanus DM, Giannakakou P. Taxane-induced blockade to nuclear accumulation of the androgen receptor predicts clinical responses in metastatic prostate cancer. Cancer Res. 2011; 71:6019–6029.
9. Gan L, Chen S, Wang Y, Watahiki A, Bohrer L, Sun Z, Wang Y, Huang H. Inhibition of the androgen receptor as a novel mechanism of taxol chemotherapy in prostate cancer. Cancer Res. 2009; 69:8386–8394.
10. Dehm SM, Schmidt LJ, Heemers HV, Vessella RL, Tindall DJ. Splicing of a novel androgen receptor exon generates a constitutively active androgen receptor that mediates prostate cancer therapy resistance. Cancer Res. 2008; 68:5469–5477.
11. Hu R, Dunn TA, Wei S, Isharwal S, Veltri RW, Humphreys E, Han M, Partin AW, Vessella RL, Isaacs WB, Bova GS, Luo J. Ligand-independent androgen receptor variants derived from splicing of cryptic exons signify hormone-refractory prostate cancer. Cancer Res. 2009; 69:16–22.
12. Guo Z, Yang X, Sun F, Jiang R, Linn DE, Chen H, Chen H, Kong X, Melamed J, Tepper CG, Kung HJ, Brodie AM, Edwards J, Qiu Y. A novel androgen receptor splice variant

is up-regulated during prostate cancer progression and promotes androgen depletion-resistant growth. Cancer Res. 2009; 69:2305–2313.

13. Sun S, Sprenger CC, Vessella RL, Haugk K, Soriano K, Mostaghel EA, Page ST, Coleman IM, Nguyen HM, Sun H, Nelson PS, Plymate SR. Castration resistance in human prostate cancer is conferred by a frequently occurring androgen receptor splice variant. J Clin Invest. 2010; 120:2715–2730.
14. Hu R, Lu C, Mostaghel EA, Yegnasubramanian S, Gurel M, Tannahill C, Edwards J, Isaacs WB, Nelson PS, Bluemn E, Plymate SR, Luo J. Distinct transcriptional programs mediated by the ligand-dependent full-length androgen receptor and its splice variants in castration-resistant prostate cancer. Cancer Res. 2012; 72:3457–3462.
15. Hornberg E, Ylitalo EB, Crnalic S, Antti H, Stattin P, Widmark A, Bergh A, Wikstrom P. Expression of androgen receptor splice variants in prostate cancer bone metastases is associated with castration-resistance and short survival. PLoS One. 2011; 6:e19059.
16. Zhang X, Morrissey C, Sun S, Ketchandji M, Nelson PS, True LD, Vakar-Lopez F, Vessella RL, Plymate SR. Androgen receptor variants cccur frequently in castration resistant prostate cancer metastases. PLoS ONE. 2011; 6:e27970.
17. Mostaghel EA, Marck BT, Plymate SR, Vessella RL, Balk S, Matsumoto AM, Nelson PS, Montgomery RB. Resistance to CYPA1 inhibition with abiraterone in castration-resistant prostate cancer: induction of steroidogenesis and androgen receptor splice variants. Clin Cancer Res. 2011; 17:5913–5925.
18. Li Y, Chan SC, Brand LJ, Hwang TH, Silverstein KAT, Dehm SM. Androgen receptor splice variants mediate enzalutamide resistance in castration-resistant prostate cancer Cell Lines. Cancer Res. 2013; 73:483–489.
19. Cao B, Qi Y, Zhang G, Xu D, Zhan Y, Alvarez X, Guo Z, Fu X, Plymate SR, Sartor O, Zhang H, Dong Y. Androgen receptor splice variants activating the full-length receptor in mediating resistance to androgen-directed therapy. Oncotarget. 2014; 5:1646–1656.
20. Antonarakis ES, Lu C, Wang H, Luber B, Nakazawa M, Roeser JC, Chen Y, Mohammad TA, Chen Y, Fedor HL, Lotan TL, Zheng Q, De Marzo AM, Isaacs JT, Isaacs WB, Nadal R, Paller CJ, Denmeade SR, Carducci MA, Eisenberger MA, Luo J. AR-V7 and resistance to enzalutamide and abiraterone in prostate cancer. N Engl J Med. 2014; 371:1028–1038.
21. Mezynski J, Pezaro C, Bianchini D, Zivi A, Sandhu S, Thompson E, Hunt J, Sheridan E, Baikady B, Sarvadikar A, Maier G, Reid AHM, Mulick Cassidy A, Olmos D, Attard G, de Bono J. Antitumour activity of docetaxel following treatment with the CYP17A1 inhibitor abiraterone: clinical evidence for cross-resistance? Ann Oncol Off J Eur Soc Med Oncol ESMO. 2012; 23:2943–2947.
22. Schweizer MT, Zhou XC, Wang H, Bassi S, Carducci MA, Eisenberger MA, Antonarakis ES. The influence of prior abiraterone treatment on the clinical activity of docetaxel in men with metastatic castration-resistant prostate cancer. Eur Urol. 2014; 66:646–652.
23. Van Soest RJ, van Royen ME, de Morrée ES, Moll JM, Teubel W, Wiemer EAC, Mathijssen RHJ, de Wit R, van Weerden WM. Cross-resistance between taxanes and new hormonal agents abiraterone and enzalutamide may affect drug sequence choices in metastatic castration-resistant prostate cancer. Eur J Cancer. 2013; 49:3821–3830.
24. Nadal R, Zhang Z, Rahman H, Schweizer MT, Denmeade SR, Paller CJ, Carducci MA, Eisenberger MA, Antonarakis ES. Clinical activity of enzalutamide in docetaxel-naïve and docetaxel-pretreated patients with metastatic castration-resistant prostate cancer. The Prostate. 2014; 74:1560–1568.
25. Cheng HH, Gulati R, Azad A, Nadal R, Twardowski P, Vaishampayan UN, Agarwal N, Heath EI, Pal SK, Rehman HT, Leiter A, Batten JA, Montgomery RB, Galsky MD, Antonarakis ES, Chi KN, Yu EY. Activity of enzalutamide in men with metastatic castration-resistant prostate cancer is affected by prior treatment with abiraterone and/or docetaxel. Prostate Cancer Prostatic Dis. 2015; 18:122–127.
26. Anbalagan M, Ali A, Jones RK, Marsden CG, Sheng M, Carrier L, Bu Y, Hangauer D, Rowan BG. Peptidomimetic Src/pretubulin inhibitor KX-01 alone and in combination with paclitaxel suppresses growth, metastasis in human ER/PR/HER2-negative tumor xenografts. Mol Cancer Ther. 2012; 11:1936–1947.
27. Cassimeris LU, Wadsworth P, Salmon ED. Dynamics of microtubule depolymerization in monocytes. J Cell Biol. 1986; 102:2023–2032.
28. Roth DM, Moseley GW, Glover D, Pouton CW, Jans DA. A microtubule-facilitated nuclear import pathway for cancer regulatory proteins. Traffic. 2007; 8:673–686.
29. Roth DM, Moseley GW, Pouton CW, Jans DA. Mechanism of microtubule-facilitated “fast track” nuclear import. J Biol Chem. 2011; 286:14335–14351.
30. Giannakakou P, Sackett DL, Ward Y, Webster KR, Blagosklonny MV, Fojo T. p53 is associated with cellular microtubules and is transported to the nucleus by dynein. Nat Cell Biol. 2000; 2:709–717.
31. Soderholm JF, Bird SL, Kalab P, Sampathkumar Y, Hasegawa K, Uehara-Bingen M, Weis K, Heald R. Importazole, a small molecule inhibitor of the transport receptor importin-β. ACS Chem Biol. 2011; 6:700–708.
32. Sweeney C, Chen Y-H, Carducci MA, Liu G, Jarrard DF, Eisenberger MA, Wong Y-N, Hahn NM, Kohli M, Vogelzang NJ, Cooney MM, Dreicer R, Picus J, Shevrin DH, Hussain M, Garcia JA, DiPaola RS. Impact on overall survival (OS) with chemohormonal therapy versus hormonal therapy for hormone-sensitive newly

metastatic prostate cancer (mPrCa): An ECOG-led phase III randomized trial. J Clin Oncol. 2014; 32:5s.

33. Seruga B, Ocana A, Tannock IF. Drug resistance in metastatic castration-resistant prostate cancer. Nat Rev Clin Oncol. 2011; 8:12–23.

34. Antonarakis ES, Armstrong AJ. Evolving standards in the treatment of docetaxel-refractory castration-resistant prostate cancer. Prostate Cancer Prostatic Dis. 2011; 14:192–205.

35. Thadani-Mulero M, Portella L, Sun S, Sung M, Matov A, Vessella RL, Corey E, Nanus DM, Plymate SR, Giannakakou P. Androgen receptor splice variants determine taxane sensitivity in prostate cancer. Cancer Res. 2014; 74:2270–2282.

36. Martin SK, Banuelos CA, Sadar MD, Kyprianou N. N-terminal targeting of androgen receptor variant enhances response of castration resistant prostate cancer to taxane chemotherapy. Mol Oncol. 2015; 9:628–639.

37. Steinestel J, Luedeke M, Arndt A, Schnoeller TJ, Lennerz JK, Wurm C, Maier C, Cronauer MV, Steinestel K, Schrader AJ. Detecting predictive androgen receptor modifications in circulating prostate cancer cells. Oncotarget. . Published online Apr 23, 2015.

38. Antonarakis ES, Lu C, Chen Y, Luber B, Wang H, Nakazawa M, Marzo AMD, Isaacs WB, Nadal R, Paller CJ, Denmeade SR, Carducci MA, Eisenberger MA, Luo J. AR splice variant 7 (AR-V7) and response to taxanes in men with metastatic castration-resistant prostate cancer (mCRPC). J Clin Oncol. 2015; 33 .

39. Clarke SJ, Rivory LP. Clinical pharmacokinetics of docetaxel. Clin Pharmacokinet. 1999; 36:99–114.

40. Chan SC, Li Y, Dehm SM. Androgen receptor splice variants activate androgen receptor target genes and support aberrant prostate cancer cell growth independent of canonical androgen receptor nuclear localization signal. J Biol Chem. 2012; 287:19736–19749.

41. Andersen RJ, Mawji NR, Wang J, Wang G, Haile S, Myung JK, Watt K, Tam T, Yang YC, Banuelos CA, Williams DE, McEwan IJ, Wang Y, Sadar MD. Regression of castrate-recurrent prostate cancer by a small-molecule inhibitor of the amino-terminus domain of the androgen receptor. Cancer Cell. 2010; 17:535–546.

42. Liu C, Lou W, Zhu Y, Nadiminty N, Schwartz CT, Evans CP, Gao AC. Niclosamide inhibits androgen receptor variants expression and overcomes enzalutamide resistance in castration-resistant prostate cancer. Clin Cancer Res. 2014; 20:3198–3210.

43. Purushottamachar P, Godbole AM, Gediya LK, Martin MS, Vasaitis TS, Kwegyir-Afful AK, Ramalingam S, Ates-Alagoz Z, Njar VCO. Systematic structure modifications of multi-target prostate cancer drug candidate galeterone to produce novel androgen receptor down-regulating agents as an approach to treatment of advanced prostate cancer. J Med Chem. 2013; 56:4880–4898.

44. Li J, Cao B, Liu X, Fu X, Xiong Z, Chen L, Sartor O, Dong Y, Zhang H. Berberine suppresses androgen receptor signaling in prostate cancer. Mol Cancer Ther. 2011; 10:1346–1356.

45. Roth DM, Harper I, Pouton CW, Jans DA. Modulation of nucleocytoplasmic trafficking by retention in cytoplasm or nucleus. J Cell Biochem. 2009; 107:1160–1167.

Published OnlineFirst June 9, 2015; DOI: 10.1158/0008-5472.CAN-15-0381

Tumor and Stem Cell Biology

Cancer Research

Androgen Receptor Splice Variants Dimerize to Transactivate Target Genes

Duo Xu[1,2,3], Yang Zhan[2], Yanfeng Qi[2], Bo Cao[1,2], Shanshan Bai[1,2], Wei Xu[4], Sanjiv S. Gambhir[5], Peng Lee[6], Oliver Sartor[7,8], Erik K. Flemington[9], Haitao Zhang[9], Chang-Deng Hu[10], and Yan Dong[1,2,11]

Abstract

Constitutively active androgen receptor splice variants (AR-V) lacking the ligand-binding domain have been implicated in the pathogenesis of castration-resistant prostate cancer and in mediating resistance to newer drugs that target the androgen axis. AR-V regulates expression of both canonical AR targets and a unique set of cancer-specific targets that are enriched for cell-cycle functions. However, little is known about how AR-V controls gene expression. Here, we report that two major AR-Vs, termed AR-V7 and AR^{v567es}, not only homodimerize and heterodimerize with each other but also heterodimerize with full-length androgen receptor (AR-FL) in an androgen-independent manner. We found that heterodimerization of AR-V and AR-FL was mediated by N- and C-terminal interactions and by the DNA-binding domain of each molecule, whereas AR-V homodimerization was mediated only by DNA-binding domain interactions. Notably, AR-V dimerization was required to transactivate target genes and to confer castration-resistant cell growth. Our results clarify the mechanism by which AR-Vs mediate gene regulation and provide a pivotal pathway for rational drug design to disrupt AR-V signaling as a rational strategy for the effective treatment of advanced prostate cancer. *Cancer Res; 75(17); 3663–71. ©2015 AACR.*

Introduction

Recurrence with lethal castration-resistant prostate cancer (CRPC) after androgen deprivation therapy remains the major challenge in treatment of advanced prostate cancer (1, 2). Significant advances in our understanding of continued androgen receptor (AR) signaling in CRPC have led to the development and FDA approval of two next-generation androgen-directed therapies, the androgen biosynthesis inhibitor abiraterone and the potent AR antagonist enzalutamide (3, 4). These drugs heralded a new era of prostate cancer therapy. However, some patients present with therapy-resistant disease, and most initial responders develop acquired resistance within months of therapy initiation (3, 4). The resistance is typically accompanied by increased prostate-specific antigen (PSA), indicating reactivated AR signaling (3, 4). Accumulating evidences indicate that prostate tumors can adapt to these androgen-directed therapies, including abiraterone and enzalutamide, by signaling through constitutively active alternative splicing variants of AR (AR-V; refs. 5–17).

To date, 15 AR-Vs have been identified (18). Structurally, AR-Vs have insertions of cryptic exons downstream of the exons encoding the DNA-binding domain (DBD) or deletions of the exons encoding the ligand-binding domain (LBD), resulting in a disrupted AR open reading frame and expression of LBD-truncated AR (6, 7, 9, 15, 19, 20). Because the N-terminal domain, which contains the most critical transactivation domain of the receptor (AF1), and the DBD remain intact in the majority of the AR-Vs, many AR-Vs display ligand-independent transactivation. AR-V7 (aka AR3) and AR^{v567es} (aka AR-V12) are two major AR-Vs expressed in clinical specimens (7–10, 15, 17). They localize primarily to the nucleus, activate target gene expression in a ligand-independent manner, and promote castration-resistant growth of prostate cancer cells both *in vitro* and *in vivo* (7, 9, 15, 19–21). Strikingly, patients with high levels of expression of AR-V7 or detectable expression of AR^{v567es} in prostate tumors have a shorter survival than other CRPC patients (8). Moreover, AR-V7 expression in circulating tumor cells of CRPC patients is associated with resistance to both abiraterone and enzalutamide (17). These findings indicate an association between AR-V expression and a more lethal form of prostate cancer, and also highlight the importance of AR-Vs in limiting the efficacy of androgen-directed therapies.

[1]College of Life Sciences, Jilin University, Changchun, China. [2]Department of Structural and Cellular Biology, Tulane University School of Medicine, Tulane Cancer Center, New Orleans, Louisiana. [3]School of Nursing, Jilin University, Changchun, China. [4]McArdle Laboratory for Cancer Research, University of Wisconsin, Madison, Wisconsin. [5]Bio-X Program and Department of Radiology, Stanford University School of Medicine, Stanford, California. [6]Department of Pathology, New York University School of Medicine, New York, New York. [7]Department of Urology, Tulane University School of Medicine, Tulane Cancer Center, New Orleans, Louisiana. [8]Department of Medicine, Tulane University School of Medicine, Tulane Cancer Center, New Orleans, Louisiana. [9]Department of Pathology and Laboratory Medicine, Tulane University School of Medicine, Tulane Cancer Center, New Orleans, Louisiana. [10]Department of Medicinal Chemistry and Molecular Pharmacology, Purdue University, West Lafayette, Indiana. [11]National Engineering Laboratory for AIDS Vaccine, Jilin University, Changchun, China.

Note: Supplementary data for this article are available at Cancer Research Online (http://cancerres.aacrjournals.org/).

D. Xu and Y. Zhan contributed equally to this article.

Corresponding Author: Yan Dong, Tulane University School of Medicine, 1430 Tulane Avenue SL-49, New Orleans, LA 70112. Phone: 504-988-4761; Fax: 504-988-0468; E-mail: ydong@tulane.edu

doi: 10.1158/0008-5472.CAN-15-0381

Published OnlineFirst June 9, 2015; DOI: 10.1158/0008-5472.CAN-15-0381

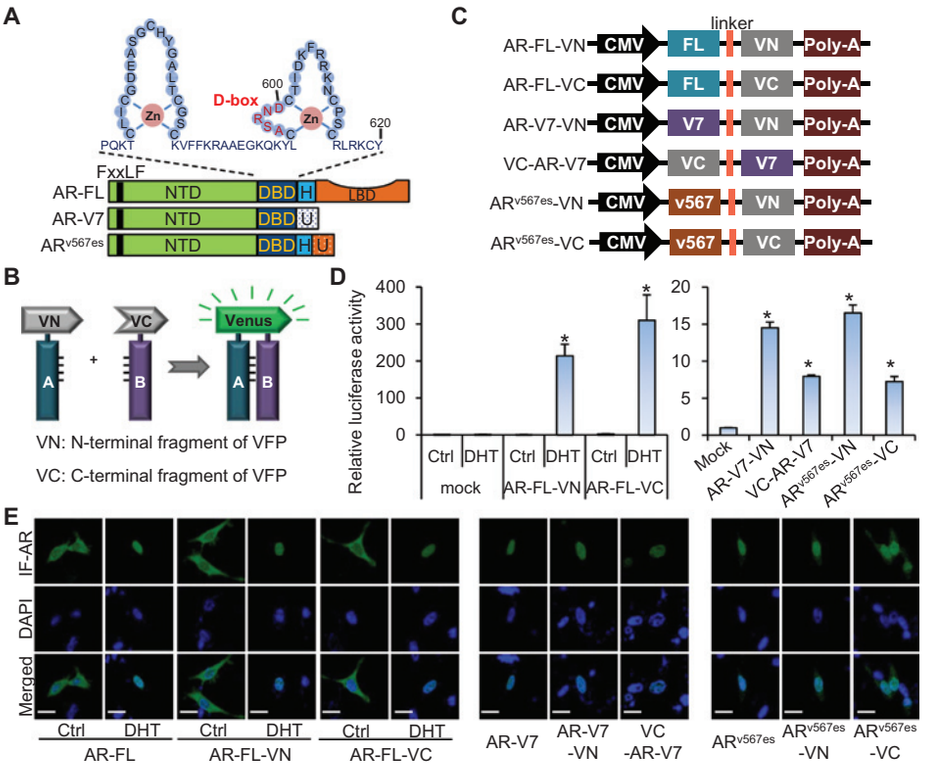

Figure 1.
AR-FL and AR-Vs in BiFC fusion proteins are functional. A, schematic representation of AR-FL, AR-V7, and AR^{v567es} protein structure. The DBD is composed of two zinc fingers. NTD, N-terminal domain; H, hinge region; U, unique C-terminal sequence. D-box and FxxLF motif mediate AR-FL dimerization. B, a schematic of the principle of the BiFC assay. VFP, Venus fluorescent protein. C, schematic diagram of the constructs used in the BiFC assay. D, luciferase assay showing AR transactivating activity in PC-3 cells cotransfected with the indicated BiFC construct and the ARE-luc plasmid. *, $P < 0.05$ from mock control. E, immunofluorescent (IF) staining showing protein fusion does not change subcellular localization of AR-FL, AR-V7, or AR^{v567es}. The indicated expression construct or BiFC fusion construct was transfected into PC-3 cells, and immunofluorescent staining was conducted at 48 hours after transfection. DAPI, nuclear stain. Scale bars, 10 μm. Cells were cultured under androgen-deprived condition unless specified. DHT, 1 nmol/L for 24 hours.

AR-V7 and AR^{v567es} can regulate the expression of both canonical AR targets and a unique set of targets enriched for cell-cycle function independent of the full-length AR (AR-FL; refs. 7, 10, 15). AR-V7 and AR^{v567es} can also activate AR-FL in the absence of androgen by facilitating AR-FL nuclear localization and coregulate the expression of canonical AR targets (5). It has long been appreciated that dimerization is required for AR-FL to regulate target gene expression (22), but little is known about AR-V dimerization. Coimmunoprecipitation of endogenous AR^{v567es} and AR-FL (15) and co-occupancy of the PSA promoter by AR-V7 and AR-FL (5) suggest that AR-Vs may form heterodimers with AR-FL. However, whether AR-Vs homodimerize or heterodimerize with each other and whether the dimerization is required for AR-Vs to regulate target genes and to confer castration-resistant cell growth are currently unknown.

Dimerization of AR-FL is mediated mainly through N/C-terminal interactions, via the FxxLF motif in the N-terminal domain and the coactivator groove in the LBD, and DBD/DBD interactions, via the dimerization box (D-box; ref. 22). Because the FxxLF motif and the D-box (Fig. 1A) are maintained in the majority of the AR-Vs identified, we hypothesize that these AR-Vs can form heterodimers with each other as well as homodimers via DBD/DBD interactions and that they can also form heterodimers with AR-FL via DBD/DBD and N/C interactions. In the current study, we tested this hypothesis by using the bimolecular fluorescence complementation (BiFC) and bioluminescence resonance energy transfer (BRET) assays, which have complementary capabilities for characterizing protein–protein interactions in live cells. BiFC allows direct visualization of subcellular locations of the interactions (23), while BRET allows real-time detection of complex formation (24, 25).

Materials and Methods

Cell lines and reagents

LNCaP, PC-3, DU145, VCaP, and HEK-293T cells were obtained from the ATCC, and cultured as described (26). C4-2 was provided by Dr. Shahriar Koochekpour (Roswell Park Cancer Institute, Buffalo, NY). All the cell lines were authenticated on April 1, 2015 by the method of short tandem repeat profiling at the Genetica DNA Laboratories. Enzalutamide was purchased from Selleck Chemicals.

Plasmid construction

To generate different BiFC fusion constructs of AR-FL, AR-V7, and AR^{v567es}, we PCR amplified the AR-FL, AR-V7, and AR^{v567es} cDNAs from their respective expression construct, and cloned the PCR amplicons separately into a TA-cloning vector (Promega). Fusion constructs of AR-FL, AR^{v567es}, and AR-V7 with either VN or VC were generated by subcloning the cDNAs from the TA plasmids into the SalI and XhoI sites of the pBiFC-VN155 and pBiFC-VC155 vectors. The mutant BiFC-AR-V and BiFC-AR-FL constructs with mutations at the FxxLF motif (F23,27A/L26A) and/or D-box (A596T/S597T) were generated by site-directed mutagenesis by using the Q5 site-Directed Mutagenesis Kit (New England BioLabs). BRET-fusion constructs of AR-FL, AR-V7, and AR^{v567es} were generated by subcloning the AR-FL, AR-V7, and AR^{v567es} cDNA from the respective TA plasmids into the BamHI and XbaI sites of the pcDNA3.1-RLuc8.6 and TurboFP635 vectors (24). The doxycycline-inducible AR^{v567es} lentiviral construct was generated by subcloning the AR^{v567es} cDNA from its TA plasmid first into the pDONR221 vector (Invitrogen) and subsequently into the doxycycline-inducible pHAGE-Ind-EF1a-DEST-GH lentiviral construct

Published OnlineFirst June 9, 2015; DOI: 10.1158/0008-5472.CAN-15-0381

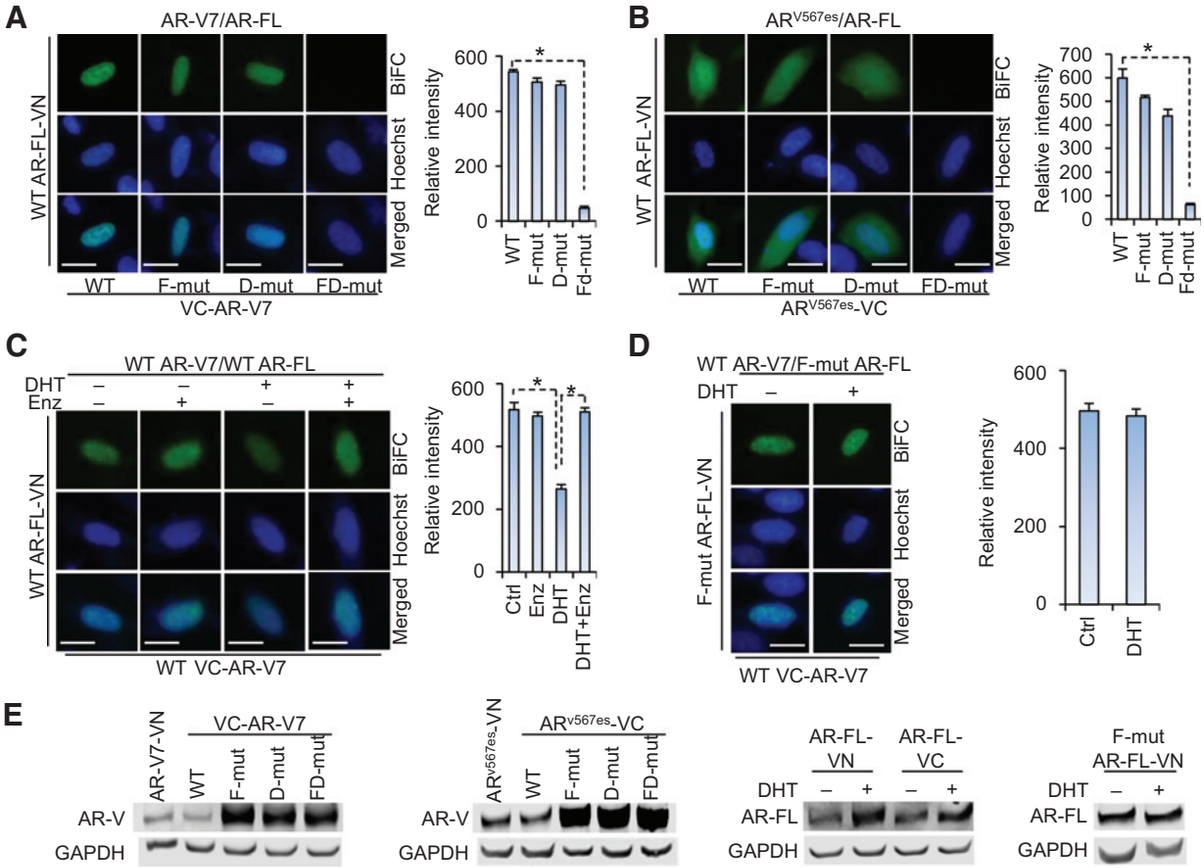

Figure 2.
AR-V7 and AR^{V567es} heterodimerize with AR-FL through both N/C and DBD/DBD interactions. wt, wild-type; F-mut, FxxLF-motif mutant; D-mut, D-box mutant; FD-mut, FxxLF-motif and D-Box double mutant. Hoechst, nuclear stain. Scale bars, 10 μm. *, $P < 0.05$. A and B, dimerization was detected by the BiFC assay in PC-3 cells under androgen-deprived condition. Right, quantitation of BiFC signals by flow cytometry. C and D, pretreatment with androgen attenuates the dimerization between AR-V7 and wt AR-FL (C) but not the dimerization between AR-V7 and F-mut AR-FL (D). PC-3 cells were treated with 1 nmol/L DHT with or without 10 μmol/L enzalutamide (Enz) right after transfection with the indicated BiFC constructs, and BiFC signal was assessed at 48 hours after transfection. Right, quantitation of BiFC signals by flow cytometry. E, Western blotting with a pan-AR antibody showing expression of the BiFC-fusion proteins. Individual fusion construct was transfected into PC-3 cells cultured under androgen-deprived condition unless specified. DHT, 1 nmol/L for 24 hours.

by using the Gateway Cloning System (Invitrogen). All plasmids were sequence verified.

DNA transfection and reporter gene assay

PC-3 and HEK-293T cells were transfected by using the TransIT-2020 (Mirus Bio LLC) and TurboFect reagents (Thermo Scientific), respectively, per instruction of the manufacturer. DU145, C4-2, and LNCaP cells were transfected by using the Lipofectamine 2000 and Plus reagent (Invitrogen) as described (27). Reporter gene assay was performed as previously described (28) with either an androgen-responsive element-luciferase plasmid (ARE-luc) containing three ARE regions ligated in tandem to the luciferase reporter or a luciferase construct driven by three repeats of an AR-V–specific promoter element of the ubiquitin-conjugating enzyme E2C (UBE2C) gene (UBE2C-luc). To ensure an even transfection efficiency, we conducted the transfection in bulk and then split the transfected cells for luciferase assay.

Immunofluorescence staining

Cells were transfected with indicated plasmids on Poly-D-Lysine–coated coverslips (neuVitro) and cultured in phenol red–free medium supplemented with 10% charcoal-stripped FBS. For the dihydrotestosterone (DHT) groups, 1 nmol/L DHT was added at 24 hours after transfection. At 48 hours after transfection, cells were fixed with 70% ethanol, and incubated with a pan-AR antibody (PG-21, Millipore; 1:200) overnight at 4°C and subsequently with Alexa Fluor 488–conjugated secondary antibody (Invitrogen; 1:1,000) for 1 hour at room temperature in the dark. Nuclei were then stained with 4′,6-diamidino-2-phenylindole (DAPI). Confocal images were obtained by using a Leica TCS SP2 system with a 40× oil-immersion objective on a Z-stage.

BiFC analysis

Cells were cotransfected with different BiFC fusion constructs. At 48 hours after transfection, cells were incubated with Hoechst33342 (Invitrogen) and observed by fluorescence microscopy (Olympus). For flow cytometry quantitation of BiFC signals, the pDsRed2-C1 construct (Clontech) was cotransfected with the BiFC fusion constructs. At 48 hours after transfection, cells were trypsinized, and the Venus and DsRed fluorescence were analyzed by flow cytometry.

Published OnlineFirst June 9, 2015; DOI: 10.1158/0008-5472.CAN-15-0381

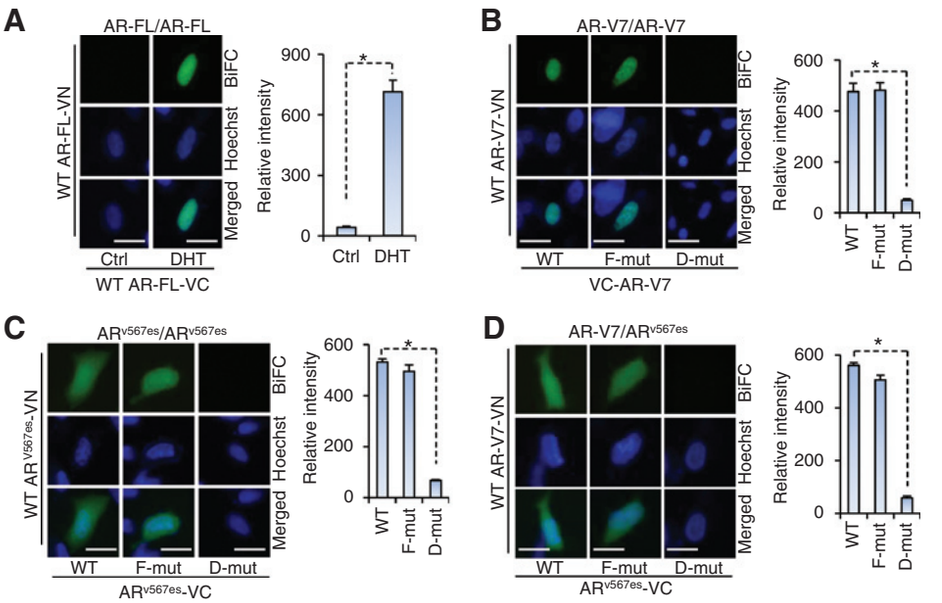

Figure 3.
AR-V and AR-V dimerize through DBD/DBD interactions. AR-FL homodimerization (A), AR-V7 homodimerization (B), AR^{v567es} homodimerization (C), and AR-V7/AR^{v567es} heterodimerization (D) were detected by BiFC assay in PC-3 cells under androgen-deprived condition unless specified. DHT, 1 nmol/L for 24 hours. Right panels, quantitation of BiFC signals by flow cytometry. wt, wild-type; F-mut, FxxLF-motif mutant; D-mut, D-box mutant. Hoechst, nuclear stain. Scale bars, 10 μm. *, $P < 0.05$. In contrast to AR-FL/AR-FL and AR-V7/AR-V7 dimerization, which were detected mainly in the nucleus (>90%), AR^{v567es}/AR^{v567es} and AR-V7/AR^{v567es} dimerization were observed in both the nucleus (37% and 57%, respectively) and the cytoplasm (63% and 43%, respectively).

Western blot analysis

The procedure was described previously (29). The anti-GAPDH (Millipore), anti-AR (N-20, Santa Cruz Biotechnology), anti-HSP70 (Abcam), anti-Turbo-red fluorescent protein (Abcam), and anti-*Renilla*-luciferase (Thermo Scientific) antibodies were used.

Quantitative RT-PCR and cell growth assay

Quantitative RT-PCR (qRT-PCR) was performed as described (30), and the qPCR primer probe sets were from IDT. Cell growth was determined by the sulforhodamine (SRB) assay as described (31). To ensure an even transduction efficiency, we conducted the transduction of the cells with packaged lentivirus in bulk, and then split the transduced cells for qRT-PCR and SRB assays.

BRET assay

Cells were either transfected with an RLuc BRET fusion plasmid or cotransfected with an RLuc and a TFP BRET fusion plasmid. At 72 hours after transfection, cells were detached with 5 mmol/L EDTA in PBS and resuspended in PBS with 1% sucrose. Cells were counted and seeded in triplicate into a 96-well white-wall microplate at 10^5 cells per well. Freshly prepared coelenterazine (Nanolight Technology) in water was added to the cells at a final concentration of 25 μmol/L. BRET readings at 528 nm and 635 nm were obtained immediately with a Synergy 2 microplate reader (BioTek). The BRET ratio was calculated by subtracting the ratio of 635-nm emission and 528-nm emission obtained from cells coexpressing the RLuc and TFP fusion proteins from the background BRET ratio resulting from cells expressing the RLuc fusion protein alone in the same experiment: BRET ratio = (emission at 635 nm)/(emission at 528 nm) − (emission at 635 nm RLuc only)/(emission at 528 nm RLuc only).

Statistical analysis

The Student two-tailed *t* test was used to determine the mean differences between two groups. $P < 0.05$ is considered significant. Data are presented as mean ± SEM.

Results

Characterization of AR-FL and AR-Vs in BiFC fusion proteins

For BiFC analysis of interaction between proteins A and B, the two proteins are fused separately to either the N- or C-terminal fragment of the Venus fluorescent protein (VN or VC, Fig. 1B). If the two proteins dimerize, the interaction allows regeneration of the Venus fluorescent protein to emit fluorescent signal (23). Because BiFC depends on the relative orientation of the fusion proteins (23), we generated all possible combinations of N- and C-terminal fusions by cloning the AR-FL, AR^{v567es}, or AR-V7 cDNA either in front of or after VN or VC. Different pairs of fusion protein constructs were transfected into the AR-null PC-3 cells (to avoid confounding effect of endogenous AR), and the fusion protein constructs exhibiting the highest BiFC signals (Fig. 1C) were chosen for further analysis. The transactivating abilities of the fusion proteins were tested by the reporter gene assay. Although the protein fusion affected the relative activities of the fusion proteins (Figs. 1D and Supplementary Fig. S1), all the fusion proteins can transactivate target genes. Immunofluorescence assay further showed that the AR-FL and AR-Vs in the fusion proteins have the same subcellular localizations as the respective nonfusion AR isoform (Fig. 1E). Collectively, the data indicated that AR-FL and AR-Vs are functional in the fusion proteins.

BiFC detection of AR-V/AR-FL heterodimerization

To assess the ability of AR-V7 and AR^{v567es} to heterodimerize with AR-FL, we cotransfected the AR-V- and AR-FL BiFC fusion constructs into PC-3 cells and quantitated the Venus fluorescence signal by flow cytometry. Both AR-V7 and AR^{v567es} dimerized with AR-FL, and the dimerization did not require androgen (Fig. 2A and B). To delineate the dimerization interface, we generated mutant BiFC-AR-V constructs with mutations at the FxxLF motif (F23,27A/L26A) and/or D-box (A596T/S597T). FxxLF motif and D-box mediate AR-FL homodimerization through N/C and DBD/DBD interactions, respectively (22). Only mutating both motifs abolished AR-V/AR-FL dimerization (Fig. 2A and B), indicating that both N/C and DBD/DBD interactions mediate

Published OnlineFirst June 9, 2015; DOI: 10.1158/0008-5472.CAN-15-0381

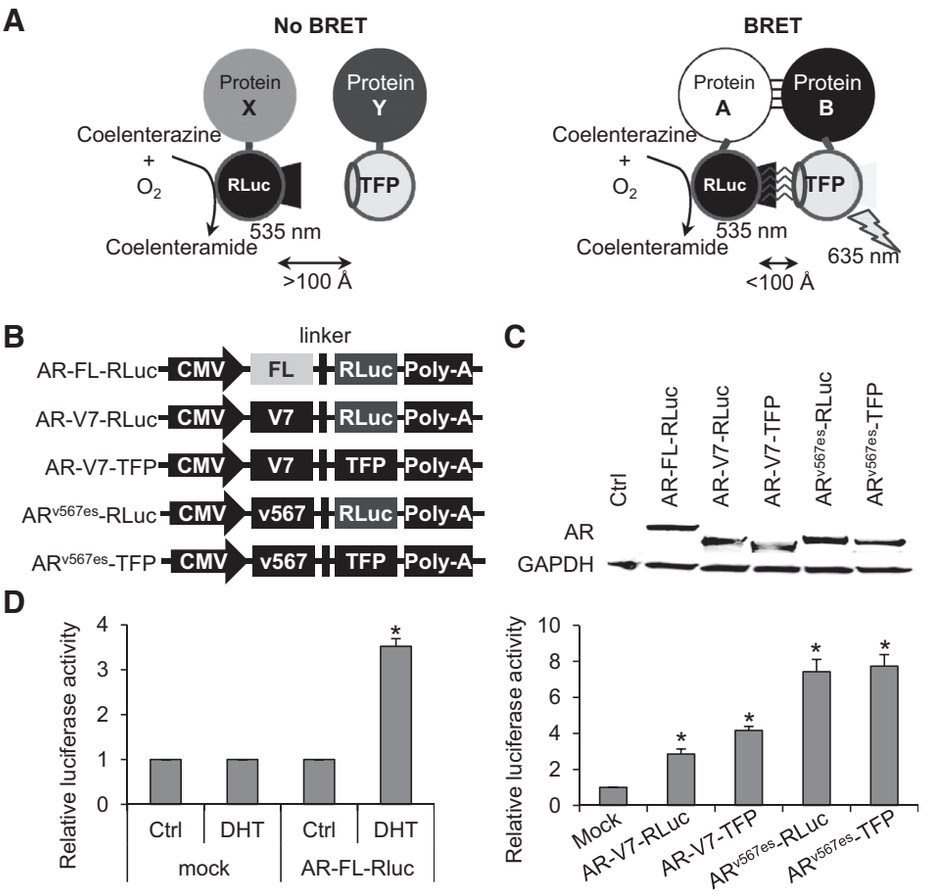

Figure 4.
AR-FL and AR-Vs in BRET fusion proteins are functional. A, a schematic of the principle of the BRET assay. B, schematic diagram of the constructs used in the BRET assay. RLuc, RLuc8.6 luciferase; TFP, TurboFP635 fluorescent protein. C, Western blotting with a pan-AR antibody showing expression of the BRET-fusion proteins. Individual fusion construct was transfected into HEK-293T cells cultured under androgen-deprived condition. D, luciferase assay showing AR *trans*-activating activity in HEK-293T cells cotransfected with the indicated BRET construct and the ARE-luc plasmid. Cells were cultured under androgen-deprived condition unless specified. DHT, 1 nmol/L for 24 hours. *, $P < 0.05$ from mock control.

the dimerization. Mutating one motif did not lead to significant change of BiFC signal (Fig. 2A and B), likely due to compensation of the loss of one mode of interaction by the other. Similar results were obtained in DU145 and HEK-293T cells (Supplementary Figs. S2 and S3). Intriguingly, although AR^{v567es}/AR-FL dimerization was observed in both the cytoplasm and the nucleus, AR-V7/AR-FL dimerization was detected primarily in the nucleus in the vast majority of the cells (Figs. 2A and B, Supplementary Figs. S2A, S2B, S3A, and S3B).

Pretreatment of cells with DHT attenuated AR-V7/AR-FL dimerization, and this effect was blocked by the antiandrogen enzalutamide (Fig. 2C). Conversely, DHT pretreatment produced minimal effect on the dimerization of AR-V7 and the FxxLF-motif–mutated AR-FL (Fig. 2D), which lost the ability to homodimerize upon androgen treatment (Supplementary Fig. S4B; ref. 32). These data indicate that AR-V7 may compete with AR-FL for dimerizing with AR-FL. Notably, the expression of each of the wild-type and mutant fusion proteins was confirmed by Western blotting (Fig. 2E). Collectively, our data demonstrated androgen-independent dimerization between AR-V and AR-FL, and indicated that AR-V/AR-FL dimerization may attenuate androgen induction of AR-FL homodimerization.

BiFC detection of AR-V/AR-V dimerization

We further showed that, like liganded AR-FL (Figs. 3A and Supplementary Fig. S4), both AR-Vs can form a homodimer when expressed alone (Figs. 3B and C and Supplementary Figs. S2C, S2D, S3C, and S3D). The homodimerization can also occur when AR-V is coexpressed with AR-FL and even when it is expressed at a much lower level than AR-FL (Supplementary Fig. S5). Moreover, AR-V7 and AR^{v567es} can heterodimerize (Fig. 3D). Mutating D-box, but not the FxxLF motif, abolished AR-V/AR-V interactions, indicating that AR-Vs homodimerize and heterodimerize with each other through DBD/DBD interactions. Interestingly, similar to AR-V7/AR-FL dimerization, AR-V7/AR-V7 dimerization was detected primarily in the nucleus (Figs. 3B and Supplementary Figs. S2C and S3C). However, AR^{v567es}/AR^{v567es} and AR-V7/AR^{v567es} dimerization were observed in both the nucleus and the cytoplasm (Fig. 3C and D and Supplementary Figs. S2D and S3D).

Characterization of AR-FL and AR-Vs in BRET fusion proteins

We then used the newest BRET system, BRET6 (24), to confirm the BiFC results. BRET6 is based on energy transfer between the Rluc8.6 *Renilla* luciferase (Rluc) energy donor and the turbo red fluorescent protein (TFP) energy acceptor when the donor and acceptor are brought into close proximity by their fused proteins (Fig. 4A). Similar to BiFC, BRET also depends on the relative orientation of the fusion proteins. We therefore generated all possible combinations of N- and C-terminal fusions by cloning the AR-FL, AR^{v567es}, or AR-V7 cDNA either in front of or after Rluc

Published OnlineFirst June 9, 2015; DOI: 10.1158/0008-5472.CAN-15-0381

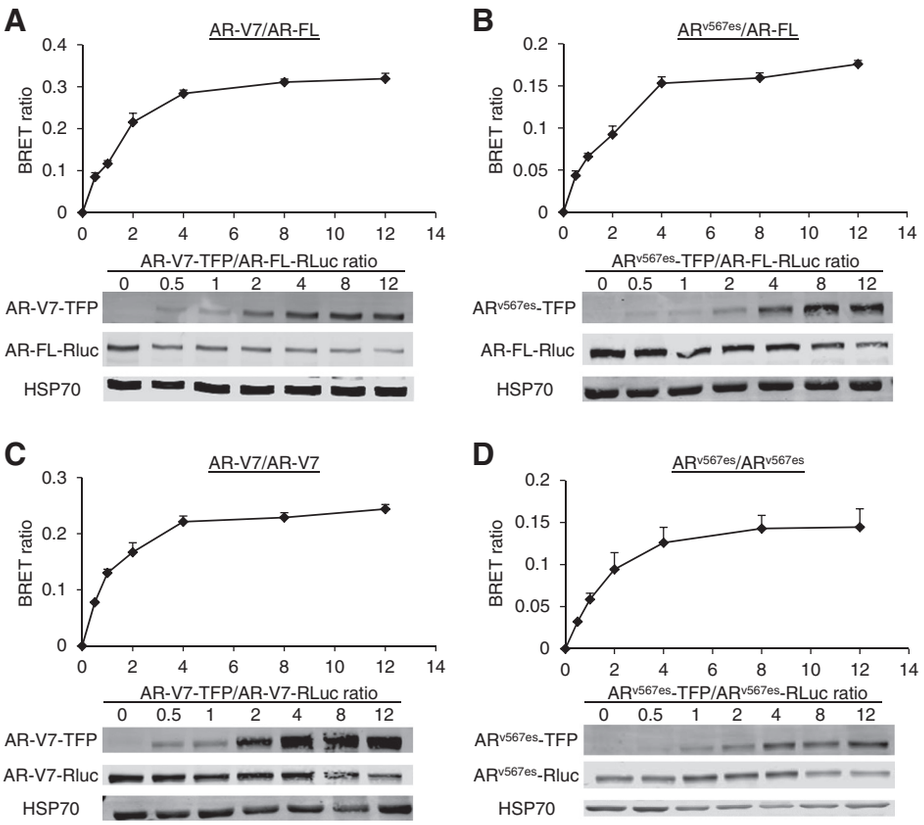

Figure 5.
BRET assay confirmation of AR-V/AR-FL and AR-V/AR-V dimerization. Indicated BRET fusion constructs were cotransfected into HEK-293T cells at different ratios, and BRET signal was measured after the addition of the coelenterazine substrate. Lower panels, Western blotting with an antibody against TFP, RLuc, or HSP70 showing the levels of the fusion proteins expressed. Cells were cultured under androgen-deprived condition.

or TFP. Different pairs of the fusion protein constructs were transfected into the AR-null HEK-293T cells (to avoid confounding effect of endogenous AR), and the fusion protein constructs exhibiting the highest BRET signals (Fig. 4B) were chosen for further analysis. The expression of these fusion proteins was confirmed by Western blotting (Fig. 4C). Furthermore, their abilities to transactivate were validated by luciferase assay with the cotransfection of the ARE-luc plasmid (Fig. 4D), indicating that AR-FL and AR-Vs are functional in the BRET fusion proteins.

BRET confirmation of AR-V/AR-FL and AR-V/AR-V dimerization

Figure 5 shows the BRET saturation curves for different combinations of the BRET fusion proteins in HEK-293T cells. The BRET ratios increased hyperbolically and rapidly saturated with the increase in the ratio of energy acceptor to energy donor, indicating specific protein–protein interaction (33). Similar to the BiFC data, mutating the FxxLF-motif and/or the D-box inhibited AR-V/AR-FL and AR-V/AR-V dimerization (Supplementary Fig. S6). Thus, the BRET data confirmed the BiFC results, showing the ability of AR-Vs to heterodimerize with AR-FL and to homodimerize. AR^{v567es}/AR^{v567es} interaction was further demonstrated by coimmunoprecipitation assay (Supplementary Fig. S7).

Dimerization is required for AR-V action

To assess the requirement of dimerization for AR-V action, we first performed reporter gene assay with the wild-type or the dimerization mutants of AR-V. As shown in Fig. 6A, the dimerization mutants completely lost the ability to transactivate, indicating a requirement of dimerization for AR-V transactivation. We then analyzed the ability of the wild-type and dimerization mutants of AR-Vs to regulate target gene expression and castration-resistant growth of prostate cancer cells. To this end, we infected the AR-FL–expressing LNCaP cells with lentivirus encoding AR-V7 or doxycycline-inducible AR^{v567es}. Mutation of the FxxLF motif alone or both the FxxLF motif and D-box attenuated AR-V induction of androgen-independent expression of the canonical AR target PSA and the AR-V–specific target UBE2C (Fig. 6B) as well as castration-resistant cell growth (Fig. 6C). The data indicated the requirement of dimerization for AR-Vs to regulate target genes and to confer castration-resistant cell growth.

Discussion

The current study represents the first to show the dimeric nature of AR-Vs in live cells. Using BiFC and BRET assays, we showed that AR-V7 and AR^{v567es} not only homodimerize and heterodimerize with each other but also heterodimerize with AR-FL. The dimerization does not require androgen. By mutating the FxxLF motif in the N-terminal domain and/or D-box in DBD of AR-Vs, we further showed that AR-V/AR-FL dimerization is mediated by both N/C and DBD/DBD interactions, whereas AR-V/AR-V dimerization is through DBD/DBD interactions. Because AR-Vs lack the C-terminal domain, the N/C interactions between AR-V and AR-FL is mediated presumably via the FxxLF motif of AR-V and the C-terminal domain of AR-FL. Significantly, dimerization mutants of AR-Vs lose the ability to transactivate target genes and to confer

Published OnlineFirst June 9, 2015; DOI: 10.1158/0008-5472.CAN-15-0381

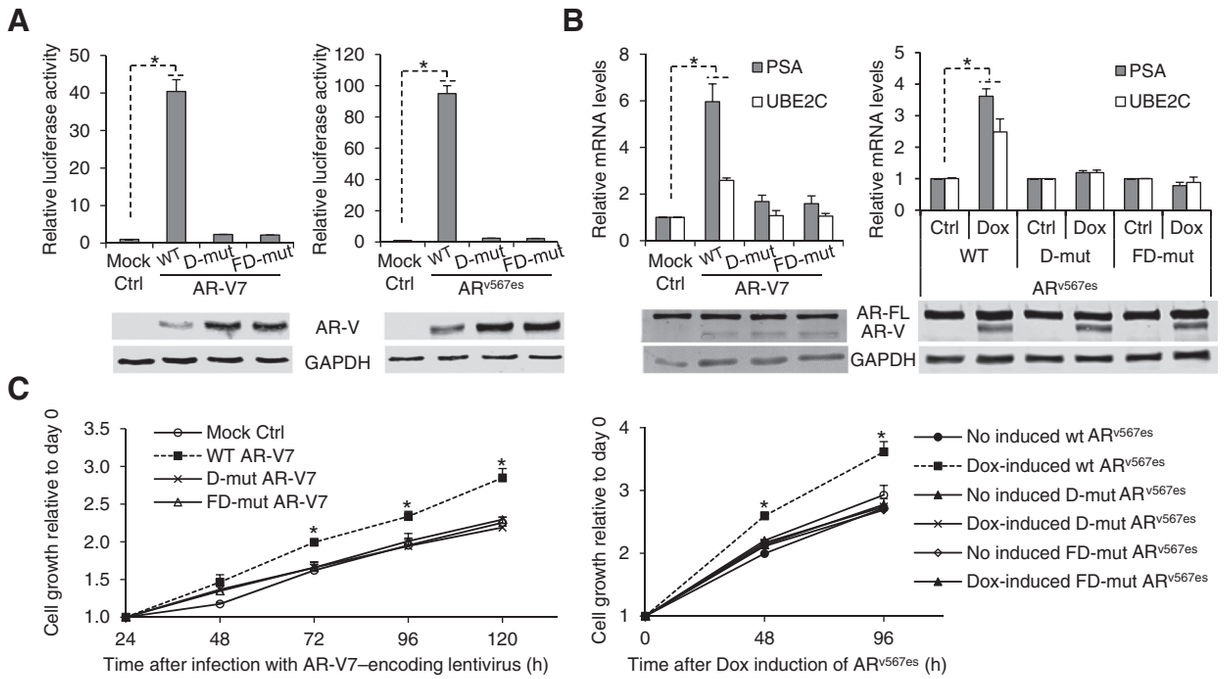

Figure 6.
Dimerization mutants of AR-Vs lose ability to transactivate and to promote castration-resistant cell growth. A, wild-type or dimerization mutant of AR-V was cotransfected with the ARE-luc plasmid, and cells were cultured under androgen-deprived condition. B and C, LNCaP cells were infected in bulk with lentivirus encoding wild-type or dimerization mutant of AR-V7 (left) or doxycycline-inducible wild-type or dimerization mutant of AR^{v567es} (right). At 24 hours after infection, cells were reseeded and treated with or without 200 ng/mL doxycycline and incubated for an additional 48 hours for qRT-PCR analysis of target genes (B) or for the indicated time for SRB assay of cell growth (C). Western blotting confirmed AR-V expression. *, $P < 0.05$ from control cells.

castration-resistant cell growth, indicating the requirement of dimerization for important functions of AR-Vs.

Our finding on AR-V/AR-FL interaction is in accordance with the previous reports on AR^{v567es} and AR-FL coimmunoprecipitation (15) as well as on AR-V7 and AR-FL co-occupancy of the PSA promoter (5), providing a direct evidence for their dimerization. Interestingly, we found that the androgen-independent dimerization between AR-V and AR-FL may mitigate androgen induction of AR-FL homodimerization. This could constitute a mechanistic basis for the ability of AR-Vs to attenuate androgen induction of AR-FL activity (5). To date, functional studies of AR-Vs have been focused mostly on their ability to regulate gene expression independent of AR-FL. Because AR-Vs are often coexpressed with AR-FL in biologic contexts, it is conceivable that the ability of AR-Vs to heterodimerize with and activate AR-FL in an androgen-independent manner could be equally important as their AR-FL–independent activity to castration resistance.

We and others showed previously that AR-V7 and AR^{v567es} localize constitutively to the nucleus and can facilitate AR-FL nuclear entry (5, 15), indicating that the initial interaction between AR-V and AR-FL is likely to be in the cytoplasm. This is supported by our data showing both cytoplasmic and nuclear localization of AR^{v567es}/AR-FL dimerization. Intriguingly, AR-V7/AR-FL dimerization is detected primarily in the nucleus in the vast majority of the cells. This may be due to the regeneration of the Venus fluorescent protein from the VN and VC fragments being slower than AR-V7/AR-FL nuclear translocation. Interestingly, AR-V7/AR-V7 dimerization was also detected primarily in the nucleus, whereas AR^{v567es}/AR^{v567es} and AR-V7/AR^{v567es} dimerization were observed in both the nucleus and the cytoplasm. Whether this is also due to slower regeneration of the Venus fluorescent protein than AR-V7/AR-V7 nuclear translocation or AR-V7 entering the nucleus as a monomer requires further investigation. In addition, the majority of the posttranslational modification sites of AR-FL are retained in AR-Vs (34). These posttranslational modifications regulate AR-FL transactivating activity, possibly via the interaction of AR-FL with other proteins or with itself (34). It is very likely that these posttranslational modifications may impact AR-V dimerization and transactivation and therefore deserve further investigation.

We reported previously that AR-V binds to the promoter of its specific target UBE2C without AR-FL, but co-occupies the promoter of the canonical AR target PSA with AR-FL in a mutually dependent manner (5). Furthermore, knockdown of AR-FL and AR-V both result in reduced androgen-independent PSA expression, but only AR-V knockdown downregulates UBE2C expression (5). The data, together with the findings from the current study, indicate that AR-Vs regulate their specific targets as an AR-V/AR-V dimer but control the expression of canonical AR targets as an AR-V/AR-FL dimer. Interestingly, while mutating D-box alone does not significantly mitigate AR-V/AR-FL dimerization, the mutation abolishes the ability of AR-V to induce the expression of PSA and UBE2C as well as to promote castration-resistant cell growth. A plausible explanation is that, although D-box–mutated AR-V can dimerize with AR-FL, the dimer cannot bind to DNA to regulate the expression of target genes. This, together with the finding that D-box–D-box interactions are required for the formation of androgen-induced AR-FL intermolecular N/C

Published OnlineFirst June 9, 2015; DOI: 10.1158/0008-5472.CAN-15-0381

interactions (32), indicates that disrupting D-box–D-box interactions could lead to inhibition of not only AR-V/AR-V dimerization and transactivation but also AR-FL activation induced by either AR-Vs or androgens. Thus, disrupting D-box–D-box interactions may represent a more effective means to suppress AR signaling than targeting the LBD of AR.

In summary, we demonstrated the dimeric nature of AR-Vs in live cells and identified the dimerization interface. Significantly, we showed that proper dimerization is required for AR-V functions. The research therefore represents a key step in delineating the mechanism by which AR-Vs mediate gene regulation. This is vital for developing effective therapeutic strategies to disrupt AR-V signaling and provide more effective treatments for prostate cancer.

Disclosure of Potential Conflicts of Interest

O. Sartor is a consultant/advisory board member for Astellas, Janssen, and Medivation. No potential conflicts of interest were disclosed by the other authors.

Authors' Contributions

Conception and design: D. Xu, Y. Zhan, Y. Qi, B. Cao, H. Zhang, Y. Dong
Development of methodology: D. Xu, Y. Zhan, Y. Qi, S.S. Gambhir, H. Zhang
Acquisition of data (provided animals, acquired and managed patients, provided facilities, etc.): D. Xu, S. Bai
Analysis and interpretation of data (e.g., statistical analysis, biostatistics, computational analysis): D. Xu, Y. Qi, S. Bai, P. Lee, Y. Dong
Writing, review, and/or revision of the manuscript: D. Xu, Y. Zhan, B. Cao, W. Xu, S.S. Gambhir, P. Lee, O. Sartor, E.K. Flemington, H. Zhang, Y. Dong
Administrative, technical, or material support (i.e., reporting or organizing data, constructing databases): D. Xu
Study supervision: Y. Qi, W. Xu, Y. Dong
Other (provided BiFC plasmids and suggestions to conduct the BiFC experiments. Also, reviewed the manuscript with comments): C.-D. Hu

Acknowledgments

The authors thank Dr. Yun Qiu (University of Maryland, College Park, MD) for the human AR-FL and AR-V7 expression constructs, Dr. Stephen Plymate (University of Washington, Seattle, WA) for the human AR^{v567es} expression construct, Dr. Jun Luo (Johns Hopkins University, Baltimore, MD) for the pEGFP-AR construct, Drs. Zhou Songyang and Nancy L. Weigel (Baylor College of Medicine, Houston, TX) for the pHAGE-Ind-EF1a-DEST-GH construct, and Dr. Shahriar Koochekpour (Roswell Park Cancer Institute, Buffalo, NY) for C4-2 cells. The authors appreciate the excellent technical assistance from Ms. Mary Price at the Louisiana Cancer Research Consortium FACS Core.

Grant Support

This work was supported by the following grants: NIH/NCI R01CA188609, NIH/NIGMS P20GM103518, DOD W81XWH-12-1-0112, W81XWH-14-1-0485, and W81XWH-12-1-0275; Louisiana Board-of-Regents LEQSF (2012–15)-RD-A-25; the Louisiana Cancer Research Consortium Fund; the Tulane University School of Medicine Research Bridge Fund; and the National Natural Science Foundation of China Projects 81272851 and 81430087.

The costs of publication of this article were defrayed in part by the payment of page charges. This article must therefore be hereby marked *advertisement* in accordance with 18 U.S.C. Section 1734 solely to indicate this fact.

Received February 6, 2015; revised May 7, 2015; accepted May 27, 2015; published OnlineFirst June 9, 2015.

References

1. Egan A, Dong Y, Zhang H, Qi Y, Balk SP, Sartor O. Castration-resistant prostate cancer: adaptive responses in the androgen axis. Cancer Treat Rev 2014;40:426–33.
2. Knudsen KE, Scher HI. Starving the addiction: new opportunities for durable suppression of AR signaling in prostate cancer. Clin Cancer Res 2009;15:4792–8.
3. Fizazi K, Scher HI, Molina A, Logothetis CJ, Chi KN, Jones RJ, et al. Abiraterone acetate for treatment of metastatic castration-resistant prostate cancer: final overall survival analysis of the COU-AA-301 randomised, double-blind, placebo-controlled phase 3 study. Lancet Oncol 2012;13:983–92.
4. Scher HI, Fizazi K, Saad F, Taplin ME, Sternberg CN, Miller K, et al. Increased survival with enzalutamide in prostate cancer after chemotherapy. N Engl J Med 2012;367:1187–97.
5. Cao B, Qi Y, Zhang G, Xu D, Zhan Y, Alvarez X, et al. Androgen receptor splice variants activating the full-length receptor in mediating resistance to androgen-directed therapy. Oncotarget 2014;5:1646–56.
6. Dehm SM, Schmidt LJ, Heemers HV, Vessella RL, Tindall DJ. Splicing of a novel androgen receptor exon generates a constitutively active androgen receptor that mediates prostate cancer therapy resistance. Cancer Res 2008;68:5469–77.
7. Guo Z, Yang X, Sun F, Jiang R, Linn DE, Chen H, et al. A novel androgen receptor splice variant is up-regulated during prostate cancer progression and promotes androgen depletion-resistant growth. Cancer Res 2009;69:2305–13.
8. Hornberg E, Ylitalo EB, Crnalic S, Antti H, Stattin P, Widmark A, et al. Expression of androgen receptor splice variants in prostate cancer bone metastases is associated with castration-resistance and short survival. PLoS ONE 2011;6:e19059.
9. Hu R, Dunn TA, Wei S, Isharwal S, Veltri RW, Humphreys E, et al. Ligand-independent androgen receptor variants derived from splicing of cryptic exons signify hormone-refractory prostate cancer. Cancer Res 2009;69:16–22.
10. Hu R, Lu C, Mostaghel EA, Yegnasubramanian S, Gurel M, Tannahill C, et al. Distinct transcriptional programs mediated by the ligand-dependent full-length androgen receptor and its splice variants in castration-resistant prostate cancer. Cancer Res 2012;72:3457–62.
11. Li Y, Chan SC, Brand LJ, Hwang TH, Silverstein KA, Dehm SM. Androgen receptor splice variants mediate enzalutamide resistance in castration-resistant prostate cancer cell lines. Cancer Res 2012;73:483–9.
12. Liu LL, Xie N, Sun S, Plymate S, Mostaghel E, Dong X. Mechanisms of the androgen receptor splicing in prostate cancer cells. Oncogene 2014;33:3140–50.
13. Mostaghel EA, Marck BT, Plymate SR, Vessella RL, Balk S, Matsumoto AM, et al. Resistance to CYP17A1 inhibition with abiraterone in castration-resistant prostate cancer: induction of steroidogenesis and androgen receptor splice variants. Clin Cancer Res 2011;17:5913–25.
14. Nadiminty N, Tummala R, Liu C, Yang J, Lou W, Evans CP, et al. NF-kappaB2/p52 induces resistance to enzalutamide in prostate cancer: role of androgen receptor and its variants. Mol Cancer Ther 2013;12:1629–37.
15. Sun S, Sprenger CC, Vessella RL, Haugk K, Soriano K, Mostaghel EA, et al. Castration resistance in human prostate cancer is conferred by a frequently occurring androgen receptor splice variant. J Clin Invest 2010;120:2715–30.
16. Zhang X, Morrissey C, Sun S, Ketchandji M, Nelson PS, True LD, et al. Androgen receptor variants occur frequently in castration resistant prostate cancer metastases. PLoS ONE 2011;6:e27970.
17. Antonarakis ES, Lu C, Wang H, Luber B, Nakazawa M, Roeser JC, et al. AR-V7 and resistance to enzalutamide and abiraterone in prostate cancer. N Engl J Med 2014;371:1028–38.
18. Zhang H, Zhan Y, Liu X, Qi Y, Zhang G, Sartor O, et al. Splicing variants of androgen receptor in prostate cancer. Am J Clin Exp Urol 2013;1:18–24.
19. Hu R, Isaacs WB, Luo J. A snapshot of the expression signature of androgen receptor splicing variants and their distinctive transcriptional activities. Prostate 2011;71:1656–67.
20. Watson PA, Chen YF, Balbas MD, Wongvipat J, Socci ND, Viale A, et al. Constitutively active androgen receptor splice variants expressed in castration-resistant prostate cancer require full-length androgen receptor. Proc Natl Acad Sci U S A 2010;107:16759–65.

21. Chan SC, Li Y, Dehm SM. Androgen receptor splice variants activate androgen receptor target genes and support aberrant prostate cancer cell growth independent of canonical androgen receptor nuclear localization signal. J Biol Chem 2012;287:19736–49.
22. Centenera MM, Harris JM, Tilley WD, Butler LM. Minireview: the contribution of different androgen receptor domains to receptor dimerization and signaling. Mol Endocrinol 2008;22:2373–82.
23. Hu CD, Grinberg AV, Kerppola TK. Visualization of protein interactions in living cells using bimolecular fluorescence complementation (BiFC) analysis. Curr Protoc Cell Biol 2006; Chapter 21:Unit 21.3.
24. Dragulescu-Andrasi A, Chan CT, De A, Massoud TF, Gambhir SS. Bioluminescence resonance energy transfer (BRET) imaging of protein–protein interactions within deep tissues of living subjects. Proc Natl Acad Sci U S A 2011;108:12060–5.
25. Pfleger KDG, Seeber RM, Eidne KA. Bioluminescence resonance energy transfer (BRET) for the real-time detection of protein–protein interactions. Nat Protocols 2006;1:337–45.
26. Liu S, Qi Y, Ge Y, Duplessis T, Rowan BG, Ip C, et al. Telomerase as an important target of androgen signaling blockade for prostate cancer treatment. Mol Cancer Ther 2010;9:2016–25.
27. Dong Y, Zhang H, Gao AC, Marshall JR, Ip C. Androgen receptor signaling intensity is a key factor in determining the sensitivity of prostate cancer cells to selenium inhibition of growth and cancer-specific biomarkers. Mol Cancer Ther 2005;4:1047–55.
28. Zhan Y, Cao B, Qi Y, Liu S, Zhang Q, Zhou W, et al. Methylselenol prodrug enhances MDV3100 efficacy for treatment of castration-resistant prostate cancer. Int J Cancer 2013;133:2225–33.
29. Dong Y, Zhang H, Hawthorn L, Ganther HE, Ip C. Delineation of the molecular basis for selenium-induced growth arrest in human prostate cancer cells by oligonucleotide array. Cancer Res 2003;63:52–9.
30. Dong Y, Lee SO, Zhang H, Marshall J, Gao AC, Ip C. Prostate specific antigen expression is downregulated by selenium through disruption of androgen receptor signaling. Cancer Res 2004;64:19–22.
31. Vichai V, Kirtikara K. Sulforhodamine B colorimetric assay for cytotoxicity screening. Nat Protoc 2006;1:1112–6.
32. van Royen ME, van Cappellen WA, de VC, Houtsmuller AB, Trapman J. Stepwise androgen receptor dimerization. J Cell Sci 2012;125:1970–9.
33. Hamdan FF, Percherancier Y, Breton B, Bouvier M. Monitoring protein–protein interactions in living cells by bioluminescence resonance energy transfer (BRET). Curr Protoc Neurosci 2006;Chapter 5:UInit 5.23.
34. van der Steen T, Tindall DJ, Huang H. Posttranslational modification of the androgen receptor in prostate cancer. Int J Mol Sci 2013;14:14833–59.

Asian Journal of Andrology (2016) 18, 607–612

www.asiaandro.com; www.ajandrology.com

Open Access

ORIGINAL ARTICLE

Prostate Disease

Berberine inhibits androgen synthesis by interaction with aldo-keto reductase 1C3 in 22Rv1 prostate cancer cells

Yuantong Tian[1,2,*], Lijing Zhao[1,*], Ye Wang[3], Haitao Zhang[4], Duo Xu[1], Xuejian Zhao[1], Yi Li[1], Jing Li[1]

Aldo-keto reductase family 1 member C3 has recently been regarded as a potential therapeutic target in castrate-resistant prostate cancer. Herein, we investigated whether berberine delayed the progression of castrate-resistant prostate cancer by reducing androgen synthesis through the inhibition of Aldo-keto reductase family 1 member C3. Cell viability and cellular testosterone content were measured in prostate cancer cells. Aldo-keto reductase family 1 member C3 mRNA and protein level were detected by RT-PCR and Western bolt analyses, respectively. Computer analysis with AutoDock Tools explored the molecular interaction of berberine with Aldo-keto reductase family 1 member C3. We found that berberine inhibited 22Rv1 cells proliferation and decreased cellular testosterone formation in a dose-dependent manner. Berberine inhibited Aldo-keto reductase family 1 member C3 enzyme activity, rather than influenced mRNA and protein expressions. Molecular docking study demonstrated that berberine could enter the active center of Aldo-keto reductase family 1 member C3 and form π-π interaction with the amino-acid residue Phe306 and Phe311. In conclusion, the structural interaction of berberine with Aldo-keto reductase family 1 member C3 is attributed to the suppression of Aldo-keto reductase family 1 member C3 enzyme activity and the inhibition of 22Rv1 prostate cancer cell growth by decreasing the intracellular androgen synthesis. Our result provides the experimental basis for the design, research, and development of AKR1C3 inhibitors using berberine as the lead compound.

Asian Journal of Andrology (2016) **18**, 607–612; doi: 10.4103/1008-682X.169997; published online: 11 December 2015

Keywords: aldo-keto reductase family 1 member C3; androgen; berberine; castration-resistant prostate cancer

INTRODUCTION

Recently, more studies have focused on castration-resistant prostate cancer (CRPC) because of high mortality rates.[1,2] One of the pivotal reasons for prostate cancer progression to CRPC is their acquired ability for intratumoral steroidogenesis from cholesterol or adrenal androgens.[3–5] Abiraterone acetate was designed to inhibit steroidogenesis mediated by CYP17A1 (cytochrome P450 17A1), a key enzyme for intratumoral *de novo* steroid synthesis from cholesterol and production of progestins, mineralocorticoids, glucocorticoids, androgens, and estrogens in the steroidogenic pathway.[6,7] Clinical trials have shown that chemotherapy combined with abiraterone acetate treatments prolonged survival among patients with metastatic CRPC.[8] However, CYP17A1 inhibitors have been associated with adrenocortical suppression and have led to an adrenocortical insufficiency because of the upstream blockage of steroidogenesis.[9,10] Therefore, more effective prostate cancer therapy that avoids this adverse effect may be targeting downstream of the *de novo* steroid synthesis from cholesterol.

Aldo-keto Reductase Family 1 Member C3 (AKR1C3) is known to be a type 5 17-hydroxysteroid dehydrogenase (17β-HSD5) and is involved in the final two steps of steroid synthesis in human prostate cancer cells, which possesses reductase activity for the catalysis of low activity hormone precursors, androstenedione and androsterone, to highly active testosterone (T) and dihydrotestosterone (DHT), as **Figure 1** depicted.[11] Other works have also shown that AKR1C3 is overexpressed in localized, advanced or recurrent prostate cancers and the CRPC,[12–14] and the expression levels of AKR1C3 were closely correlated with the Gleason grade of prostate cancer progression.[15] The up-regulation of AKR1C3 was likely to be a survival adaptation to the T/DHT-deprived environment. Moreover, *in vitro* studies have shown that AKR1C3-overexpressed LNCaP prostate cancer cells (LNCaP-AKR1C3) were prone to generating significantly higher amounts of testosterone.[16] Therefore, AKR1C3 is regarded to be a vital therapeutic target in the treatment of CRPC through suppressing intratumoral production of androgen.

In recent years, researchers have focused on the development of AKR1C3 inhibitors. A series of chemical compounds, such as medroxyprogesterone acetate (MPA), steroidal lactones, benzodiazepines, jasmonates, cinnamic acids, flavonoids, nonsteroidal anti-inflammatory drug (NSAIDs), and EM1404, were investigated for their efficacies in inhibiting the enzymatic activity of AKR1C3.[17] However, more work needs to be done for these drugs in the clinical applications of CRPC. Therefore, the purpose of our

[1]Department of Pharmacology, College of Basic Medical Science, Jilin University, Changchun 130021, China; [2]Gannan Medical University, Ganzhou, Jiangxi 341000, China; [3]School of Life Science, Jilin University, Changchun 130012, China; [4]Tulane Cancer Center, Tulane University School of Medicine, 1430 Tulane Avenue SL-79, New Orleans, LA 70112, USA.
*These authors contributed equally to this work.
Correspondence: Dr. J Li (lijing@jlu.edu.cn)
Received: 10 April 2015; Revised: 26 June 2015; Accepted: 15 October 2015

study is to find out AKR1C3 inhibitor in "old," nontoxic drugs. Berberine (2,3-methylenedioxy-9,10-dimenthoxyproto-berberine chloride; BBR), an isoquinoline alkaloid (**Figure 2**), was screened from a traditional Chinese medicine (TCM) monomer library and had been used as an anti-diarrheal agent for hundreds of years in China; Recently, it has been demonstrated possession of high antitumor activities against prostate cancer.[18–20] Our prior study found that BBR could delay the latent periods to the progression of CRPC in castrated nu/nu mice bearing a subcutaneous LNCaP xenograft.[19] However, the blocking mechanism by which BBR prevents AKR1C3-mediated intratumoral steroidogenesis in the inhibition of the development of CRPC has yet to be elucidated.

Herein, we first investigated the inhibitory capacity of BBR on a human recombinant AKR1C3 enzyme *in vitro* and the effect of BBR on the cell proliferation. In addition, we studied androgen synthesis in the AKR1C3-overexpressing cell line 22Rv1. Finally, we used AutoDock Tools to elucidate the molecular interactions between BBR and AKR1C3. This work provides new insights on strategies for the prevention and treatment of CRPC.

MATERIALS AND METHODS

Materials

Androstendione, NADPH, and other chemicals were obtained from Sigma-Aldrich (St. Louis, MO, USA). Recombinant human AKR1C3 enzymes were obtained from (PROSPEC: Cat#enz-406, Ness-Ziona, Israel). The primary anti-AKR1C3 (NP6.G6.A6, mouse monoclonal antibody, 1:150) was purchased from Abcam Inc., (Cambridge, MA, USA) and anti-β-actin (mouse polyclonal antibody, 1:1000) was purchased from Santa Cruz Biotechnology, Inc., (Dallas, TX, USA). The secondary antibody was HRP-conjugated anti-mouse IgG (1:10 000, Gaithersburg, MD, USA). Human LNCaP, PC3, PC3M cells and 22Rv1 were obtained from the American Type Culture Collection (Manassas, VA, USA). Tris–HCl gel, polyvinylidene difluoride (PVDF) membranes, and nonfat dry milk were purchased from Bio-Rad Laboratories, Inc., CA, USA.

Methods

Screening for AKR1C3 expression human prostate cancer cell

Cellular proteins were prepared from LNCaP cells, PC3 cells, PC3M cells and 22Rv1 cells in a modified RIPA buffer (50 mmol l^{-1} Tris–HCl, pH 7.4), 1% NP-40, 0.25% sodium deoxycholate, 150 mmol l^{-1} NaCl, 1 mmol l^{-1} EDTA and 2 mmol l^{-1} phenylmethylsulfonyl fluoride). Total soluble proteins (50 μg) were electrophoresed on a 12% Tris–HCl gel. Proteins were transferred onto PVDF membranes. The membranes were blocked with 5% nonfat dry milk in Tris-buffered saline containing 1% Tween 20. Antigens were detected by incubating with mouse anti-human AKR1C3 mAb (1:500) or anti-β-actin mAb (1:5000) at room temperature for 2 h followed by incubation with HRP-conjugated anti-mouse IgG (1:10 000, Gaithersburg, MD, USA) secondary antibody at room temperature for another 1 h. Immunoreactive protein was then detected using enhanced chemiluminescence reagent (Pierce, Rockford, IL, USA) according to the manufacturer's protocol.

Cell proliferation assay by MTT

The cells were maintained in RPMI 1640 medium supplemented with 10% FBS, 2 mmol l^{-1} glutamine, 100 units ml^{-1} penicillin, and 100 μg ml^{-1} streptomycin at 37°C in a humidified incubator containing 5% CO_2. MTT assay was performed in 96-well plates in quintuple. Cells were seeded at a density of 1.5×10^4 cells/well overnight, and the medium was changed to RPMI 1640 with 10% charcoal-dextran stripped serum (CSS) and BBR (12.5 μmol l^{-1}, 25 μmol l^{-1} and 50 μmol l^{-1}) for 48 h with or without 0.1 μmol l^{-1} androstendione; 30 μmol l^{-1} indomethacin was used as positive control. Data are expressed as the means ± s.d. of at least three independent experiments.

Determination of testosterone formation

22Rv1 cells were seeded into 6-well plates in duplicate at a density of 2.5×10^5 cells/well overnight, and the cells were divided into three groups, including the negative control group (solvent only), the BBR group (25 μmol l^{-1}) and the INN group (30 μmol l^{-1}). In the cellular testosterone formation experiment, finasteride, an inhibitor of 5α-reductase (SRD5A1), was used to blocked metabolism of 0.1 μmol l^{-1} androstendione to 5α-andostane-3,17-dione and block T to the formation of DHT. Simply, cells were treated with chemicals for 24 h, and then androstendione was added to the medium with a final concentration of 0.1 μmol l^{-1} in each group. Then, the medium of the culture was separated, and the metabolism of androstendione was analyzed by determining the concentration of testosterone in the medium using chemiluminescence. Data are expressed as the means ± s.d. of at least three independent experiments.

AKR1C3 mRNA expression analysis using reverse transcription PCR (RT-PCR)

22Rv1 cells were divided into solvent control (DMSO) and BBR (25 μmol l^{-1}). Total RNA was extracted from the cells using the Trizol reagent (Invitrogen, Grand Island, NY, USA) according to the manufacturer's instructions. First-strand cDNA was generated

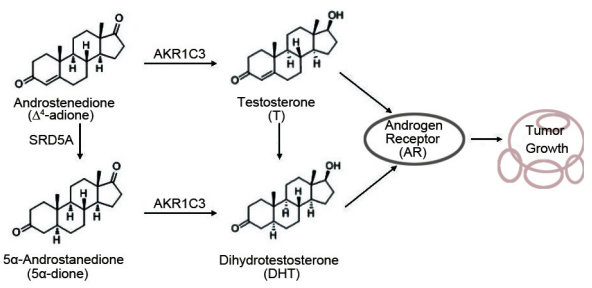

Figure 1: The synthesis of T/DHT under AKR1C3 catalysis. AKR1C3 catalyzes Δ^4-adione to T and 5α-dione to DHT. SRD5A catalyzes Δ^4-adione to 5α-dione and T to DHT. Then, T and DHT promote prostate cancer cell growth by activation of androgen receptor (AR).

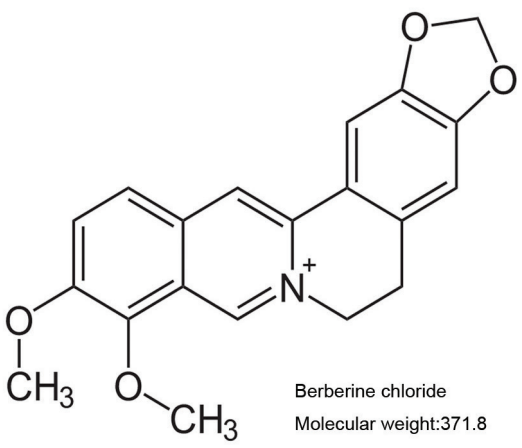

Figure 2: Berberine (BBR) chemical structure.

by reverse transcription of 5 μg RNA samples using a one-step gDNA removal and cDNA synthesis supermix (Transgene biotech, Beijing, China). One-tenth of the reverse-transcribed RNA was used in the PCR reaction. Absolute gene transcription was normalized to β-actin. The primer sequences were as follows: β-actin sense: 5'-dATCTGGCACCACACCTTCTACAATGAGCTGCG-3' and antisense: 5'-dCGTCATACTCCTGCTTGCTGATCCACATCTGC-3'; AKR1C3 sense: 5'-dGTAAAGCTTTGGAGGTCAC-3' and antisense: 5'-dCACCCATCGTTTGTCTCGT-3'. The PCR products were separated using electrophoresis on 1% agarose gels containing ethidium bromide. The PCR products were visualized using a Tanon-1600 figure gel image processing system and analyzed with a GIS 1D gel image system software (Tanon, Shanghai, China). For Western blot analysis, cellular proteins were prepared and performed as described in Screening for AKR1C3 expression human prostate cancer cell for 22Rv1 cells.

AKR1C3 protein expression by Western blot analysis

22Rv1 cells were divided into solvent control (DMSO) and BBR (25 μmol l^{-1}). The protein was prepared from cells treated with BBR for 48 h. Protein extraction, quantification and Western blot steps were conducted the same as the screening for AKR1C3 expression human prostate cancer cells.

Enzyme activity assays

Enzyme activity was monitored in 200 μl volumes containing 6.25–100 μmol l^{-1} androstendione in 4% (v/v) DMSO, 0.2 mmol l^{-1} NADPH, 100 mmol l^{-1} potassium phosphate buffer (pH 7.0) and human recombinant AKR1C3 enzyme. The IC50 values for AKR1C3 inhibitors were carried out in a range of eight inhibitor concentrations (0.39–50 μmol l^{-1}) with 50 μmol l^{-1} androstendione in the same reaction mixture mentioned above. All reactions were initiated by the addition of enzyme. The activities of the enzymes were determined at 37°C by measuring the rate of change in NADPH fluorescence (at 455 nm with an excitation wavelength of 340 nm). A standard curve was constructed by monitoring fluorescence changes with incremental additions of NADPH. Indomethacin was used as a positive control in the inhibition studies.

Molecular modeling

To estimate the potential interaction and the conformation of the protein-ligand complex, inhibitors were docked into the AKR1C3 protein using the AutoDock 4.2 program based on Lamarkian Genetic Algorithm (Scripps Research Institute, La Jolla, CA, USA). The amino acid sequence of AKR1C3 was collected from the UniProtKB (P42330), in which 323 amino acid residues were involved. The atomic coordinates for the AKR1C3-$NADP^+$-E1404 acid complex (PDB code 1ZQ5) were obtained from the RCSB Protein Data Bank. The 3D structure of inhibitors was acquired from the Internet (http://zinc.docking.org/). The predicted complexes were optimized and ranked according to the empirical scoring function, ScreenScore, which estimated the binding free energy of the ligand-receptor complex. Each docking was performed twice, and each operation screened 250 conformations for the protein-ligand complex that were advantageous for docking; each docking had 500 preferred conformations. The most stable conformation had the minimal binding energy as shown by Discovery Studio (DS) 3.5 Visualizer (Accelrys, Inc).

Statistical analysis

Statistical evaluation of the data was performed using independent Student's *t*-test and ANOVA followed by Fisher's test. A P value < 0.05 was considered statistically significant. IC50 was calculated by probit analysis using SPSS (SPSS Inc., Chicago, IL, USA).

RESULTS

Characterization of AKR1C3 protein expression in prostate cancer cell lines

To find a model to mimic the CRPC state, we screened for a prostate cancer cell line with high AKR1C3 expression. The characterization of AKR1C3 protein expression was conducted for a panel of prostate cancer cell lines, including LNCaP cells, PC3 cells, PC3M cells and 22Rv1 cells. Western blot analyses confirmed that the expression of AKR1C3 was relatively strong in PC3M cells and 22Rv1 cells (**Figure 3**). Because the 22Rv1 cell line was derived from the androgen-dependent 22Rv1 cells and has castration-resistant prostate cancer characteristics, the following experiments were carried out with 22Rv1 cells.

Cell proliferation assay in 22Rv1 cells

To investigate the dose-effect relationship of BBR on 22Rv1 cell growth, an MTT assay was carried out using a 48 h treatment with three concentrations of BBR (12.5 μmol l^{-1}, 25 μmol l^{-1} and 50 μmol l^{-1}). The results showed that BBR exhibited a dose-dependent inhibition on the proliferation of 22Rv1 cells at 48 h. When 0.1 μmol l^{-1} androstenedione was added to the culture medium, the inhibitive effect of BBR on cell proliferation was partially counteracted, indicating that the additional androstenedione increased the synthesis of androgen and indirectly reversed the BBR effect (**Figure 4**).

BBR on testosterone formation in 22Rv1 cells

To explore whether BBR influenced androgen synthesis, cellular T production was measured after the treatment with 25 μmol l^{-1} BBR for 48 h in 22Rv1 cells. As shown in **Figure 1**, T and DHT are the primary androgen species stimulating prostate cell growth, which are converted from Δ^4-adione and 5α-dione by AKR1C3 catalysis, respectively. Herein, we used a potent 5α-reductase inhibitor, finasteride, to block conversion of Δ^4-adione to 5α-dione and also block T to the formation of DHT, respectively. The aim is to confirm the efficacy of BBR on the inhibition of AKR1C3 activity. The results showed that after blockage of 5α-reductase, finasteride with the final concentration of 2 μmol l^{-1} increased T production approximately 2.19 folds to Control group. As shown in **Figure 5**, BBR and INN significantly reduced the formation of total testosterone, even slightly lower to the finasteride ($P < 0.05$).

Effects of BBR on AKR1C3 gene expression

To investigate whether BBR influences gene expression, RT-PCR and Western blot analysis were carried out. The results showed that BBR did not change the mRNA level or the protein level after the treatment of 22Rv1 cells with 25 μmol l^{-1} BBR for 48 h (**Figure 6**). This indicates that BBR did not influence the transcription or expression of the AKR1C3 gene.

In vitro inhibition of AKR1C3 enzyme activity

The aforementioned results demonstrated that AKR1C3 did not change the mRNA expression or the protein expression after a 48 h treatment with 25 μmol l^{-1} BBR. However, along with cell proliferation, the intracellular testosterone production significantly reduced. Therefore, we inferred that the inhibition of enzymatic activity by AKR1C3 was the main reason for the suppression of prostate cancer cell growth. Regarding the AKR1C3-catalyzed reduction of Δ^4-adione to T, we examined the inhibition of BBR on AKR1C3 reductive enzyme activity by using Δ^4-adione as a substrate and INN as a positive control. It is shown that both BBR and INN displayed potent inhibitory effects

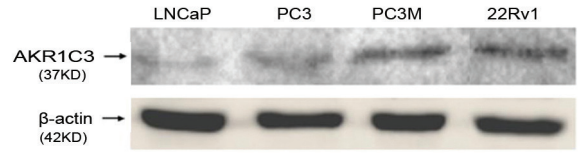

Figure 3: Protein expression of AKR1C3 in human prostate cancer cell lines.

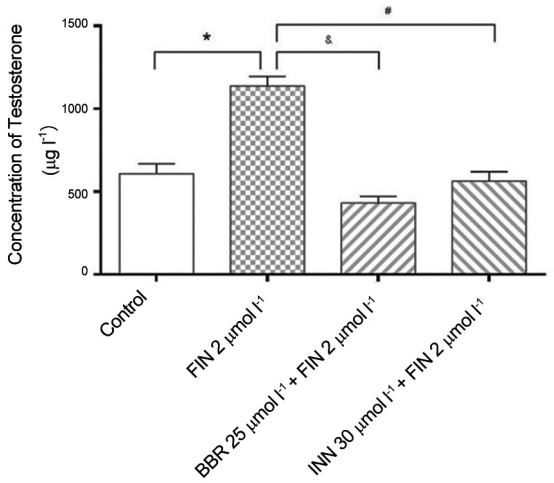

Figure 5: The influence of berberine on the formation of testosterone. $^{*}P < 0.05$, compared with the control group. $^{\#}$and $^{\&}P < 0.05$, compared with the finasteride group.

on the activity of recombinant human AKR1C3 (**Figure 7a** and 7**b**). The IC50 values for BBR was 4.08 μmol l^{-1} with a 95% Confidence Intervals of 3.47 μmol l^{-1} to 4.69 μmol l^{-1}. The IC50 values for INN was 7.26 μmol l^{-1} with a 95% Confidence Intervals of 6.82 μmol l^{-1} to 7.70 μmol l^{-1}. The IC50 value for BBR was much lower than that for INN implicating that BBR had higher efficacy in inhibiting the activity of AKR1C3.

Molecular docking studies

To gain insight into interactions inside the enzyme binding sites of BBR, we used AutoDock 4.2 to observe the optical interactions of BBR (**Figure 8 Ia–Ic**) with the cavity center of AKR1C3. Two control drugs were involved in the analysis, INN (**Figure 8 IIa–IIc**) and EM1404 (**Figure 8 IIIa–IIIc**), which are potent AKR1C3 inhibitors. Our data showed that BBR could enter the steroid/inhibitor binding cavity of AKR1C3 and form π-π interactions with amino-acid residues Phe306 and Phe311 (**Figure 8 Ic**). To identify the binding forces contributing to the interaction between the inhibitors and AKR1C3, the estimated free energy of binding (FEB), which predicts the Van der Waals energy, electrostatic energy, hydrogen-bond energy, de solv energy, final total internal energy, torsional free energy, and unbound system energy, were calculated. As estimated by Discovery Studio (DS) 3.5 Visualizer software, the most stable conformation exhibited the lowest FEB. The binding energies of BBR, INN, and EM1404 were –9.63, –9.79, and –12.55 kcal mol^{-1}, respectively (**Table 1**). These results provided theoretical support for and explanation of the effects of BBR on AKR1C3 activity.

DISCUSSION

Recently researchers demonstrated that prostate cancer cells acquired

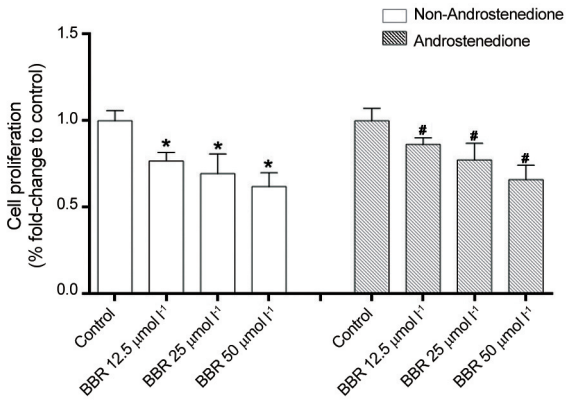

Figure 4: Effect of berberine (BBR) on 22Rv1 cell proliferation by MTT assay in conditions with or without androstenedione (4-adione) addition. *and $^{\#}P < 0.05$, compared with their control groups.

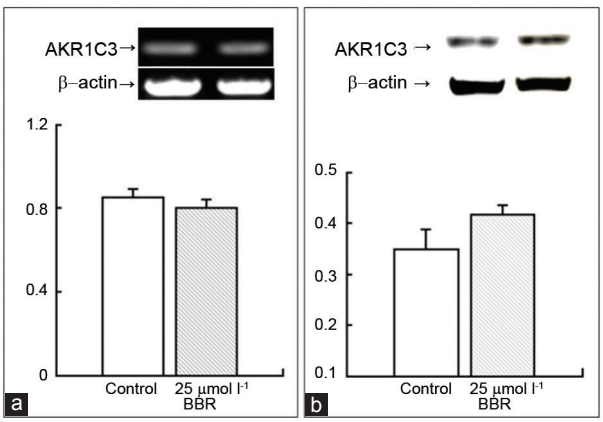

Figure 6: The influence of BBR on AKR1C3 in the level of mRNA and protein. (**a**) RT-PCR for AKR1C3 gene, the upper panel shows the mRNA bands for the control group and the BBR group, and the lower panel shows the bars for their quantification. (**b**) Western blot for AKR1C3 gene, the upper panel shows the protein bands for the control group and the BBR group, and the lower panel shows bars for their quantification.

ability of intratumoral steroidogenesis from cholesterol or adrenal androgens in the absence of blood androgens, which made prostate cancer evolve from an endocrine disease to an autocrine/paracrine one.[3,5] AKR1C3 is a key steroidogenic enzyme to catalyze the conversion of low active androstenedione and androsterone hormone precursors to highly active testosterone and dihydrotestosterone in steroid synthesis pathway.[11] In recent, accumulating amount of data reported that AKR1C3 is associated with the transformation from hormone-dependent prostate cancer to CRPC.[11,15] This concept has led to the increasing interest in the development of AKR1C3 inhibitors. Until now, several AKR1C3 inhibitors, such as ASP9521and SN33638, were evaluated in multi-center phase I/II study in patients with metastatic CRPC or in high AKR1C3-expressing cell lines. The results suggested that a subpopulation of CRPC patients with high AKR1C3 might benefit from AKR1C3 inhibitor therapy.[21,22]

BBR, as an isoquinoline alkaloid, has high capacity and spectrum for various tumors. Recent studies have found that BBR displays potent antitumor activity for prostate cancer without toxicity.[19,23] In this research, BBR exhibited a dose-dependent inhibition on the proliferation of 22Rv1 cells at 48 h without influencing the mRNA level

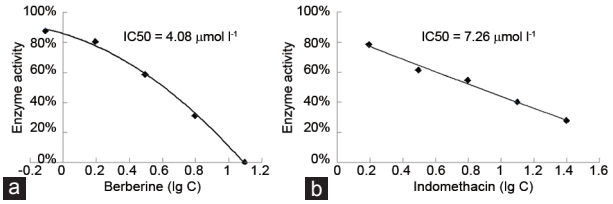

Figure 7: The enzyme inhibition curve of (**a**) BBR and (**b**) INN.

Table 1: The binding energy of BBR, INN and EM1404 with AKR1C3

Zinc number	*Compound*	*Binding energy (kcal mol^{-1})*
Zinc_3779067	BBR	–9.63
Not acceptable	EM1404	–12.55
Zinc_27643987	INN	–9.79

BBR: berberine; INN: indomethacin

or the protein level of AKR1C3, but significantly reducing the formation of total testosterone. In enzyme assays, BBR displayed potent inhibition on the activity of recombinant human AKR1C3 with lower IC50 value than that for INN, implicating that BBR had higher efficacy in inhibiting the activity of AKR1C3. Some studies had shown that CRPC cells were prone to generate significantly higher amounts of T, rather than DHT to promote prostate cancer growth.[5,11,24] Therefore, AKR1C3 is regarded as a vital therapeutic target in the treatment of CRPC. In cell proliferation assay, BBR exhibited dose-dependent growth inhibition on high AKR1C3-expressing 22Rv1 cell, but INN had only a limited effect on the cell growth mediated by Δ^4-adione. After blocking AKR1C3, prostate cancer cells reverted to their overall androgen metabolic profile from the conversion Δ^4-adione to the 5α-dione, which bound with the mutated AR to stimulate androgen signaling pathway.[16] Therefore, the desired therapeutic effect of AKR1C3 inhibitors could be weakening in this circumstance. In our previous study, we confirmed the BBR also induced the truncated AR splice variants degradation. Consequently, BBR could block cell proliferation either by intratumoral steroidogenesis or by AR antagonist. That's why the more potent effect was shown in BBR than that of INN.

In order to better understanding the molecular mechanism of BBR on AKR1C3, we used AutoDock Tools to study the molecular interaction between BBR and AKR1C3. According to the X-ray crystal structure, AKR1C3 consists of 323 amino acids, which form a (β/α) 8-barrel structure with a large, multi-cavity active site that exhibits flexibility at the level of individual side chains and entire loop regions on ligand binding.[25] AKR1C3 catalytic sites were consist of five compartments, an oxyanion site (formed by Tyr55, His117, and $NADP^+$), a steroid channel (Trp227 and Leu54), and three subpockets, SP1 (Ser118, Asn167, Phe306, Phe311, and Tyr319), SP2 (Trp86, Leu122, Ser129, and Phe311), and SP3 (Tyr24, Glu192, Ser221, and Tyr305).[17] The difference among the AKR1C enzymes lies in the three subpockets. The SP1 pocket is expected to give more potent and selective AKR1C3 inhibitors.[17,26] Structural differences at position 306 in SP3 and 311 in SP2 make the AKR1C3 differ from the other enzymes.[17] Our data show that BBR could enter the steroid/inhibitor binding cavity of AKR1C3 and formed π-π interaction in the amino-acid residue Phe306 and Phe311. Although further study should be carried out to certificate this interaction, this molecular docking theoretically gave the supports and explanation on the effects of BBR on AKR1C3 enzymatic activity.

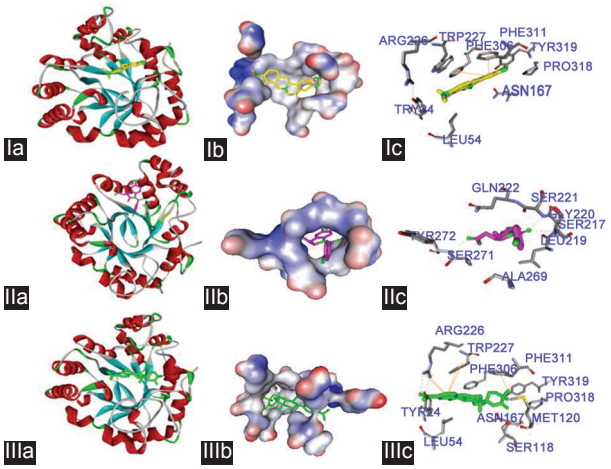

Figure 8: The interaction of BBR (**I**), INN (**II**) and EM1404 (**III**) with AKR1C3. BBR (yellow), INN (pink) and EM1404 (green). (**a**) The optimize graphic performance of ligands with AKR1C3. (**b**) The created surface around ligands in the active center of AKR1C3. (**c**) Ligand binding site atoms of AKR1C3. Hydrogen bonds and π-π interaction formed between BBR (**I**), INN (**II**) and EM1404 (**III**) with the active center of AKR1C3. Hydrogen bonds are shown by green dash lines. π-π interactions are shown by yellow solid line.

CONCLUSIONS

The present findings reveal that BBR could decrease intracellular androgen synthesis due to the suppression of AKR1C3 enzyme activity. The mechanisms of BBR on CRPC provide a basis on the design, research, and development of future AKR1C3 inhibitors using BBR as the lead compound.

AUTHOR CONTRIBUTIONS

JL conceived the study, coordinated the experimental design of the study. YTT and LJZ carried out the critical revision of results, analyzed the data and drafted the manuscript. YW carried out the computer analysis. DX carried out an *in vitro* pharmacology study. HTZ, YL, and XJZ helped to draft and to revise the manuscript. All authors read and approved the final manuscript.

COMPETING INTERESTS

The authors declare that they have no competing interests.

ACKNOWLEDGMENTS

This work was supported by grants from the National Natural Science Foundation of China (81302206 and 81560422), the Development and Reform Commission of Jilin Province (2013C026-2), and the Young Scholars Program of Norman Bethune Health Science Center of Jilin University (2013201012), the Health and Family Planning Commission of Jiangxi Province (20143207) and the Natural Science Foundation of Jiangxi Province of China (20151BAB205016 and 20132BAB205008).

REFERENCES

1 Titus M, Tomer KB. Androgen quantitation in prostate cancer tissue using liquid chromatography tandem mass spectrometry. *Methods Mol Biol* 2011; 776: 47–57.
2 Shah RB, Mehra R, Chinnaiyan AM, Shen R, Ghosh D, *et al*. Androgen-independent prostate cancer is a heterogeneous group of diseases: lessons from a rapid autopsy program. *Cancer Res* 2004; 64: 9209–16.
3 Mostaghel EA, Nelson PS. Intracrine androgen metabolism in prostate cancer progression: mechanisms of castration resistance and therapeutic implications. *Best Pract Res Clin Endocrinol Metab* 2008; 22: 243–58.
4 Locke JA, Guns ES, Lubik AA, Adomat HH, Hendy SC, *et al*. Androgen levels increase by intratumoral *de novo* steroidogenesis during progression of castration-resistant prostate cancer. *Cancer Res* 2008; 68: 6407–15.

5 Montgomery RB, Mostaghel EA, Vessella R, Hess DL, Kalhorn TF, *et al*. Maintenance of intratumoral androgens in metastatic prostate cancer: a mechanism for castration-resistant tumor growth. *Cancer Res* 2008; 68: 4447–54.
6 Pezaro CJ, Mukherji D, De Bono JS. Abiraterone acetate: redefining hormone treatment for advanced prostate cancer. *Drug Discov Today* 2012; 17: 221–6.
7 Rehman Y, Rosenberg JE. Abiraterone acetate: oral androgen biosynthesis inhibitor for treatment of castration-resistant prostate cancer. *Drug Des Devel Ther* 2012; 6: 13–8.
8 de Bono JS, Logothetis CJ, Molina A, Fizazi K, North S, *et al*. Abiraterone and increased survival in metastatic prostate cancer. *N Engl J Med* 2011; 364: 1995–2005.
9 Attard G, Reid AH, Yap TA, Raynaud F, Dowsett M, *et al*. Phase I clinical trial of a selective inhibitor of CYP17, abiraterone acetate, confirms that castration-resistant prostate cancer commonly remains hormone driven. *J Clin Oncol* 2008; 26: 4563–71.
10 O'Donnell A, Judson I, Dowsett M, Raynaud F, Dearnaley D, *et al*. Hormonal impact of the 17alpha-hydroxylase/C (17,20)-lyase inhibitor abiraterone acetate (CB7630) in patients with prostate cancer. *Br J Cancer* 2004; 90: 2317–25.
11 Adeniji AO, Chen M, Penning TM. AKR1C3 as a target in castrate resistant prostate cancer. *J Steroid Biochem Mol Biol* 2013; 137: 136–49.
12 Nakamura Y, Suzuki T, Nakabayashi M, Endoh M, Sakamoto K, *et al*. *In situ* androgen producing enzymes in human prostate cancer. *Endocr Relat Cancer* 2005; 12: 101–7.
13 Pelletier G, Luu-The V, El-Alfy M, Li S, Labrie F. Immunoelectron microscopic localization of 3beta-hydroxysteroid dehydrogenase and type 5 17beta-hydroxysteroid dehydrogenase in the human prostate and mammary gland. *J Mol Endocrinol* 2001; 26: 11–9.
14 Lapouge G, Marcias G, Erdmann E, Kessler P, Cruchant M, *et al*. Specific properties of a C-terminal truncated androgen receptor detected in hormone refractory prostate cancer. *Adv Exp Med Biol* 2008; 617: 529–34.
15 Tian Y, Zhao L, Zhang H, Liu X, Zhao X, *et al*. AKR1C3 overexpression may serve as a promising biomarker for prostate cancer progression. *Diagn Pathol* 2014; 9: 42.
16 Byrns MC, Mindnich R, Duan L, Penning TM. Overexpression of aldo-keto reductase 1C3 (AKR1C3) in LNCaP cells diverts androgen metabolism towards testosterone resulting in resistance to the 5alpha-reductase inhibitor finasteride. *J Steroid Biochem Mol Biol* 2012; 130: 7–15.
17 Byrns MC, Jin Y, Penning TM. Inhibitors of type 5 17beta-hydroxysteroid dehydrogenase (AKR1C3): overview and structural insights. *J Steroid Biochem Mol Biol* 2011; 125: 95–104.
18 Wang Y, Liu Q, Liu Z, Li B, Sun Z, *et al*. Berberine, a genotoxic alkaloid, induces ATM-Chk1 mediated G2 arrest in prostate cancer cells. *Mutat Res* 2012; 734: 20–9.
19 Li J, Cao B, Liu X, Fu X, Xiong Z, *et al*. Berberine suppresses androgen receptor signaling in prostate cancer. *Mol Cancer Ther* 2011; 10: 1346–56.
20 Mantena SK, Sharma SD, Katiyar SK. Berberine, a natural product, induces G1-phase cell cycle arrest and caspase-3-dependent apoptosis in human prostate carcinoma cells. *Mol Cancer Ther* 2006; 5: 296–308.
21 Loriot Y, Fizazi K, Jones RJ, Van den Brande J, Molife RL, *et al*. Safety, tolerability and anti-tumour activity of the androgen biosynthesis inhibitor ASP9521 in patients with metastatic castration-resistant prostate cancer: multi-centre phase I/II study. *Invest New Drugs* 2014; 32: 995–1004.
22 Yin YD, Fu M, Brooke DG, Heinrich DM, Denny WA, *et al*. The activity of SN33638, an inhibitor of AKR1C3, on testosterone and 17beta-estradiol production and function in castration-resistant prostate cancer and ER-positive breast cancer. *Front Oncol* 2014; 4: 159.
23 Choi MS, Oh JH, Kim SM, Jung HY, Yoo HS, *et al*. Berberine inhibits p53-dependent cell growth through induction of apoptosis of prostate cancer cells. *Int J Oncol* 2009; 34: 1221–30.
24 Stanbrough M, Bubley GJ, Ross K, Golub TR, Rubin MA, *et al*. Increased expression of genes converting adrenal androgens to testosterone in androgen-independent prostate cancer. *Cancer Res* 2006; 66: 2815–25.
25 Schlegel BP, Jez JM, Penning TM. Mutagenesis of 3 alpha-hydroxysteroid dehydrogenase reveals a "push-pull" mechanism for proton transfer in aldo-keto reductases. *Biochemistry* 1998; 37: 3538–48.
26 Bauman DR, Rudnick SI, Szewczuk LM, Jin Y, Gopishetty S, *et al*. Development of nonsteroidal anti-inflammatory drug analogs and steroid carboxylates selective for human aldo-keto reductase isoforms: potential antineoplastic agents that work independently of cyclooxygenase isozymes. *Mol Pharmacol* 2005; 67: 60–8.